COPPE
Instituto Alberto Luiz Coimbra de Pós-Graduação e Pesquisa de Engenharia
UFRJ

LIPASE PRODUCTION BY *YARROWIA LIPOLYTICA* WITH SOYBEAN HULLS IN TRAY AND PACKED-BED BIOREACTORS: EXPERIMENTAL STUDIES AND PROCESS MODELING

Felipe Valle do Nascimento

Tese de Doutorado apresentada ao Programa de Pós-graduação em Engenharia Química, COPPE, da Universidade Federal do Rio de Janeiro, como parte dos requisitos necessários à obtenção do título de Doutor em Engenharia Química.

Orientadores: Argimiro Resende Secchi
Maria Alice Zarur Coelho
Aline Machado de Castro

Rio de Janeiro
Junho de 2021

LIPASE PRODUCTION BY *YARROWIA LIPOLYTICA* WITH SOYBEAN HULLS IN TRAY AND PACKED-BED BIOREACTORS: EXPERIMENTAL STUDIES AND PROCESS MODELING

Felipe Valle do Nascimento

TESE SUBMETIDA AO CORPO DOCENTE DO INSTITUTO ALBERTO LUIZ COIMBRA DE PÓS-GRADUAÇÃO E PESQUISA DE ENGENHARIA DA UNIVERSIDADE FEDERAL DO RIO DE JANEIRO COMO PARTE DOS REQUISITOS NECESSÁRIOS PARA A OBTENÇÃO DO GRAU DE DOUTOR EM CIÊNCIAS EM ENGENHARIA QUÍMICA.

Orientadores: Argimiro Resende Secchi
Maria Alice Zarur Coelho
Aline Machado de Castro

Aprovada por: Prof. Argimiro Resende Secchi
Profa. Maria Alice Zarur Coelho
Pesq. Aline Machado de Castro
Prof. Tito Lívio Moitinho Alves
Profa. Andréa Medeiros Salgado
Profa. Fernanda Perpétua Casciatori

RIO DE JANEIRO, RJ – BRASIL
JUNHO DE 2021

Nascimento, Felipe Valle do

Lipase production by *Yarrowia lipolytica* with soybean hulls in tray and packed-bed bioreactors: experimental studies and process modeling/Felipe Valle do Nascimento. – Rio de Janeiro: UFRJ/COPPE, 2021.

XXV, 129 p.: il.; 29, 7cm.

Orientadores: Argimiro Resende Secchi
Maria Alice Zarur Coelho
Aline Machado de Castro

Tese (doutorado) – UFRJ/COPPE/Programa de Engenharia Química, 2021.

Referências Bibliográficas: p. 106 – 129.

1. Solid-state fermentation. 2. *Yarrowia lipolytica*. 3. Lipase. 4. Modeling. I. Secchi, Argimiro Resende *et al.* II. Universidade Federal do Rio de Janeiro, COPPE, Programa de Engenharia Química. III. Título.

Às minhas sobrinhas Mariane
(em memória) e Catarina.

Agradecimentos

Em meio à pandemia de COVID-19, as percepções sobre os agradecimentos tomam outras dimensões e, em confinamento social, destaca-se o evidente papel daqueles que sempre estão ao meu lado: minha família. Não existem palavras suficientes para agradecer por toda compreensão, pelo esforço que meus pais Jailton e Maria de Fátima sempre fizeram para que eu tivesse condições estruturais, econômicas e emocionais para concluir mais esta etapa acadêmica. Sempre foram os que mais me estimularam a tentar e a seguir em frente, mesmo em momentos de incerteza e dificuldade. Sinto que nunca conseguirei expressar o quanto eu valorizo isso tudo e nossa relação. Muito, muito obrigado por tudo! Agradeço também à família com quem não divido a mesma casa: meu irmão e meu tio José Luiz (e suas respectivas famílias), que sempre estiveram presentes, me apoiaram e serviram de maior exemplo de perseverança e estudo. Muito obrigado também!

Fora do ambiente de trabalho e da minha casa, meus amigos sempre foram minha base. Era com eles que eu gostaria de estar e, muitas vezes, eu abdiquei dessas oportunidades por conta de outras obrigações. Sei que vocês sempre me apoiaram independente da minha ausência. Muito obrigado pelos raros e felizes encontros!

Em seguida, gostaria de agradecer aos meus amigos do grupo BIOSE (incluindo os professores), tanto os que permanecem quanto os que já deixaram o grupo. Tenham certeza que a cada troca com cada um de vocês eu aprendi muito, não somente sobre o contexto óbvio das nossas atividades laboratoriais, mas também sobre a vida no seu sentido mais amplo. Peço desculpas pelos momentos de angústia e dificuldade, pois sei que vocês foram afetados por isso, mas sempre me acolheram. Agradeço também pelos incontáveis momentos de alegria e leveza que pude partilhar com vocês. Nao vejo a hora em que poderemos nos encontrar novamente!

Em especial, em função dos nossos temas de pesquisa (mas definitivamente não limitado a isso), gostaria de agradecer à Ariane, Verônica e Caê, com quem sempre pude tirar dúvidas, e à Alanna e ao Júlio, com quem discuti infinitamente nossas dificuldades e felicidades da tese. Agradeço também a Ana Beatriz e a Larissa, que além da amizade, me obrigavam a estudar com elas (só posso dizer que apesar de reclamar, sempre foi um prazer para mim). Por fim, agradeço também à Nanci, pelo puro carinho e cuidado que sempre teve comigo.

Marselle, Gabriel L., Carol, Sara e Gabriel S: talvez vocês não saibam o quanto vocês são importantes para mim e me ajudaram nisso tudo. Que foram meu porto seguro para conseguir chegar ao fim dessa jornada. Saibam que esse trabalho também é fruto da presença de vocês na minha vida.

Aos amigos do PEQ que fiz enquanto cursava as disciplinas, agradeço profundamente, sobretudo por estar sobrecarregado naquele momento. Graças a vocês também pude atravessar esse caminho de forma mais tranquila. Aos funcionários da secretaria do PEQ eu agradeço por sempre ajudarem prontamente quando tive dúvidas.

Aproveito também o espaço para agradecer aos funcionários e professores do Departamento de Engenharia Bioquímica (DEB) da Escola de Química da UFRJ, pelos inúmeros aprendizados e oportunidades que tive enquanto fui professor auxiliar nos anos iniciais. Em especial, agradeço aos professores do setor de Bioengenharia, sobretudo à professora Eliana Alhadeff, com quem dividi disciplinas e que confiou no meu trabalho. Agradeço também ao Christiano pela ajuda nas incontáveis aulas práticas e ao Bruno, por toda ajuda mais burocrática. Ainda, agradeço aos professores Bernardo Dias e Karen Signori, que me deram inúmeras oportunidades desde que cheguei no laboratório. Além disso, um professor não é ninguém sem seus alunos. Nesses quatro semestres de atuação, fui muito feliz trocando conhecimentos com vocês. Espero que entendam que vocês também tem seu papel na construção desse trabalho e na pessoa que eu me tornei.

Nesse sentido, agradeço também aos meus ex alunos e colegas de trabalho do pré-vestibular comunitário SBS. Obrigado pela confiança e por me ensinarem sempre, em todos os encontros semanais que tivemos e teremos.

Gostaria também de agradecer aos meus orientadores anteriores, pois sei que sou fruto de uma jornada de muitos anos de treinamento. Primeiramente, aqueles que estiveram comigo durante a graduação no período da iniciação científica, estágio e projeto final. À Juliana H., minha primeira orientadora e que disse para eu "não desistir da Engenharia de Bioprocessos", Érica S., Adriana Y., Ioana G., Juliana C., Rimenys C. e à professora Leda Castilho (que sempre me ajudou e continua ajudando desde a iniciação científica). Agradeço também à professora Priscilla Amaral, por toda a troca durante o mestrado e enquanto professor substituto do DEB.

Em seguida, agradeço aos meus atuais orientadores. Principalmente durante esse último ano de pandemia, sempre estiveram dispostos a me ajudar e corrigir o que fosse necessário, respeitando meus momentos de dificuldade. Sei que para vocês esse momento também foi e ainda está sendo exaustivo e, por isso, não posso deixar de enfatizar o quanto valorizo o papel de vocês enquanto professores/orientadores. Essa oportunidade que tive de trabalhar com vocês me ensinou muito, pude confiar em vocês e sou grato por isso. À Aline Machado, apesar de não termos interagido

pessoalmente muitas vezes, sinto que mesmo à distância suas percepções, ideias e sugestões sempre me levaram a um caminho melhor. Só consigo enxergar positivade na troca que tivemos, muito obrigado. Ao Professor Argimiro, pelo qual minha admiração vem desde a época da graduação, agradeço infinitamente por toda ajuda. Todas as correções, ensinamentos e paciência. Finalmente, agradeço à professora Maria Alice, a grande mãe do laboratório 103, sempre correndo atrás para garantir o melhor e que pudéssemos trabalhar em condições adequadas. Que sempre ressaltou que o produto principal da tese de doutorado é o aluno. Foram inúmeras as "cordas que você jogou", que eu fui tentando pegar e só posso ser grato por elas. Além disso, foram inúmeros os cafés, almoços e conversas, por vezes sérias, por vezes não, mas que fazem parte da cultura do grupo e desse sentimento de coletividade que encontrei no BIOSE e pelo qual ele também é conhecido e que certamente também fizeram parte do meu crescimento profissional.

Por fim, agradeço aos demais professores do PEQ e EQ, à Coordenação do PEQ e aos representantes discentes, que contribuíram para o andamento do meu trabalho. Agradeço também ao apoio financeiro da Coordenação de Aperfeiçoamento de Pessoal de Nível Superior (CAPES), ao Conselho Nacional de Desenvolvimento Científico e Tecnológico (CNPq), à Fundação de Amparo à Pesquisa do Estado do Rio de Janeiro – FAPERJ e à Petrobras.

Resumo da Tese apresentada à COPPE/UFRJ como parte dos requisitos necessários para a obtenção do grau de Doutor em Ciências (D.Sc.)

PRODUÇÃO DE LIPASE POR *YARROWIA LIPOLYTICA* COM CASCA DE SOJA EM BIORREATORES DE BANDEJA E LEITO EMPACOTADO: ESTUDOS EXPERIMENTAIS E MODELAGEM DO PROCESSO

Felipe Valle do Nascimento

Junho/2021

Orientadores: Argimiro Resende Secchi
Maria Alice Zarur Coelho
Aline Machado de Castro

Programa: Engenharia Química

Este trabalho teve como objetivo a produção de lipase por *Yarrowia lipolytica* na fermentação no estado sólido de casca de soja. Meios definidos e complexos foram testados como suplementação para produção de lipase em biorreator de bandeja e leito empacotado (BLE). Com os dados de temperatura, lipase e protease adquiridos com BLE, equações de balanço de massa e energia foram implementadas visando a descrição matemática do processo. Além disso, uma rotina computacional para processar imagens de casca de soja foi desenvolvida para determinação do diâmetro de partícula. Os resultados da investigação da suplementação de meio indicaram que a produção de lipase foi maior com meios complexos e atingiu 1,35 kU L^{-1} com o meio contendo extrato de levedura, bactopeptona e óleo de soja. Neste caso, a temperatura do leito no BLE atingiu 35 °C, o que pode ter influenciado a produção de proteases e lipases. Modelos de distribuição de tamanho de partícula foram ajustados aos dados obtidos com a rotina de processamento digital de imagens e o diâmetro equivalente foi melhor descrito pelo modelo Sigmóide. Finalmente, simulações foram realizadas e valores do número de Nusselt (Nu) menores do que os calculados com correlações para uma esfera foram necessários na simulação. Uma análise de sensibilidade paramétrica indicou que a atividade de água na entrada (a_{w_0}) teve influência mais relevante no modelo. Portanto, esses dois parâmetros foram estimados e o valor de Nu foi $3{,}96\times10^{-4} \pm 7{,}33\times10^{-5}$, enquanto a_{w_0} não apresentou significância estatística. Os resultados finais da simulação foram consistentes com os dados experimentais em relação aos picos de temperatura e produção de lipase.

Abstract of Thesis presented to COPPE/UFRJ as a partial fulfillment of the requirements for the degree of Doctor of Science (D.Sc.)

LIPASE PRODUCTION BY *YARROWIA LIPOLYTICA* WITH SOYBEAN HULLS IN TRAY AND PACKED-BED BIOREACTORS: EXPERIMENTAL STUDIES AND PROCESS MODELING

Felipe Valle do Nascimento

June/2021

Advisors: Argimiro Resende Secchi
Maria Alice Zarur Coelho
Aline Machado de Castro

Department: Chemical Engineering

This study aimed at lipase production by *Yarrowia lipolytica* in solid-state fermentation (SSF) of soybean hulls. Defined and complex media were tested as supplementation for lipase production in tray and packed-bed bioreactor (PBB). With the temperature, lipase and protease data acquired from PBB fermentations, energy and mass balance equations were implemented aiming at the mathematical process description. Also, a computational routine to process soybean hull images was developed for particle diameter determination. The results from medium supplementation investigation indicated that lipase production was higher with complex media and reached 1.35 kU L^{-1} with the medium containing yeast extract, bactopeptone and soybean oil (YPO). In this case, the bed temperature in the PBB reached 35 °C, which may have influenced protease and lipase production. Size distribution models were fitted to the data obtained with the digital image processing routine, and the equivalent diameter was better described by the Sigmoid model. Finally, simulations were performed and the Nusselt number (Nu) values smaller then those calculated with single sphere correlations were required in the simulation. A parameter sensitivity analysis indicated that the inlet water activity (a_{w_0}) had the most relevant influence on the model, Therefore, these two parameters were estimated. The value for Nu was $3.96\times10^{-4} \pm 7.33\times10^{-5}$, while a_{w_0} presented no statistical significance. The final simulation results were consistent with experimental data in terms of peak temperatures and lipase production.

Contents

List of Figures **xii**

List of Tables **xv**

List of Symbols **xvii**

List of Abbreviations **xxiii**

1 Introduction **1**

1.1 Motivation 1
1.2 Goals 3
1.3 Thesis structure 4
1.4 Publications 4

2 Literature Review **5**

2.1 Lipases 5
2.2 *Yarrowia lipolytica* 9
2.2.1 General features of *Yarrowia lipolytica* 9
2.2.2 Lipase and protease production by *Yarrowia lipolytica* in solid-state fermentation 11
2.2.3 Regulation and characteristics of lipases and proteases from *Yarrowia lipolytica* 15
2.3 Solid-state fermentation 22
2.3.1 Cell analysis in solid-state fermentation 22
2.3.2 Solid matrix - soybean hulls production and characteristics . . 25
2.3.3 Bioreactors in solid-state fermentation and modeling of the process 30

3 Characterization of the soybean hulls and lipases **38**

3.1 Soybean hull analysis 38
3.1.1 Introduction 38
3.1.2 Material and methods 39

3.1.3 Results . . . 41
3.2 Lipase activity assays . . . 46
3.2.1 Introduction . . . 46
3.2.2 Material and methods . . . 48
3.2.3 Results . . . 49

4 Production of lipase by *Y. lipolytica* by solid-state fermentation of soybean hulls 53
4.1 Preliminary experimental development . . . 53
4.1.1 Material and methods . . . 53
4.1.2 Results and discussion . . . 59
4.2 Insights into media supplementation in solid-state fermentation of soybean hulls by *Yarrowia lipolytica*: impact on lipase production in tray and insulated packed-bed bioreactors . . . 67
4.2.1 Abstract . . . 67
4.2.2 Introduction . . . 68
4.2.3 Material and methods . . . 70
4.2.4 Results and discussion . . . 74
4.2.5 Conclusions . . . 86

5 Thermal and growth modeling of lipase production in insulated packed bed bioreactor with *Yarrowia lipolytica* 87
5.1 Mathematical model description . . . 88
5.1.1 Model simulation . . . 94
5.1.2 Sensitivity Analysis and Parameter Estimation . . . 94
5.2 Results . . . 95
5.2.1 Base case simulation . . . 95
5.2.2 Sensitivity analysis and parameter estimation . . . 99

6 Conclusions and perspectives 104
6.1 Suggestions for future work . . . 105

References 106

List of Figures

1.1 Accumulated number of articles published per year in Scopus assessed on January 18 2021 2

2.1 Mechanism of hydrolysis catalyzed by lipases. 6
2.2 Schematic representation of the action mode of lipases and esterases. 8
2.3 Structure of the main lipase (Lip2p) from *Yarrowia lipolytica*. 17
2.4 Distribution of the total amount of soybeans produced in 2019 in Brazil (left) and global production share (right). 26
2.5 Simplified steps of soybean processing. 27
2.6 Water isotherms of soybean (a), soybean meal (b) and soybean cellan (c). 29

3.1 Steps of digital image analysis implemented on Matlab R2008a (The Mathworks, Natick, Mass.) used for soybean hull shape and size determination. 39
3.2 Digital images obtained by bright-filed optical microscopy at a total of 40 x magnification of soybean hulls after autoclave sterilization and their binary versions after automatic image processing. 42
3.3 Cumulative distributions of length, width, equivalent diameter, aspect ratio and roundness of soybean hulls ($0.5<d_P<1.18$ mm) after heat sterilization in autoclave. 43
3.4 Absorption spectra for 4-nitrophenol solutions at different buffered solutions. 47
3.5 Absorbance of the blank (enzyme replaced by buffer) in the presence of the mixture of Triton X-100 (detergent/solvent) and DMSO. 49
3.6 Lipase activity in the presence of the mixture of Triton X-100 (detergent/solvent) and DMSO in various 4-nitrophenyl dodecanoate concentrations bulk concentrations. 51
3.7 Lineweaver-Burk plots of lipase activity *versus* Triton X-100 concentration for various 4-nitrophenyl dodecanoate bulk concentrations. . . 52

4.1 Fixed-bed bioreactors used for solid-state fermentation. In the center, the insulated packed-bed bioreactor with a vacuum-sealed jacket is filled with soybean hulls. 56
4.2 Temperature profiles measured at two different radii for fermentation of soybean hulls in insulated packed-bed bioreactors (PBB). 59
4.3 Enzymes (a), *N*-acetylglucosamine and pH (b) profiles observed in packed-bed bioreactor fermentation of soybean hulls by *Yarrowia lipolytica* IMUFRJ 50682 for the heights 7 (diamond), 14 (square) and 21 (triangle) cm from the bottom of the bioreactor. 60
4.4 Enzymes (a), *N*-acetylglucosamine and pH (b) profiles observed in tray (polyproylene beaker) bioreactor fermentation of soybean hulls by *Yarrowia lipolytica* IMUFRJ 50682. 60
4.5 *N*-acetylglucosamine content, pH (a), and enzyme (lipase and protease) activities (b) for tray bioreactor (polypropylene beakers) fermentation of soybean hulls with 1.5 % g g^{-1} glucose (white bars and squares), ammonium phosphate and glucose (gray bars and diamonds) and soybean oil (control, black bars and cross) by *Y. lipolytica* IMUFRJ 50682. 62
4.6 Lipase (hydrolytic) activity (bars) and pH for tray bioreactor (glass bottles) fermentation of soybean hulls with 1.5 % g g^{-1} supplementation of carbon (a) and nitrogen (b) sources, including glycerol (gray bars and diamonds), glucose (white bars and squares) and soybean oil (black bars and triangles), urea (gray bars and diamonds), diammonium phosphate (white bars and squares) and sodium nitrate (black bars and triangles) by *Y. lipolytica* IMUFRJ 50682. 63
4.7 Schematic representation of the insulated packed-bed bioreactor. . . . 72
4.8 Lipase (bars) and protease (marks) activity (A, C) and pH (marks) (B, D) profiles for fermentation of soybean hulls supplemented with different complex (left column) and defined (right column) medium in tray bioreactors. 75
4.9 Lipase (bars), protease (void marks), pH (grey marks) (A, B, and C) and temperature profiles measured at two different radii (D,E, and F) for fermentation of soybean hulls in tray and insulated packed-bed bioreactors (PBB) supplemented with different complex medium (YPD: A and D; YPDO: B and E; YPO: C and F). 78
4.10 Figure 4. Axial temperature (monitored at two radii) and moisture profiles (measured after solid sampling) for fermentation of soybean hulls in insulated packed-bed bioreactors supplemented with different complex medium at various moments of the bioprocess. 81

5.1 Gas and solid temperatures, gas and solid moisture content for the base case at different radii. 96
5.2 Gas (A,B) and solid (C,D) temperatures, gas (E,F) and solid (G,H) moisture content for $Nu = 0.0001$ at different radii. 98
5.3 Heat map for the normalized sensitivity of different variables towards the physical parameters Nu, ϵ_0, a_{w0}, and α_{wall} at different radii for the simulation of lipase production by *Y. lipolytica*. 99
5.4 Gas (A, B) and solid (C, D) temperatures, gas (E, F) and solid (G, H) moisture content after parameter estimation at different radii. . . 101
5.5 Cell (A, C) and LIpase (B, D) calculated values after parameter estimation at different radii. 102
5.6 Temperature (A, C), solid moisture content (B) and lipase (D) data from experiments (symbols) and the model (lines). 102

List of Tables

2.1 Morphology responses of *Yarrowia lipolytica* to different environmental conditions. 10
2.2 Main process conditions used for solid-state cultivation of *Yarrowia lipolytica* strains. 12
2.3 Compilation of general features of lipases from *Yarrowia lipolytica*. . 18
2.4 Composition of soybean hull and meal.* 27
2.5 Empirical growth equations used in models of solid-state fermentation. 32

3.1 Parameters for the cumulative distribution fit of length (l), width (w) and equivalent diameters (d_{eq}). 41
3.2 Bulk densities and porosity for different packing techniques of soybean hulls. 44
3.3 Elemental composition and moisture content of soybean hulls. 46
3.4 Volume fraction of DMSO and Triton X-100 used in the enzyme assays development. The calculation was made on the basis of 20 μL stock substrate solution 48

4.1 Solid-state fermentation bioreactors used in this work. 55
4.2 Central composite orthogonal rotational design (CCORD) for evaluation of humidity, carbon and nitrogen sources for lipase production by *Yarrowia lipolytica*. 58
4.3 Lipase activity obtained after 14 h of fermentation of soybeans hulls by *Y. lipolytica* IMUFRJ 50682 in glass bottles for a central composite orthogonal rotational experimental design. Values in parenthesis represent the coded variables used for analysis in the software Statistica 7.0. 65
4.4 Assay conditions for complex and defined media formulation for lipase production by *Yarrowia lipolytica*. 71
4.5 General design characteristics of solid-state fermentation bioreactors. 72
4.6 Responses obtained for the fermentation of soybean hulls supplemented with either complex or defined media 79

4.7 Compilation of main results for lipase production by solid-state fermentation. 84

5.1 Parameters used for the simulation of *Y. lipolytica* growth, temperature and lipase production in solid-state fermentation of soybean hulls. 92

List of Symbols

A	Frequency factor, p. 33
AR	Particle aspect ratio, p. 40
B	Frequency factor, p. 33
Bi	*Biot* number, p. 34
C_{p_a}	Air heat capacity, p. 33
C_{p_b}	Bed heat capacity, p. 33
C_{p_s}	Solid heat capacity, p. 34
C_{p_w}	Water heat capacity, p. 36
$C_{p_{vap}}$	Vapor heat capacity, p. 35
D_0	Constant for water activity-dependent specific cell growth rate calculation, p. 33
D_1	Constant for water activity-dependent specific cell growth rate calculation, p. 33
D_2	Constant for water activity-dependent specific cell growth rate calculation, p. 33
D_3	Constant for water activity-dependent specific cell growth rate calculation, p. 33
D_4	Constant for water activity-dependent specific cell growth rate calculation, p. 33
D_g	Water molecular diffusivity in the air, p. 90
D_s	Water dispersion coefficient in the solid, p. 36
$D_{Feret_{max}}$	Particle maximum Feret diameter, p. 39

$D_{Feret_{min}}$	Particle minimum Feret diameter, p. 40
D_{eq}	Particle equivalent diameter, p. 40
$D_{g,r}$	Gas effective mass dispersion coefficient in the radial direction, p. 36
$D_{g,z}$	Gas effective mass dispersion coefficient in the axial direction, p. 36
D_{red}	Reduced packed-bed mass transfer coefficient, p. 90
E	Enzyme bulk concentration, p. 7
EMC	Equilibrium moisture content, p. 28
E_A	Energies for thermal activation of internal components of cells, p. 33
E_D	Energies for thermal denaturation of internal components of cells, p. 33
F_{obj}	Objective function of the paramter estimation, p. 94
K_S	Dissociation constant for the surface, p. 7
K_M	Michaelis-Menten constant, p. 7
L	Bioreactor length, p. 34
L_{as}	Fraction of active segments, p. 32
Lip	Lipase activity, p. 73
MC	Moisture content, p. 54
MC_{adj}	Desired moisture content after adjustment, p. 55
MC_{sample}	Actual moisture content of the sample, p. 55
N	Constant, p. 90
Nu	*Nusselt* number, p. 91
P	Particle perimeter, p. 40
P	Pressure, p. 93
Pe_{0_T}	Thermal molecular *Péclet* number, p. 91

Pe_{0_m}	Mass molecular *Péclet* number, p. 90
Q_{Lip}	Lipase productivity, p. 73
R	Bioreactor Radius, p. 34
R_g	Universal gas constant, p. 33
Rd	Particle roundness, p. 40
Re_p	*Reynolds* number of the particle, p. 91
S	Total dry solid concentration, p. 35
S_{bulk}	Substrate bulk concentration, p. 7
$S_{surface}$	Substrate surface concentration, p. 7
S_{total}	Total surface, p. 7
Sh	*Sherwood* number, p. 91
T	Temperature, p. 28
T_g	gas temperature, p. 35
T_s	Solid temperature, p. 35
T_∞	Temperature of surroundings, p. 34
T_{g_0}	Gas initial temperature, p. 93
T_{g_i}	Inlet gas temperature, p. 34
T_{opt}	Temperature optimum value for growth, p. 33
T_{s_0}	Solid initial temperature, p. 93
$V_{extraction}$	Extractant volume, p. 73
X	Solid moisture content, p. 35
Y	Moisture content of the air, p. 35
Y^*	Saturation moisture content of the air, p. 35
Y_H	Heat yield, p. 33
Y_w	Yield of water on biomass, p. 35

$Y_{B/Glu}$	Biomass yield on glucose, p. 92
$Y_{P/Glu}$	Lipase yield on biomass, p. 92
ΔH_{vap}	Enthalpy of water evaporation, p. 33
$\Lambda_{g,r}$	Gas effective radial thermal conductivity, p. 36
Λ_{red}	Reduced packd-bed heat transfer coefficient, p. 90
α_{wall}	Heat transfer coefficient between the gas and the wall, p. 90
β	Interfacial mass transfer coefficient, p. 35
$\dot{\nu}(X)$	Normalized drying rate, p. 35
ϵ_0	Bed porosity, p. 33
γ_D	Frequency factor for denaturation of the physiological factor, p. 31
γ_S	Frequency factor for synthesis of the physiological factor, p. 31
λ_s	Solid-state stagnant thermal conductivity, p. 36
$\lambda_{g,z}$	Gas effective axial thermal conductivity, p. 36
λ_g	Molecular thermal conductivity of the air, p. 90
μ	Specific cell growth rate, p. 31
μ_T	Temperature-dependent specific cell growth rate, p. 33
μ_W	Water activity-dependent specific growth rate, p. 33
$\mu_{T_{opt}}$	Specific growth rate at optimum temperature, p. 33
μ_{opt}	Optimum specific growth rate, p. 33
ν_{air}	Air viscosity, p. 91
$\overline{r}$	Dimensionless radial coordinate, p. 88
$\overline{z}$	Dimensionless axial coordinate, p. 88
ϕ	Physiological factor, p. 31
$\psi_{j,t}$	j-th calculated process variable, p. 94
ρ_a	Air density, p. 33

ρ_b Bed density, p. 33

ρ_s Solid density, p. 33

ρ_{ds} Dried bulk density, p. 40

ρ_{ws} Wet bulk density, p. 40

$\tilde{\psi}_{j,t}$ Experimental value of the j-th process variable, p. 95

ξ_i Variation of parameter i-th used in sensitivity analysis, p. 94

a Interfacial area, p. 35

a_W Water activity, p. 28

b Cell mass, p. 32

b_0 Initial cell concentration, p. 93

b_T total cell mass, p. 32

b_{max} Maximum cell mass, p. 32

b_v Viable cell mass, p. 32

d_P Particle diameter, p. 39

f Water carrying capacity, p. 33

f_{deform} Deformation parameter, p. 90

f_{shape} Particle shape factor, p. 90

h Interfacial heat transfer coefficient, p. 35

k_D First order death decay constant, p. 32

k_a Air thermal conductivity, p. 34

k_a First order decay constant for the fraction of active segments, p. 32

k_b Bed thermal conductivity, p. 33

k_c Reduced thermal conductivity of the core unit cell, p. 90

k_p Reduced thermal conductivity of the particle, p. 90

k_s Solid thermal conductivity, p. 34

k_{cat}	Catalytic turnover, p. 7
l	Particle length, p. 39
m	Constant of the size distribution model, p. 40
m_{ds}	Dried mass of the solid sample, p. 55
$m_{inoculum}$	Mass of the inoculum solution, p. 55
m_{liq}	Mass of liquid in the solid material, p. 55
$m_{supplementation}$	Mass of the supplementation solution, p. 55
m_{ws}	Wet mass of the solid sample, p. 55
n_1	Exponent of weight function, p. 94
n_2	Exponent of weight function, p. 94
n_T	Sensitivity of the specific growth rate to temperature, p. 33
p_i	Parameter i-th of the model, p. 94
r	Radial direction, p. 33
s	Particle evaluated property (length, width or equivalent diameter), p. 40
$s_{i,j,t}$	Sensitivity of the j-th process variable calculated at the time t to the i-th parameter, p. 94
$s^*_{i,j,t}$	Normalized sensitivity of the j-th process variable calculated at the time t to the i-th parameter, p. 94
t	time, p. 32
t_a	time when deceleration phase begins, p. 32
t_f	Fermentation time when maximum lipase activity was measured, p. 73
v_z	Axial gas superficial velocity, p. 33
w	Particle width, p. 40
$w(x)$	Weight function, p. 94
y	Cumulative count, p. 40
z	Axial direction, p. 33

List of Abbreviations

AEP	Alkaline Extracellular Protease, p. 21
ANOVA	Analysis of Variance, p. 66
ATCC	American Type Culture Collection, p. 12
AXP	Acidic Extracellular Protease, p. 21
BET	Brunauer-Emmet-Teller, p. 28
CBLF	Cell-bound lipase fraction, p. 16
CCORD	Central Composite Orthogonal Rotational Design, p. 59
CCRD	Central composite rotational designs, p. 15
CECT	Coleccion Española de Cultivos Tipo, p. 12
CMC	Critical Micelar Concentration, p. 7
CM	Complex Medium, p. 68
D.W.	Dry Weight, p. 28
DMSO	Dimethyl Sulfoxide, p. 18
DM	Defined Medium, p. 68
DNA	Deoxyribonucleic acid, p. 23
E.C.	Enzyme Commission Number, p. 5
EDTA	Ethylenediaminetetraacetic acid, p. 19
EMSO	Environment for Modeling, Simulation and Optimization, p. 4
GGS	Gates–Gaudin–Schumann, p. 40
GRAS	Generally Regarded As Safe, p. 70

HXK1	Hexokinase-1 gene, p. 16
LIP2	Triacylglycerol lipase 2 gene, p. 16
Lip2p	Triacylglycerol lipase 2, p. 16
Lip7p	Triacylglycerol lipase 7, p. 16
Lip8p	Triacylglycerol lipase 8, p. 16
NBIMCC	National Bank for Industrial Microorganisms and Cell Cultures, p. 62
NCIM	National Collection of Industrial Microorganisms, p. 12
NCYC	National Collection of Yeast Cultures, p. 13
NRBC	NITE Biological Research Center, p. 12
NRRL	Agricultural Research Service Culture Collection, p. 12
PBB	Packed-bed Bioreactor, p. 59
PET	Polyethylene terephthalate, p. 15
POPG	1-palmitoyl-2-oleoyl-sn-glycero-3-phosphoglycerol, p. 9
RIM/Pal	Signal Transduction Pathway Responsive to pH genes, p. 21
RRB	Rosin–Rammler–Bennett, p. 40
SEM	Scanning Electron Microscopy, p. 45
SEP	Solid enzymatic preparation, p. 15
SOA	Specific for Oleic Acid gene, p. 16
SSF	Solid-State Fermentation, p. 19
SmF	Submerged Fermentation, p. 16
W.S.	Wet Solids, p. 67
XPR2	Alkaline Extracellular Protease gene, p. 21
YNB	Yeast Nitrogen Base, p. 21
YPDO	Yeast Peptone Dextrose Soybean oil, p. 68
YPD	Yeast Peptone Dextrose, p. 54

YPO	Yeast Peptone Soybean oil, p. 68
p-NPC$_X$	p-nitrophenyl alkanoate with X carbons in the acyl chain, p. 18
aa	amino acid, p. 18
cAMP	cyclic adenosine monophosphate, p. 10
mRNA	Messenger Ribonucleuc Acid, p. 21

Chapter 1

Introduction

1.1 Motivation

Lipases are enzymes that, in aqueous or non-aqueous media, act on water-insoluble substrates mainly catalyzing reactions on carboxyl ester bonds (STAUCH *et al.*, 2015), such as hydrolysis, aminolysis and (trans)esterifications (FATIMA *et al.*, 2020). Therefore, they have a broad substrate specificity and are "promiscuous", since they also catalyze reactions other than their natural physiological ones (GUPTA, 2016). These characteristics and the fact that they were available very early in industry for use in fat splitting make them be applied in biotechnology in the most diverse industries (KAPOOR and GUPTA, 2012).

The global market of enzymes is majorly represented by carbohydrolases, proteases and lipases (in decreasing order of market share relevance), and it was estimated at US$ 5-5.5 billion in 2016 (GUERRAND, 2017), and around US$ 7 billion in 2019 (ARBIGE *et al.*, 2019). In 2015, a technological forecast in four sectors of lipase application (namely kinetic resolution, detergent formulation, food technology and biodiesel production) indicated a potential for expansion in these industrial sectors, except for the resolution of enantiomers, which seemed to still be attractive in academic research at that moment (DAIHA *et al.*, 2015).

Fungi and bacteria are known to produce lipases. In some cases, the fungal lipases are secreted, which is advantageous for production purposes (MEUNCHAN *et al.*, 2015). In solid-state fermentation processes, residues from oleaginous cultures are preferable, once they may already have some lipid content that acts as inducers for lipase production. Residues from soybean (*Glycine max*), olive (*Olea europaea*), and other systems could be employed (SALIHU *et al.*, 2012). When the residues lack any component for microbial development, medium supplementation can also be used to fulfill these requirements.

Yarrowia lipolytica is a non-conventional (non-*Saccharomyces*) yeast known for

secreting large amounts of lipases (either the wild-type or the genetically modified strains). This yeast is of great interest in diversified fields of scientific development (NICAUD, 2012). A research for papers related to this yeast was performed in the Scopus platform for this work and evidenced the increasing number of publications (2740 search results until the end of 2020, Figure 1.1). Since 2003, lipase production in solid-state fermentation has received some attention, accounting for 0.55 % of total publications, and typically being conducted in tray bioreactors.

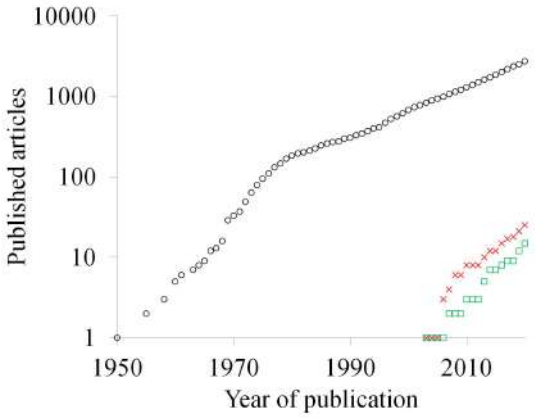

Figure 1.1: Accumulated number of articles published per year in Scopus assessed on January 18 2021 using the search keywords "lipolytica and (candida or yarrowia)" (black dots), "lipolytica and (candida or yarrowia) and (("solid state fermentation") or ("solid state culture") or ("solid-state fermentation") or ("solid-state culture")" (red crosses) and "lipolytica and (candida or yarrowia) and (("solid state fermentation") or ("solid state culture") or ("solid-state fermentation") or ("solid-state culture")) and lipase" (green squares) for abstract search.

Industrial use of solid-state fermentation could be of great interest within countries which benefit from the availability of large amounts of agro-industrial residues, such as Brazil. These are low-cost materials, which aid at process economical viability (CASTILHO *et al.*, 2000). Process scale-up using tray bioreactors require high surface (ARORA *et al.*, 2018), which make packed-bed bioreactors promising. For these bioreactors, mathematical models describing two-phase and two-dimensional heat and mass transfer have been developed for filamentous fungi (CASCIATORI *et al.*, 2016), but they have never been used to describe this type of bioprocess with *Y.lipolytica*.

Soybean hulls are the first products obtained during soybean processing, once it is removed from the seeds before oil extraction and meal processing (DE PRETTO *et al.*, 2018). Their composition varies in a large range, as seen in Table 2.4, because it depends on local and seasonal growing conditions and the treatments applied to it LOMAN and JU (2016). Some applications are being investigated despite its main use for animal feed and include the use as adsorbents, extraction of naturally existing peroxidases, feedstock in bioprocesses, and pectin extraction (DE PRETTO

et al., 2018).

The low lignin content is a very attractive characteristic for the use of this major source of carbohydrates as fermentable sugars (LOMAN and JU, 2016). Thus they have have been used for cultivation of several fungi aiming the production of cellulolytic enzymes by *Trichoderma reesei*, *Aspergillus oryzae*, and *Phanerochaete chrysosporium* with corn residue (YANG *et al.*, 2012); by *A. niger* with waste paper (JULIA *et al.*, 2016); *T. reesei* and *A. oryzae* with wheat bran (BRIJWANI *et al.*, 2010) or without it (BRIJWANI and VADLANI, 2011); lipids by *Mortierella isabellina* (ZHANG and HU, 2012); monacolin K and isoflavones by *Monascus pilosus* (SIMU *et al.*, 2018); oxygenase by *Funalia trogii* with wheat bran (DEVECI *et al.*, 2004); and peptidase by *A. niger* with orange peels (LÓPEZ *et al.*, 2018). The hulls had not been studied with the yeast *Yarrowia lipolytica* before, only the meal and oil.

Thus, the present work investigated a solid-state system for production of lipases by *Yarrowia lipolytica* in packed-bed bioreactors, which could be scaled-up to pilot or industrial scale. For this purpose, analytical tools, medium supplementation strategies and mathematical models were studied.

1.2 Goals

The purpose of this thesis is to investigate medium supplementation for the production of lipase by *Yarrowia lipolytica* in solid-state fermentation of soybean hulls in a packed-bed bioreactor, and mathematically describe the process by means of heat and water mass balances. The specific objectives of this work are:

- to adapt the available digital image analysis tool for the quantification and characterization of the soybean hulls in a less subjective manner;
- to study different medium supplementation strategies to provide conditions for increased growth and lipase production using soybean hulls as agroindustrial residue;
- to obtain experimental data of lipase production by *Y. lipolytica* in packed-bed bioreactor;
- to propose a mathematical model for the packed-bed bioreactor based on mass and energy balances and estimate the model parameters with the available experimental data.

1.3 Thesis structure

The thesis has been structured in 6 chapters.

This chapter presents the motivation, goals and communications (papers and conferences) resulting from this thesis. The Chapter 2 provides the reader with a summary of information regarding the main aspects of the yeast *Y. lipolytica*, the lipases and how they have been investigated with this yeast in the area of solid-state fermentation from a temporal evolution perspective, focusing on the most relevant topics. This logic was also used to explore the mathematical models used in this type of process in the second part of the literature review.

The Chapters 3 to 5 present the results obtained through the development of this work. In Chapter 3, analytical developments are discussed, which were performed in parallel to provide useful information required for Chapters 4 and 5. The Chapter 4 covers experimental results of lipase production in both tray and packed-bed bioreactors, focusing on media supplementation. Chapter 5 presents the results of simulations performed in the software EMSO (Environment for Modeling, Simulation and Optimization)(SOARES and SECCHI, 2003).

Finally, in Chapter 6, the main conclusions of this thesis are presented and new lines of investigation for future work are proposed.

1.4 Publications

The following works resulted from this thesis:

- Investigation of bioreactors and supplementations for lipase production in solid-state fermentation of soybean hulls by Yarrowia lipolytica. XXII National Bioprocesses Symposium (SINAFERM) XIII Enzymatic Hydrolysis of Biomass Symposium (SHEB), 2019 (ISSN: 2447-2816);

- Insights into media supplementation in solid-state fermentation of soybean hulls by *Yarrowia lipolytica*: Impact on lipase production in tray and insulated packed-bed bioreactors. Biochemical engineering Journal, Volume 166, February 2021(https://doi.org/10.1016/j.bej.2020.107866);

Chapter 2

Literature Review

2.1 Lipases

Lipases belong to the group of enzymes characterized as serine hydrolases (triacylglycerol acyl hydrolases, E.C. 3.1.1.3)(MEUNCHAN *et al.*, 2015) and are relevant for industrial use mainly due to their selectivity. They are resistant to organic solvents, catalyze synthesis reactions (FICKERS *et al.*, 2011) and act on diverse substrates with varying reaction rates (REIS *et al.*, 2009). They also allow the design of molecules with specific functional and nutritional properties (PAIVA *et al.*, 2000).

KAPOOR and GUPTA (2012) summarized the following five structural features found in lipases based on the available X-ray cristallographic data:

- They belong to the $\alpha\beta$-hydrolase fold family;
- A conserved catalytic triad made of the amino acids serine, histidine and aspartic/glutamic acid;
- A "nucleophilic elbow", where the nucleophilic serine is found between an α helix and a β strand (except for Lipase B from *Candida antarctica*);
- A structural motif (lid or flap) covering the catalytic site;
- An oxyanion hole and three pockets for fatty acids (for triglycerides).

The lid is a mobile motif that controls the substrate molecules access to the catalytic pocket (BORDES *et al.*, 2010) and some of their characteristics can be predicted by their structure, making them a target for protein engineering (KHAN *et al.*, 2017). However, its presence is controversial. KHAN *et al.* (2017) classified a selected group of lipases from the Protein Data Bank according to their lid domain. In their classification, lipases may or may not present lids, with one, two

or more loop/helices. The authors also concluded that higher optimal temperature were related to larger lids, while small loop/helix lids were found in all mono- and diacylglycerol lipases.

The catalytic activity of lipase is dependent on changes of the enzyme and substrate conditions. The interfacial activation commonly observed in lipases is the result of combined effects of the amino acid composition of the lid (and therefore the structure resulting from interactions with the environment) and the properties of the interface (such as the dieletric constant and ionic strength) (STAUCH *et al.*, 2015). The enzyme undergoes rearrangements at an water-oil interface upon exposure to a less polar solvent, making the catalytic site available for substrate access (SKJOLD-JØRGENSEN *et al.*, 2016). The exception to this is the lipase B from *Candida antartica*. Although it presents lids with open and closed structures confirmed, the activation seems to be dependent on pH and associated to a unusual mechanism (STAUCH *et al.*, 2015). Despite that, conformational changes in response to the environment are still responsible for its activation.

The mechanism of action in hydrolysis reaction (Figure 2.1) requires the action of the three amino acid residues found in the conserved catalytic triad: histidine and aspartic/glutamic acid activate the hydroxyl group of serine, which in turn attacks the substrate carbonyl, forming a stable tetrahedral intermediate stabilized by the oxianion hole residues (Figure 2.1 a). Next, an available nucleophile (found at the interface) proceeds with the deacylation step (Figure 2.1 b), leading to product formation and enzyme regeneration (Figure 2.1 c) (REIS *et al.*, 2009).

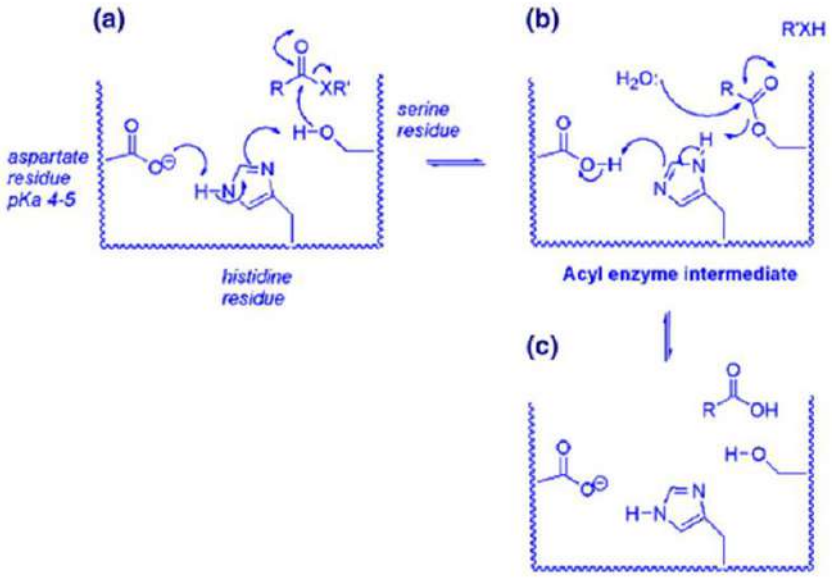

Figure 2.1: Mechanism of hydrolysis catalyzed by lipases (REIS *et al.*, 2009).

The key feature that differentiate esterases from lipases is that esterases act on water soluble substrate (REIS *et al.*, 2009), which is relevant for enzyme identifica-

tion, given that simultaneous production of these enzymes are possible. Figure 2.2 shows a scheme with the differences between the curve of activity *versus* substrate concentration for lipases and esterases.

Esterases show activity before the critical micelar concentration (CMC) and may be produced concomitantly with lipases. The later acts majorly after interaction with an interface, after structural rearrangement to reach an active conformation (SKJOLD-JØRGENSEN *et al.*, 2016), therefore the reaction media may be formulated differently to favor either types of enzymatic activity. Detergents may be used to form mixed-micelles structures may not not interfere on enzyme activity if they do not interact with the enzyme (DEEMS, 2000). In contrast, if enzyme-detergent interaction occurs, this can result in enzyme inhibition or denaturation. In addition, anything that alters the properties or the size of the surface may alter the reaction rates. For instance, smaller droplets are logically beneficial for higher reaction rates (YAO *et al.*, 2013) and calcium ions tend to neutralize negative charges maintaining a low dieletric constant at the interface (SKJOLD-JØRGENSEN *et al.*, 2016).

As esterases show no interfacial activation, their reaction rates may be described by Michaelis-Menten equations, as shown in Equation 2.1(REIS *et al.*, 2009), considering that water is an excess reagent in the reaction. In this case, S_{bulk} is the substrate bulk concentration (mol L^{-1}), E is the enzyme concentration (g L^{-1}), k_{cat} is the catalytic turnover (min^{-1}), and K_M is the Michaelis-Menten constant (mol L^{-1}).

$$v = \frac{Ek_{cat}S_{bulk}}{K_M + S_{bulk}} \tag{2.1}$$

In contrast, lipase reaction rates increase considerably after an interface is formed (REIS *et al.*, 2009), and after this, reaction occurs at the two-dimensional space of the interface. Theoretically, substrate concentration should not be calculated in relation to the bulk concentration, but in relation to the surface concentration ($S_{surface}$) (mol $area^{-1}$) or as a mole fraction. The bulk concentration of the surface should also be described, as shown in Equation 2.2 (DEEMS, 2000). This equation represents the two-step process of enzyme sequestration at the interface followed by catalysis.

$$v = \frac{Ek_{cat}S_{total}S_{surface}}{K_SK_M + K_MS_{total} + S_{total}S_{surface}} \tag{2.2}$$

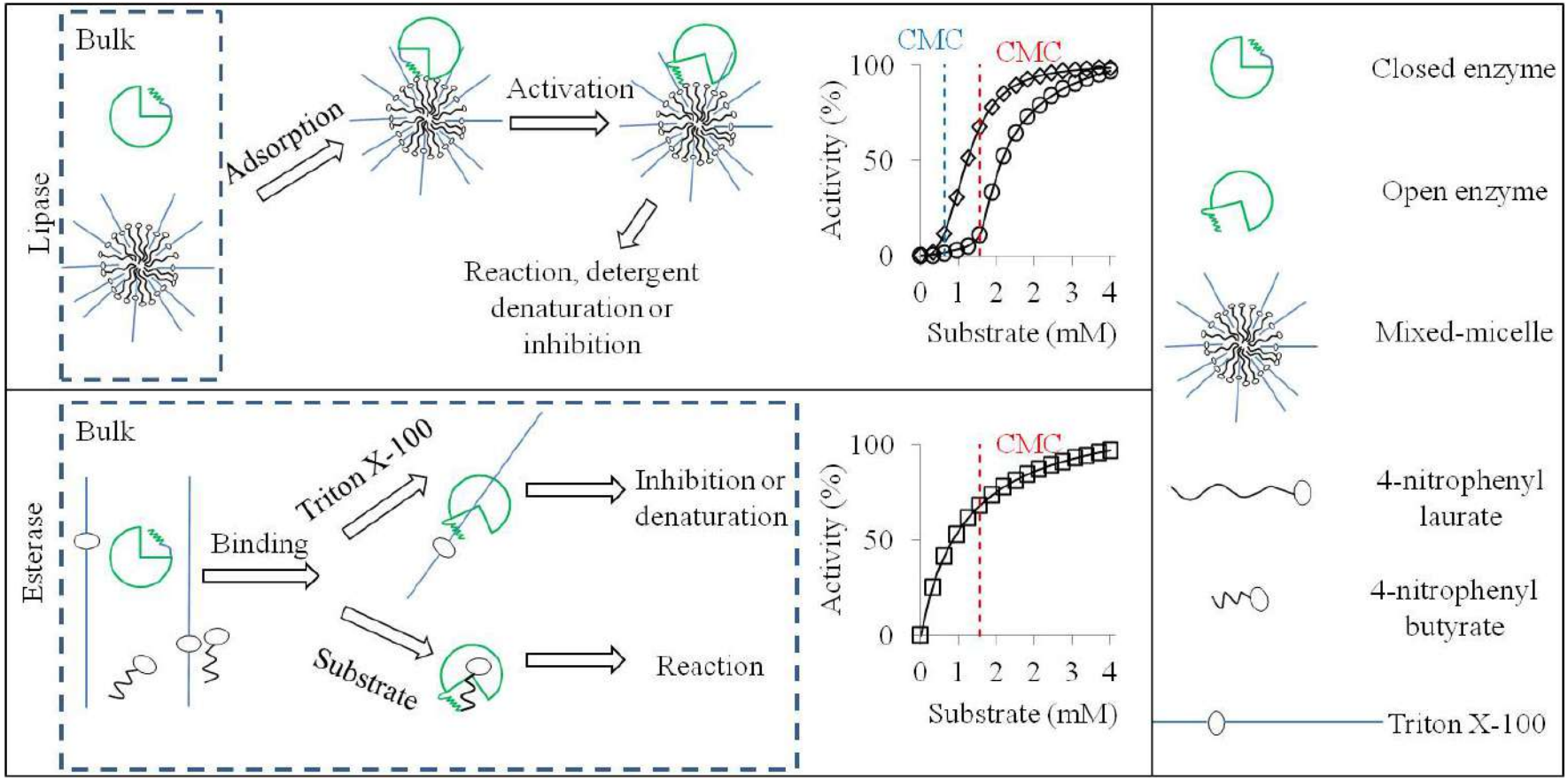

Figure 2.2: Schematic representation of the action mode of lipases and esterases. Lipases show interfacial activation, changing its conformation from closed (inactive) to partially/fully open (active). The graphic depicts the use of substrates with different sizes, where blue represents a bigger acyl chain and activity is shown to increase when substrate concentration is higher than the critical micellar concentration (CMC). In contrast, esterases act on insoluble or soluble substrate, showing no interfacial activation. In the drawings, Triton X-100 is shown to exemplify the formation of mixed micelles. Besides, the interaction between detergent and enzyme is represented, which can inhibit or denature it. Based on DEEMS (2000) and SKJOLD-JØRGENSEN *et al.* (2016).

Here, S_{total} is no longer the substrate bulk concentration, but the total surface available, that is, the sum of bulk molar concentration of the components forming vesicles, micelles or any other type of structure with the substrate that actually interact with the enzyme.K_S is the dissociation constant for the surface and has the same unit as S_{total}. K_M now is shown in the same unit as $S_{surface}$ (DEEMS, 2000). Since the substrate is now diluted in the surface, a solubility value is also expected in this case, limiting the highest values of substrate that can be used in reaction. For instance, BERG *et al.* (1998) found the maximum mole fractions of 0.37 and 0.15 for 4-nitrophenyl butyrate and tributyrin in 1-palmitoyl-2-oleoyl-sn-glycero-3-phosphoglycerol (POPG) vesicles. This equation may also reflect Michaelis-Menten behavior if one fixes the concentration of surfaces and varies the substrate mole fraction and vice-versa. Moreover, inhibition effects may still occur, leading to alterations in the mathematical description.

2.2 *Yarrowia lipolytica*

2.2.1 General features of *Yarrowia lipolytica*

Yarrowia lipolytica, an ascomycete previously known as *Candida lipolytica*, was named Yarrowia after David Yarrow identified it in 1972 and from its relation with hydrophobic substrates consumption. It has emerged as a model for many types of studies, including lipase production, dimorphism, lipid body biogenesis, among others (NICAUD, 2012). The main characteristics for growth have already been described, including protocols for media preparation, genetic manipulations, and environmental conditions such as pH, temperature and oxygen demand, which can be found in the book "Nonconventional Yeasts", edited by Klaus Wolf in 1996 (WOLF, 1996). It has a dedicated chapter for *Y. lipolytica*, written by Gerold Barth and Claude Gaillardin. Other features have been edited in a series of two monographs by Gerold Barth, including its biotechnological applications (BARTH, 2013a), genetics, and physiology (BARTH, 2013b). Therefore, only specific topics will be briefly covered along the text since a deeper description can be found in the literature aforementioned.

As a strict aerobe, aeration is essential to maintain high growth rates as well as appropriate temperature (until 34 °C) and pH (from 3 to 8). Furthermore, these conditions influence the morphology of the cells that can be ovoid, pseudo-hyphae or true (septate) hyphae. Septate hyphae can be millimeters long and 3 to 5 µm in width (BARTH and GAILLARDIN, 1996).

TIMOUMI *et al.* (2018) has recently reviewed how the environmental conditions, namely physicochemical (pH, temperature, dissolved oxygen concentration

and osmotic stress), mechanical (agitation rate and pressure) and nutritional effectors (carbon and nitrogen sources and metal ions), impact over morphology and product (citric acid and lipid) formation. Information about morphology is found in Table 2.1 (once the product of interest is lipase, citric acid or lipids will not be covered). However, the authors state that specific strain behaviors may be determinant and a further study comparing strains in the same conditions need to be performed, especially in controlled bioreactors to observe mono-effector responses. One example that reassures this statement is the observed effect for agitation rates, which has a correlation to dissolved oxygen. BRAGA *et al.* (2015) proposed that the mechanical stress could have induced pseudohypha formation, but oxygen supply was not the same and the medium in the experiment did not have glucose. Thus multiple effectors could have provoked the final results.

Table 2.1: Morphology responses of *Yarrowia lipolytica* to different environmental conditions.

Environmental condition	Effector	Observed effect
Physico-chemical	pH	Controversial observations of ovoid and mycelium forms in acid and neutral values
	Temperature	A decrease in intracellular cAMP*, Heat shock (4 or 37 °C) increases filament formation
	Dissolved oxygen	Limited oxygen favors filament formation, except for glucose-limited conditions
	Osmotic stress	Osmotic stress block hyphae formation in media with *N*-acetylglucosamine and cells become round and smaller, but not in serum.
Mechanical	Agitation rate	Controversial observation regarding mechanical and pneumatical agitation
	Pressure	Until 8 bar no effect is observed (no oxidative stress)
Nutritional	Carbon source	Glucose, N-acetylglucosamine, serum and hydrophobic substrates (oils in general, except for castor oil) induce hyphae formation.
	Nitrogen source	Controversial observations regarding organic and inorganic sources
	Metal ions	Deficiency of Mg^{+2} ($<2x10^{-5}$ M), Fe^{3+} ($<10^{-7}$ M) suppress mycelia development. Controversial reports over Ca^{+2} ions.

*cAMP: cyclic adenosine monophosphate. Adapted from TIMOUMI *et al.* (2018).

For novel processes with immobilization steps, such as the one developed by LI *et al.* (2017), efficient and stable colonization (12 repeated batches with a total process time of 460 hours) of cotton towel was observed, with the same cell

concentrations in free and immobilized cultures, as proven by scanning electronic microscopy, and increased production rates. However, the authors did not define the morphology distribution of immobilized cells. Therefore, it is not clear whether there is a correlation between morphology and production.

More recently, VANDERMIES *et al.* (2018) generated a morphological mutant strain (deletion in the YlHSL1 gene involved in mitotic cell cycle regulation) growing in a pseudohyphal form that could efficiently colonize stainless steel structured packing (98.3 % of attached cells). They emphasized that the yeast was able to attach to the material without an "immobilization step" and total cell concentration was higher, thus for an immobilized-cell process, total time would be reduced and it would be more efficient, as cells could be removed removed.

Studies of morphological transition normally use carbon sources like glucose, *N*-acetylglucosamine and serum to induce a morphological transition in this yeast (PÉREZ-CAMPO and DOMÍNGUEZ, 2001, RUIZ-HERRERA and SENTANDREU, 2002). Besides these, *Y. lipolytica* is able to consume most of the commonly available sugars (glucose, fructose), including hydrophobic substrates, such as alkanes (FICKERS *et al.*, 2005), triacylglycerols, fatty acids, glycerol and acetate (SPAGNUOLO *et al.*, 2018). However, it is not capable of hydrolyzing industrial polymeric raw materials, such as starch, inulin, xylan, cellulose and hemicelluloses, monomeric sugars like xylose, arabinose, rhamnose, and galactose and also molasses. Non-consumption of dimeric polymeric substrates is due to the lack of genes encoding for the enzymes or they are very poorly expressed and synthetic biology tools are of interest to build robust industrial strains (LEDESMA-AMARO and NICAUD, 2016). Nevertheless, despite the efforts to obtain promoters for reliable and reproducible mutations that add desired features to this microorganism, LARROUDE *et al.* (2018) have reviewed the available tools (including 5 genomic-scale metabolic models) and stated that synthetic biology alternatives for strain development are emerging as tools to make *Yarrowia* a model strain, but still need further advances.

2.2.2 Lipase and protease production by *Yarrowia lipolytica* in solid-state fermentation

Among the publications found for solid-state fermentation by *Yarrowia* (Figure 1.1), 60 % were related to lipase production. All of the publications had their experiments performed in Erlenmeyer flasks, Petri-dish plates or slants, being considered as tray bioreactors, except for the work of TRY *et al.* (2018) that employed a forcefully aerated bioreactor. The main characteristics of these processes regarding the vessels and environmental conditions are summarized in Table 2.2. Regardless of the product, temperature choice was mostly 28 or 30 °C, the usual temperature range

for increased growth, while particle diameter was usually smaller than 2 mm. The moisture content, however, greatly varied in the range of 50 to 90 %. When taking into consideration the use of soybean products, Okara has also been used as a source of nutrients by *Yarrowia lipolytica*.

Table 2.2: Main process conditions used for solid-state cultivation of *Yarrowia lipolytica* strains.

Y. lipolytica strain	Product or Process	Temperature (°C)	Initial moisture content (%)	Particle diameter (mm)	Ref.
CECT 1240 (ATCC 18942)	Lipase	30	-	-	DOMÍNGUEZ *et al.* (2003)
NCIM 3589	Lipase	30	80	-	IMANDI and GARAPATI (2007)
NCIM 3589	Citric acid	30	70	2	IMANDI *et al.* (2008)
NRBC-10073	Lipid reduction	30	67	-	YANO *et al.* (2008)
NCIM 3589	Lipase	30	60	2	IMANDI *et al.* (2010a)
NCIM 3472	L-asparaginase	30	55	2	KARANAM and MEDICHERLA (2010)
NCIM 3589	Lipase	30	70	2	IMANDI *et al.* (2010c)
NCIM 3589	Lipase	30	50	2	IMANDI *et al.* (2013a)
NRRL Y-1095	Lipase	30	55	0.2-0.5	MOFTAH *et al.* (2013)
NRRL Y-1095	Lipase	30	-	1.5	UR REHMAN *et al.* (2014)
IMUFRJ 50682	Lipase	28	58, 63	$<$1.18	FARIAS *et al.* (2014)
ATCC 24060	Astaxanthin	24	90	0.85	DURSUN and DALGIÇ (2016)

Y. lipolytica strain	Product or Process	Temperature (°C)	Initial moisture content (%)	Particle diameter (mm)	Ref.
NCYC 2904	Okara fermentation	30	75	-	VONG *et al.* (2016)
IMUFRJ 50682	Lipase	28	53	<2	LOPES *et al.* (2016)
NCYC 2904	Okara fermentation	30	-	-	VONG and LIU (2017)
IMUFRJ 50682	Lipase	28	55, 62	<1.18	SOUZA *et al.* (2017)
M53	Erythritol	30	60	-	LIU *et al.* (2018)
W29	$\gamma-$decalactones	27	60, 70	>1	TRY *et al.* (2018)
M53	Erythritol and Lipase	30	70	-	LIU *et al.* (2018)
IMUFRJ 50682	Lipase	28	55	<1.18	DA SILVA *et al.* (2019)
IMUFRJ 50682	Lipase	28	55	<1.18	DE SOUZA *et al.* (2019)
NCYC 2904	Aroma enhancement	20	40	4-8	ZHANG *et al.* (2019)
W29	Protein enrichment	20	60-80	<2.5	VUONG *et al.* (2021)
MIUG D5 and ATCC 18942	Pork lard and Okara biotransformation	30	55	-	COTÂRLEȚ *et al.* (2020)
IMUFRJ 50682	Lipase and esterase	28	55	<1.18	SALES *et al.* (2020)

Specific reports from lipase production by *Y. lipolytica* in solid-state fermentation date from 2003. The strain *Yarrowia lipolytica* CECT 1240 (ATCC 18942) was used for individual investigation of nylon sponge (inert support employed as control), barley bran (supplemented or not with corn, sunflower or olive oil) and triturated nut, all of them impregnated with culture media composed of glucose, urea, minerals, and vitamins, with production of 23 kU L^{-1} of lipolytic activity on tributyrin for

the triturated nut (the highest obtained) (DOMÍNGUEZ *et al.*, 2003).

In Asia, Indian researchers started publishing a series of papers on this subject in 2007. The first, by IMANDI and GARAPATI (2007), aimed at evaluating the combination of abundant solid substrates in India, namely sugarcane bagasse, wheat bran and rice bran, with carbon, nitrogen and humidity sources by univariate exploration in slanting position, resulting in 9.3 U g D.W.$^{-1}$ (hydrolytic activity) for 10 g of sugarcane bagasse with wheat bran, 80% moisture content and supplementation with 1 g of urea and glucose. Later on 2010, Imandi and colleagues published two reports on media formulation for the same strain (*Y. lipolytica* NCIM 3589), but this time the solid material was niger seed (*Guizotia Abyssinica*) oil cake (IMANDI *et al.*, 2010b) and palm kernel (*Elaeis guineensis*) cake (this paper was not counted for Figure 1.1) (IMANDI *et al.*, 2010c), using Plackett-Burman designs for evaluation of carbon and nitrogen sources. They obtained 26.42 and 18.58 U g D.W.$^{-1}$ of hydrolytic activity, with 60 and 50 % moisture content, 5 and 6 % m/m glucose, respectively and 1.5 % m/m urea on both cases. Finally, IMANDI *et al.* (2013a) reported lipase production on mustard oil cake, with the same type of methodology for the verification of influencing variables, with final production of 57.89 U g D.W.$^{-1}$ (hydrolytic activity), for 50 % moisture content, 1.5 % m/m urea and and 7 % m/m glucose. Common issues investigated by these authors within their publications are the diverse range of nitrogen (1 to 5 %m/m) and carbon sources (1 to 9 % m/m). In all cases, glucose and urea were the best options.

In the same year as the last report by the Indian group, MOFTAH *et al.* (2013) used crude olive oil cake (5 g in 150 mL Erlenmeyer flasks) with 0.5 mL inoculum of the strain NRRL Y-1095. The authors found 40 U g D.W.$^{-1}$ (hydrolytic activity) for the alkaline-pretreated (NaOH 3 % w/V) with yeast extract (3 % m/m) as the better nitrogen source to be supplemented.

In Brazil, production started with the strain IMUFRJ 50682, in 2014. FARIAS *et al.* (2014) examined for 48 hours the production of lipases and proteolytic enzymes having cottonseed cake and soybean cake supplemented with its sludge. Proteolytic activity was always observed after the peak of lipase production for the two agro-industrial wastes, which corresponded to hydrolytic activities (for p-nitrophenyl dodecanoate) of 102 and 139 U g D.W.$^{-1}$, respectively.

LOPES *et al.* (2016) investigated the combination of two-phase olive mill waste and wheat bran with nitrogen sources such as urea and ammonium sulfate, finding that the later one was the best option. pH remained acidic throughout the cultivation time with this nitrogen source and this was stated as one of the possible reasons that could have avoided the decay of hydrolytic activity once alkaline proteases would not be produced. The highest activity of 486 U g D.W.$^{-1}$ was obtained at 96 h.

In a more detailed study, SOUZA *et al.* (2017) applied the fractional factorial and central composite rotational designs(CCRD) to investigate how to increase lipase production with soybean cakes and compared it to canola cakes without supplementations. The evaluated variables were inoculum size, moisture content, soybean oil, and urea. Oil supplementation was in the highest case equal to 1.8 % m/m, once the purpose was to induce lipase production and avoid that cells consume added oil as the main carbon source. For canola cake, the highest lipolytic activity (for olive oil as substrate) of 72.6 U g D.W.$^{-1}$ was obtained with 62 % moisture content and 1.44 mg g D.W.$^{-1}$ inoculum, while for soybean cake it was 93.9 U g D.W.$^{-1}$, with 55 % moisture content, 0.73 mg g D.W.$^{-1}$ inoculum and 1.5 % m/m soybean oil. The cell growth was assayed for both cases and different profiles were obtained. Apparently, linear growth was observed for canola cake and it was observed along the protein production. However, for soybean cake, cell growth was verified only after the lipase activity decay with a behavior that seems to be exponential, which could be confirmed for a longer fermentation process. For these cakes, optimal pH and temperature for lipolytic activity were also evaluated by CCRD and the results were 7.6 and 41.9 °C for lipases from canola and 7.2 and 40.3 °C for lipases from soybean meal.

The later served as a basis for other studies on lipase production and application. DA SILVA *et al.* (2019) used the solid enzymatic preparation (SEP) in esterification reactions to decrease the free fatty acid content in acid oils used for biodiesel production. The authors also evaluated the catalyst properties regarding its reuse, reaching a total of 6 batches of reused SEP. DE SOUZA *et al.* (2019) improved lipase production by using higher inoculum and soybean oil supplementation. The authors also investigated its application in the synthesis of short, medium and long-chain esters. Finally, aiming at polyethylene terephthalate (PET) degradation, SALES *et al.* (2020) tested the combined use of watermelon peels and soybean meal to induce esterase and lipase production. This enzyme pool led to a higher concentration of terephthalic acid during PET hydrolysis than the enzyme pool obtained with soybean meal alone, showing its potential for other hydrolysis applications.

2.2.3 Regulation and characteristics of lipases and proteases from *Yarrowia lipolytica*

Genomic data from this yeast has revealed the presence of protein families of 16 lipases, 4 esterases, 38 aspartyl proteases and 10 alkaline proteases (BARTH, 2013b), indicating the ability to produce a diverse amount of proteins. Among those, lipases have been extensively studied, regarding biochemical characterization, culture conditions for production, industrial and *in vivo* applications (ALOULOU *et al.*, 2007b,

DE POURCQ *et al.*, 2012, PIGNÈDE *et al.*, 2000).

Lipases expression is proven to be repressed by glucose. Overexpression of the hexokinase HXK1 gene resulted in reduced lipase production in a superproducer mutant strain that was incapable of performing hexose phosphorylation as the wild-type strain (FICKERS *et al.*, 2005b), suggesting that the activity of this enzyme was correlated to repression of LIP2 and lower activities.

Lipase is also regulated by triacylglycerol molecules which activate the SOA (specific oleic acid) genes. This regulation is somehow performed by two intracellular proteins and is not related to $\beta-$oxidation POX2 gene or to oleic acid induction. The deletion of these genes still allows the induction by oleic acid of LIP2 expression and thus indicates the existence of another mechanism for free fatty acid consumption (DESFOUGÈRES *et al.*, 2010).

Recently, SASSI *et al.* (2016) observed that co-fermentation of oleic acid and glucose in complex media composed of tryptone was able to induce LIP2 expression ten-fold higher than without glucose and concluded that as glucose is also present, cells metabolize both carbon sources simultaneously, with glucose used for energy production and oleic acid for induction, instead of using it for lipid storage. Lastly, complex nitrogen source also seems to regulate lipase production, once TURKI *et al.* (2010) observed that pepsin and tryptic casein digests promoted high lipase synthesis. However, the authors verified that commercial peptone and tryptone worked better than the digests they prepared or yeast extract and attributed this to the degree of casein hydrolysis. Full hydrolysis of proteins are not of interest, instead, small peptides are the ones who induce the production of lipases.

Some lipases expressed by *Yarrowia lipolytica* in submerged fermentation (SmF) have been characterized and the main features reviewed by FICKERS *et al.* (2011). They include the Lip2p, Lip7p, and Lip8p. These authors concluded that the 3 lipases have complementary functions based on their substrate specificity for medium-long chain acids, but Lip7p should be classified as an esterase due to specificity for smaller ester molecules. Besides, specific information of lipases produced from the strain IMUFRJ 50682 (used for this study) has also been reported (BRÍGIDA, 2010, PEREIRA-MEIRELLES *et al.*, 2000, 1997). More recently, naturally immobilized lipases (possibly a mixture of Lip2p, Lip7p and Lip8p) from this strain were also studied. These were obtained either from cell debris (after SmF and followed by cell disruption, named cell-bound lipase fraction - CBLF) (FRAGA *et al.*, 2018, 2020, NUNES *et al.*, 2021) or from the liophilized SEP (DE SOUZA *et al.*, 2019). All these data are summarized in Table 2.3. One important aspect of produced lipases Lip2p and Lip8p is that they seem to be irreversibly inactivated by extreme pH changes and also by the lack of an emulsifying agent in the reaction media, as it was shown by ALOULOU *et al.* (2007b) and KAMOUN *et al.* (2015) using the lipolytic

method.

The cristallographic structure of the main lipase produced by *Y. lipolytica* has already been published (BORDES *et al.*, 2010) revealing that it is a α/β-hydrolase with its catalytic triad composed of the serine (S162), histidine (H289) and aspartic acid (D230) residues (Figure 2.3). However, one of the amino acid residues of the oxianion hole (T88) differs from other lipases. Homology studies and molecular dynamic simulations done by these authors indicated that this lipase requires drastic conformational rearrangements to have the lid opened and this is done in a two-step process. In the first step, the lid was found in a semi-open conformation at the octane-water interface that did not prevent substrate binding. The lid is then fully opened after substrate binding. Meanwhile, lid opening and closing follows different pathways. In organic solvents (which are relevant in esterification reactions), hydrophilic residues have to be exposed for its closure, which explains the loss of activity when methanol is used. In contrast, the weaker interaction of hexane, a nonpolar organic solvent can only leave its lid partially opened (JIANG *et al.*, 2014).

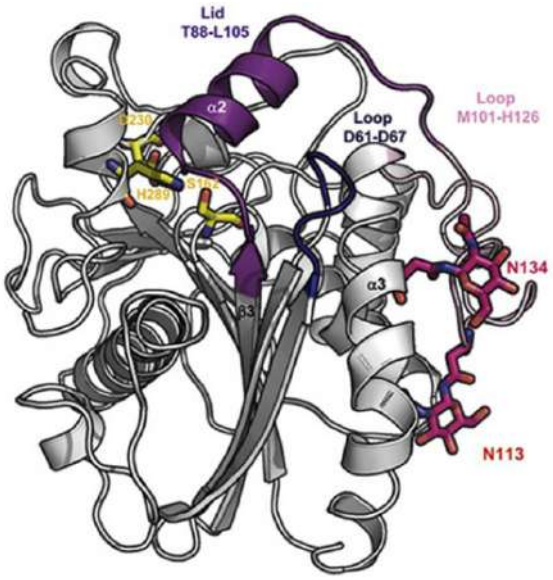

Figure 2.3: Structure of the main lipase (Lip2p) from *Yarrowia lipolytica* (BORDES *et al.*, 2010).

Table 2.3: Compilation of general features of lipases from *Yarrowia lipolytica*.

Lipase and production system	Activators	Inhibitors	pH and Temperature (optimal)	Localization and Glycosylation sites	Solvent Stability	Substrate Specificity	Ref
Lip2p, SmF	Ca^{+2}, Mg^{+2}, bile salt	Zn^{+2}, Ni^{+2}, Cu^{+2}, oleic acid	6-10, 37 °C (most reported), 55 °C	Cell wall (growth phase) and extracellular (end of growth phase), 2 sites (N113 and N134)	90% in acetone, methanol, ethanol, isopropanol, DMSO (10%), 60% in methanol (20%) and DMSO (95%)	$C_{8:0}$ and $C_{18:1}$ triglyceride, C_{12-16} methyl fatty acid	BRÍGIDA (2010), FICKERS *et al.* (2011), PEREIRA-MEIRELLES *et al.* (2000, 1997)
Lip7p, SmF	-	-	-	Cell wall (phosphate buffer extraction), 1 site at aa 140	-	*p*-NPC_6	FICKERS *et al.* (2011)
Lip8p, SmF	Bile salts	-	7.5-9.5, <30 °C	Cell wall (phosphate buffer extraction), 1 site at aa 140	-	*p*-NPC_8, *p*-NPC_{10}, and *p*-NPC_{12} (after enzyme engineering)	FICKERS *et al.* (2011), KAMOUN *et al.* (2015), SHENG *et al.* (2014)

Lipase and production system	Activators	Inhibitors	pH and Temperature (optimal)	Localization and Glycosylation sites	Solvent Stability	Substrate Specificity	Ref
CBLF, SmF	-	-	7 (37 °C)	bound to cell membrane/wall	80 % in 10% V/V) in ethanol and acetone	*p*-NPC$_{16}$	FRAGA *et al.* (2018), NUNES *et al.* (2021)
SEP, SSF	Ca^{+2} (2 mM)	Ca^{+2} and Mn^{+2} (>20 mM), Hg^{+2}, Fe^{+3}, EDTA	7 (50 °C), 8 (37 °C)	-	Stable (at 9% V/V) in hydrophobic solvents, glycerol, methanol, ethanol, acetone, acetonitrile, ether, DMSO; Stable (at 30% V/V) in hexane and heptane	$C_{8:0}$ triglyceride, coconut oil and palm kernel oil	DE SOUZA *et al.* (2019)

SEP: Solid enzymatic preparation obtained by lyophilization. SmF: Submerged Fermentation; SSF: Solid-State Fermentation; aa: amino acid; *p*-NPC$_X$: *p*-nitrophenyl alkanoate with X carbons in the acyl chain; CBLF: cell-bound lipase fraction.

These structural information are important for selectivity and process application (BORDES *et al.*, 2010). For *Y. lipolytica* Lip2p, CAO *et al.* (2017) used β-cyclodextrin to keeping its activity in methanol, demonstrating by molecular simulation that it stabilized the "pathway" for lid closure, holding it partially opened. SHENG *et al.* (2014) rationally chose a region close to the lid region for mutagenesis of Lip8p, altering its optimal operational temperature substrate specificity towards longer acyl-chain esters. AUGUSTYNIAK *et al.* (2012) used the available crystal structure of *Bacillus subtilis* lipase to improve its thermostability, which resulted in a modified protein with reduced tendency to precipitate in high temperatures due to changes in the superficial amino acid residues.

Other characteristics are also found in the literature for these lipases, such as enzyme aggregation. BRÍGIDA (2010) attributed the observed high molecular weight bands while studying the purification of lipases supernatants to the aggregation of enzymes in the concentrated extracts. ALOULOU *et al.* (2007b) verified lip2p aggregation to lipids after performing gel-filtration on supernatant from production with oleic acid as lipase inducer. KAMOUN *et al.* (2015) also reported aggregate formation due to the presence of lipids in samples of Lip8p. After purification with gel filtration and anion exchange chromatography, the authors have immunodetected Lip8p in supernatants as 2 species, one of 39-40 kDa and another of 37 kDa (majority), and speculated that this difference could be related to the production of a pro-enzyme that undergoes further processing outside the cell or a membrane-anchored enzyme (most likely) that suffers some cleavage to be released into the extracellular media. Similar results were observed by FICKERS *et al.* (2005a).

Deglycosylation of the enzyme showed that sugar moiety corresponded to 4 % of the enzyme mass in its mature form. Lip7p seems to have a similar molecular size compared to Lip8p. ALOULOU *et al.* (2007b) found that multiple isoforms of Lip2p are generated through the post-translational processing of proteins related to glycosylation inside the Golgi apparatus. Until leaving the endoplasmic reticulum, where as a net result a 10-residue Man8GlcNAc2 is transferred to the protein (BARNAY-VERDIER *et al.*, 2004), yeast glycosylation is conserved among other types of eukaryotes (either higher or lower eukaryotes), differing in the Golgi apparatus after the action of glycosyltransferases (DE POURCQ *et al.*, 2012).

However, the *N*-glycosylation patterns at N113 and N134 of lipase produced by *Yarrowia lipolytica*, that is, the ones obtained from LIP2 expression, do not seem to be critical for its catalytic activities (retain more activity for longer chain acyl substrates than for *p*-nitrophenyl butyrate) and secretion (JOLIVET *et al.*, 2007). Even though only two sites of *N*-glycosylation are observed, it seems that the occurrence increases adsorption of the enzymes at the lipid-water interfaces (ALOULOU *et al.*, 2013). The level of glycosylation thus depends on the microorganism, ranging

from 8.3 % in *Pichia pastoris* (ALOULOU *et al.*, 2013) to 13.5 % in *Yarrowia lipolytica* (ALOULOU *et al.*, 2007b, JOLIVET *et al.*, 2007) in mass, representing highly glycosylated proteins. Also, increased resistance to proteolytic activities observed through assays with pepsin (aspartic protease or "acidic" protease), chymotrypsin and trypsin (serine proteases), are observed in samples of the wild-type strains with regular glycosylation patterns, with a higher sensibility towards the serine proteases (ALOULOU *et al.*, 2013).

Taking into consideration that *Yarrowia lipolytica* is also capable of producing high amounts of protease, as it was previously mentioned by number of protease families, it is important to have in mind that for accumulation of lipases in the fermentation media, any sort of strategy may be crucial for maintaining its activity, including the absence of production of inhibition of protease activities. Different authors working with strain IMUFRJ 50682 have observed that proteolytic activity increased while lipase activity decayed, either in SmF (SANTOS *et al.*, 2019) or SSF (SOUZA *et al.*, 2017).

The two main proteases studied for *Y. lipolytica* are the alkaline (AEP, subtilisin-like) and acidic (AXP, pepsin-like) extracellular proteases (BARTH, 2013a). In a very interesting study, GLOVER *et al.* (1997) evaluated the pH regulation over this two types of proteases for different strains grown on YNB media without amino acids in pH-controlled vessels within the range of 3.5 – 7.5, both in batch and continuous submerged culture. Their findings revealed that AXP and AEP mRNA were the highest at pH 5.5 and 6.5, respectively, with no detection of AEP mRNA in pH values below or equal to 5.5 and no detection of AXP mRNA in pH above 7.0.

Although the AEP mRNA was not detected at certain pH, western blot analysis with a specific antibody proved the existence of AEP with 31 kDa structure in all the tested values of pH, even if the activity measurements could not detect it in the supernatant, emphasizing that for this protein activity assays might not be enough to completely understand the dynamics of protease regulation (GLOVER *et al.*, 1997). This fact reflects the complexity of AEP regulation, which involves the XPR2 gene expression. Derepression is achieved by starvation of either carbon, nitrogen or sulfur sources (OGRYDZIAK *et al.*, 1977), meaning that nutrient-rich media is required to avoid AEP production.

Mutations that affect the RIM/Pal genes would also serve the purpose of avoiding XPR2 expression (LAMBERT *et al.*, 1997). This pathway, generally proposed for yeast and filamentous fungi, involves different proteins, including transmembrane sensor proteins and intracellular polypeptides that would be recruited to the membrane in case of external neutral or alkaline pH, generating a response of proteolysis of intracellular promoters that would further travel into the nucleus for activation of transcription of these specific genes (BARTH, 2013b). In this context, acidic

products from transcription and translation would be repressed.

Besides, it has been found that AEP is expressed as a 55 kDa precursor that suffers intracellular processing by a dipeptidyl aminopeptidase (DPAPase). The product, a 52 kDa protein, is secreted and processed into a pro-peptide of 20 kDa and the 32 kDa mature-AEP (MATOBA *et al.*, 1997). Given that the existence of this 52 kDa protein and that mixing the supernatants of this protein with the mature-AEP decreases its activity, BARTH (2013a) proposed a model for inhibition of activity based on dimer formation between the mature-AEP and pro-peptide, after HU *et al.* (1996) showed evidence of the existence of a folded prosubtilisin structure.

AXP secretory pathway is a simpler process, with links between the absence of mRNA and protein quantification through activity measurements (GLOVER *et al.*, 1997). It is an endopeptidase secreted as a 42 kDa pro-peptide which undergoes extracellular autocatalytic processing at acidic pH to a final 39 kDa structure, with faster processing at the pH range of 4.0 – 4.6 and autoprocessing is not inhibited by pepstatin, a common aspartic proteinase inhibitor. The active enzyme does not present glycosylation and processing is not done by AEP (MCEWEN and YOUNG, 1998).

2.3 Solid-state fermentation

2.3.1 Cell analysis in solid-state fermentation

Biomass estimation is still a relevant topic of research in the area of solid-state fermentation. The natural limitations imposed in this type of process, such as the system heterogeneity and the microorganism ingrowth into the solid matrix, makes direct determination of biomass challenging (BOTELLA *et al.*, 2019, MITCHELL *et al.*, 2004, STEUDLER and BLEY, 2015).

When microorganisms grow on solid matrices and penetrate the material, like in most solid-state fermentation, offline cell analysis methods are majorly based on the estimation of cell components, such as the cell wall components like chitin (AIDOO *et al.*, 1981, PLASSARD *et al.*, 1982, RIDE and DRYSDALE, 1972). However, extraction of cellular material is time consuming, including hydrolysis and chemical reactions based on the compound to be assayed. Beyond that, hydrolysis of the fermented material may generate background signal from the solid matrix (MITCHELL *et al.*, 2004). AIDOO *et al.* (1981) compared four different methods based on chitin quantification and found that alkaline depolymerization and deacetylation of Koji fermentation samples produced the lowest background signals.

SOUZA *et al.* (2017) evaluated the growth of *Y. lipolytica* IMUFRJ 50682 in

canola cake and soybean meal after acid hydrolysis with 6 M HCl and no variation of *N*-acetyl glucosamine was observed in both growth phases after 4 and 20 h. The values seem to have been blankly discounted since AIDOO *et al.* (1981) found high initial values of this component at the beginning of Koji fermentation. Thus, it is difficult to determine if cells did not grow and remained in a lag phase or if they initially decreased in number and this was masked by the supposed blank discounting.

Besides the existence of the target component in the solid matrix, cell composition and products may vary in response to the environmental conditions (MITCHELL *et al.*, 2004). For example, VEGA and DOMÍNGUEZ (1986) analyzed the wall components of *Y. lipolytica* and found that chitin represented approximately 7 and 15 % of the wall in yeast cells and septa in hypha, respectively, after chemical hydrolysis. Hence, two main aspects should be taken in consideration: cells may or may not undergo morphological transition, meaning that the increase in the chitin content may not be appropriate to evaluate growth in SSF; if cells do not grow well on the solid matrix or they are from the beginning of fermentation, data interpretation may be disturbed by the influence of the solid support since the chitin percentage on the cell wall is quite small.

A systematic approach on quantification methods has been performed by STEUDLER and BLEY (2015). After evaluation of several methods of analysis (quantification of ergosterol, glucosamine, nuclei number, nucleic acids, protein content and genomic DNA, lignolytic and cellulolytic enzymes, glucose content and respiratory analysis), the authors verified that respiratory analysis, nuclei count (aided by flow cytometry for a rapid procedure) and ergosterol quantification were the most suitable for monitoring of the fungus *Trametes hirsuta*.

Respiratory analysis has been used as an indirect online method (BOTELLA *et al.*, 2019, PITOL *et al.*, 2017). This analysis is based on the offstream gas leaving the bioreactor in solid-state fermentation. CO_2 and O_2 are measured with online sensors in the gas stream, which sometimes passes by a silica column to remove water and other components, and a simple mass balance in the gas phase is used to quantify production and consumption of these gases. BOTELLA *et al.* (2019) also used capacitance measurement as a potential new method, although developments are still required to have absolute biomass values. Other than that, these authors also used a total mass balance to estimate fungal growth, assuming that the only product removed from the bed is CO_2 and that product formation followed a Luedeking-Piret model.

To circumvent the time-consuming and labor-intensive procedures used in ergosterol quantification, MANSOLDO *et al.* (2020) studied strategies for rapid ergosterol extraction and simple quantification using ergosterol autofluorescence. Their

results proved that ultrasound assisted extraction for 20 min was sufficient for later detection by excitation-emission matrix measurements, even in the presence of an interferent component. However, it is unclear if the method could present limitation in extraction with real fermented material, since the samples consisted of solid residue commonly testes in SSF processes mixed with the target fungus (*Schizophyllum comune*).

Even though these indirect quantification procedures give an idea of growth, no information of the physiological state is obtained, although respiratory analysis gives an indication of cell metabolic activity. Cell viability is also important because it reflects its active state and as reactions rates depend on the cells, monitoring becomes necessary (WEI *et al.*, 2007). Various methods were already used to distinguish morphologies and size distribution of *Y. lipolytica*, including morphonogranulometry, coulter counter, density gradient centrifugation, diffraction light scattering, flow cytometry, and electronic or optical microscopy, as it was reviewed by TIMOUMI *et al.* (2018), being the techniques cited in ascending amount of reports. The authors state that the more recent techniques provide information on a single-cell level allowing studies of the subpopulations.

Digital image analysis has also received some attention as a potential tool for biomass monitoring. Once images have been acquired, processing is required to extract information. The main steps of image processing include preprocessing, where contrast enhancement and filters are used; segmentation, where cells are separated from the background of the image; and classification and information extraction, when cells are separated into different populations, usually by means of measured properties (WOLLMANN *et al.*, 2017). Besides, proper cell preparation and visualization prior to image acquisition are necessary. COELHO *et al.* (2004) had to focus the cell borders for images with greater differentiation from the background of the image, while LOPES (2015) and BRAGA *et al.* (2015) used safranin to stain the cell surface.

In this sense, dark-field microscopy has already been applied to extract information for various types of cells. The dark background and the objects provide enough contrast, which is an advantage when comparing with bright field microscopy (ANTOLOVIĆ *et al.*, 2014). Also, the light scattering produced by the microscope allows expansion of the resolution of the images, with increased signal to noise ratio. Nevertheless, errors from light scattering may occur if cells are in contact, since it happens at the cell edges and therefore the signal will not be proportional to the number of cells (LAWRENCE *et al.*, 1989). Examples of application of this type of microscopy include examination of bacterial biofilms and their motility (LAWRENCE *et al.*, 1989), cell tracking of amoebae (ANTOLOVIĆ *et al.*, 2014), *in situ* viability classification of *S. cerevisiae* (WEI *et al.*, 2007) and viability classification of animal cell

cultures (BURGEMEISTER *et al.*, 2010).

For the yeast *Y. lipolytica*, a few works have been described using digital image analysis. KAWASSE *et al.* (2003) used this technique to analyze dimorphism under thermal and oxidative stress. BRAGA *et al.* (2015) evaluated the cells stained with safranin in the study of aroma production in SmF. Later, the same group reported on morphology study of the same strain without safranin staining in bright field microscopy (BRAGA *et al.*, 2016). In a more recent publication, BOTELHO *et al.* (2020) studied *Y. lipolytica* adhesion onto polystyrene, PET, Teflon and glass. The authors quantified the area colonized by the cells using strains IMUFRJ 50682 and W29 and associated the higher adhesion to polystyrene to the more hydrophobic characteristic of this material. In SSF, LOPES (2015) developed a protocol for biomass sampling from after fermentation and was able to verify the evolution of *Y. lipolytica* population obtained in solid-state fermentation in bright field microscopy, but with safranin staining, being a promising tool for better understanding of this type of process. A limitation found in the later is the manual choice of threshold limit for segmentation.

Images have also been used for filamentous fungi quantification without performing cell extraction. In this case, images of the fermented solid are made and directly analyzed. DUAN *et al.* (2012) extracted the contours of the material and used fractal geometry to quantify over time the changes in the solid fermented by *Penicillium decumbens* system, being promising as a non-destructive method of analysis and online cell monitoring of solid-state fermentation. This idea of whole-material analysis was also studied in fermentation with *Rhizopus oryzae* NRRL 195 and *Aspergillus awamori* with sugarcane bagasse and industrial wheat residues (LÓPEZ-GÓMEZ *et al.*, 2019), although in this case the authors used the color development to extract biomass information. They also point out that a natural limitation to this method may exist if the fungal colony does not differ from the solid matrix considerably in color.

2.3.2 Solid matrix - soybean hulls production and characteristics

Soybean is greatly produced in Brazil, being spread through the interior of the country and limited until last year to some extent by the Amazon Rainforest and the states of southeast and northeast Figure 2.4. Global production is mainly done in the America and Asian continents, having Brazil, the United States, and Argentina as the biggest producers with 114.3, 96.8 and 55.3 Mtons in 2019. These three countries account for nearly 80 % of the worldwide production.

The use of soybeans reflects its processing, which generates a diverse range of

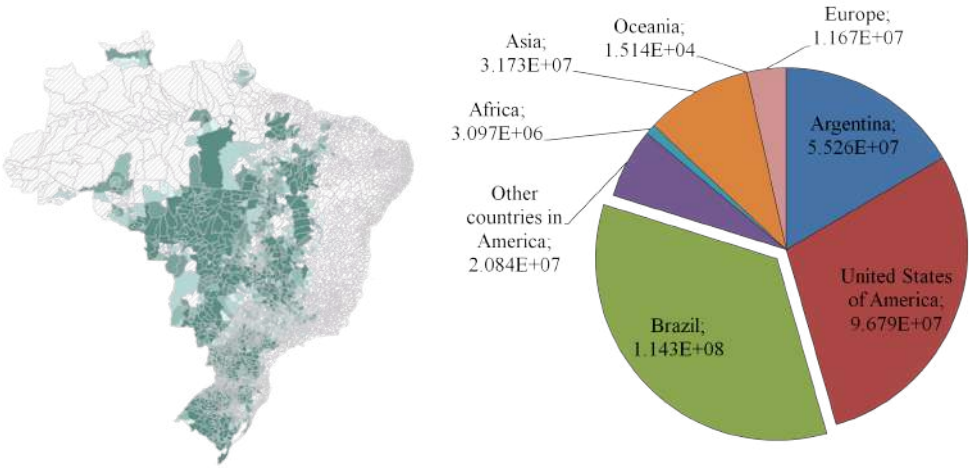

(a) (b)

Figure 2.4: Distribution of the total amount of soybeans produced in 2019 in Brazil (left) and global production share (right). Grey regions represent the part from where there is no available data. The intensity of production was depicted in green scale, with darker green representing the highest amounts produced. Scaling was divided into equal intervals of production. Source: IBGE (2020) and FOOD AND AGRICULTURE ORGANISATION (FAO) (2020), accessed on April 17, 2021.

products, with attention to the soybean refined oil, soybean protein concentrate and soybean isolate and soybean itself. The main steps concerning the processing of the soybeans are represented in Figure 2.5, where the components used for solid-state fermentation with *Y.lipolytica* are highlighted. After harvest, soybeans are usually dehulled to increase protein concentration in the flakes and follows extraction, generating as the two major fractions the crude oil and the meal, which may be defatted. Refining steps may occur to obtain the refined oil and protein concentrates and isolates, Okara and whey and the products are then destined for human or animal consumption (DE PRETTO *et al.*, 2018). The fermentation possibilities for the hulls usually comprehend production of biofuels or lignocellulolytic enzymes (LOMAN and JU, 2016).

The composition of the meal and the hulls (used herein) are very different, as it is summarized in Table 2.4. The hulls have lower commercial value, being destined to animal nutrition and the major differences of these materials lie in the protein and holocellulose (sum of cellulose and hemicellulose) content, as the meal contains a lot more protein than the hulls and much less cellulose (LOMAN and JU, 2016).

The values cited here are in accordance with what BRIJWANI and VADLANI (2011) measured. They also investigated the influence of mild conditions for pretreatment with steam, HCl, H_2SO_4, and NaOH over hulls of 0.61 mm of diameter and found that all of them increased crystallinity and the porosity of the hulls without changes in holocellulose content. Specific effects over enzyme production by the fungi *T. reesei* and *A. oryzae* were also verified. Some relevant characteristics of the

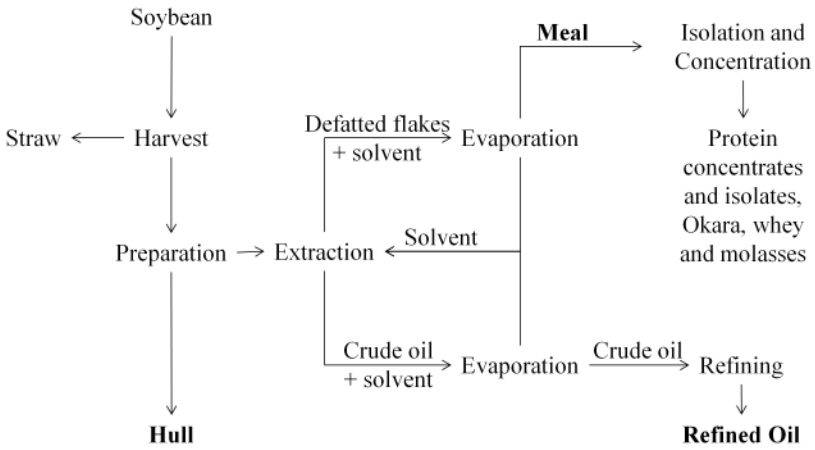

Figure 2.5: Simplified steps of soybean processing. Parts that have been used by *Y. lipolytica* IMUFRJ 50682 for fermentation are represented in bold.

Table 2.4: Composition of soybean hull and meal.*

Components	Composition (weight %)	
	Hull	Meal
Cellulose	29-51	2-4
Hemicellulose	10-20	8-10
Soluble oligosaccharides	5-10	10-12
Lignin	1-4	0.5-1
Pectin	6-15	10-12
Protein	9-14	50-52
Ash	1-4	5-6
Fat	-	2-3

*Adapted from LOMAN and JU (2016).

soybean hulls for solid-state fermentation include its swelling capacity (7.35 mL g^{-1}) and oil holding capacity bigger than those of wheat and barley bran, measured for its powder (MATIN *et al.*, 2013). These two last features are important once they will determine whether swelling of the material will influence the porosity of the bed or not and if the material will absorb the inducer for lipase production.

When using the soybean products in solid-state fermentation, the water binding properties of these material have great relevance, since they help in retaining the water used by the microorganism to grow. Water sorption and desorption isotherms are obtained by reaching equilibrium moisture content by absorbing water from the environment or losing it. These isotherms may not superimpose and present a hysteretic loop (AVIARA, 2020). They are available for a variety of products, such as the soybean seeds (AVIARA *et al.*, 2004, PIXTON and WARBURTON, 1975), meal (LUZ *et al.*, 2006, PIXTON and WARBURTON, 1975) and cellan (DONGOWSKI and EHWALD, 1999), and are drawn in Figure 2.6. The later (also refered as vesiculary particles) is obtained after treatment with enzymes to remove proteins,

starch and other digestible materials (DONGOWSKI and EHWALD, 1999).

These plots explicit the equilibrium moisture content behavior as a function of water activity and temperature. The soybean meal present very little hysteretic behavior (PIXTON and WARBURTON, 1975), as it is shown in Figure 2.6b. The temperature effect on desorption isotherms is less pronounced in the meal (Figure 2.6b) than in the soybean (Figure 2.6a, as also shown by Equations 2.3 (LUZ *et al.*, 2006) and 2.4 (AVIARA *et al.*, 2004), respectively:

$$EMC = \frac{0.834}{1 + 0.036\ T\ ln\frac{1}{a_W}} \tag{2.3}$$

$$EMC = (61.831 - 0.151\ T)\left(\frac{a_W}{1 - a_W}\right)^{\frac{1}{3.72}} \tag{2.4}$$

where EMC is the equilibrium moisture content, a_w is the water activity, and T is the temperature. AVIARA *et al.* (2004) also estimated the parameters for the explicit calculation of water activity, shown in Equation 2.5:

$$a_W = exp[-exp(18.605 + 0.0387\ T)EMC^{-2.597}] \tag{2.5}$$

For the cellan (Figure 2.6c), a small hysteresis is observed. Its water retention capacity increases as a function of the pH and range from 7.28 to 8.90 g H_2O g^{-1} D.W. at 20 °C. Brunauer-Emmet-Teller (BET) isotherms for desorption (Equation 2.6b) and sorption (Equation 2.6a) obtained at 25 °C are also available for it, showing that monolayer water content is around 0.08 g H_2O g^{-1}. All these values were smaller than those for other types of cellans, such as apple, cabbage, sugar-beet, and wheat bran, including its oil holding capacity (DONGOWSKI and EHWALD, 1999).

$$EMC = 0.074\frac{12.62a_W}{(1 - a_W)(1 - a_W + 12.62a_W)} \tag{2.6a}$$

$$EMC = 0.088\frac{14.57a_W}{(1 - a_W)(1 - a_W + 14.57a_W)} \tag{2.6b}$$

It is noteworthy that the data for the (de)sorption isotherms were all for particles with variable sizes, although little difference is observed. CARDOSO *et al.* (2013) studied density, particle size and shape distributions of soybean hulls, tobacco waste, fiber sorghum, and sweet sorghum, in three size ranges (150-425, 425-710 and 710-850 μm). They observed that soybean hulls presented higher roundness than the other materials, which also increased as their particle sizes diminished. Density of soybean hulls presented small changes in true density upon drying, for three size ranges. Soy hulls also had higher bulk and apparent densities than the other tested materials. The values found for the higher size range are in accordance with the ones reported by OLIVEIRA *et al.* (2015) for soybeans hulls sieved with apperture

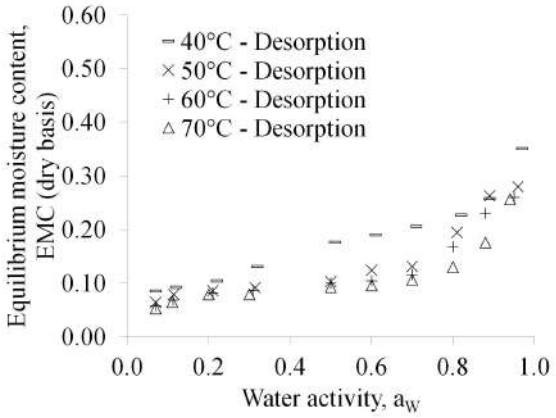

(a)

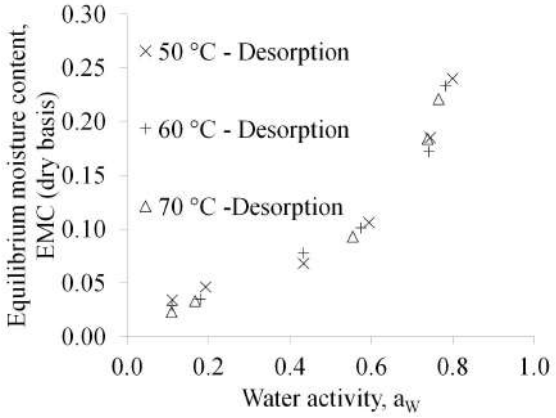

(b)

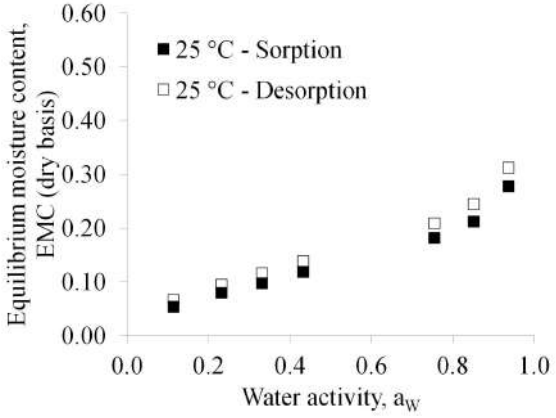

(c)

Figure 2.6: Water isotherms of soybean (a)AVIARA *et al.* (2004), soybean meal (b)LUZ *et al.* (2006) and soybean cellan (c)DONGOWSKI and EHWALD (1999). Different symbols were used for each temperature. Sorption and desorption data were calculated with the original authors adjusted equations and represented with filled or empty symbols, respectively.

diameters between 1000 and 500 μm. The apparent densities found in these two works are the same (1.432 g cm^{-3}), while the bulk and apparent densities are only given in the first (0.46 and 1.09 g cm^{-3}). MUZILLA *et al.* (1991) measured the apparent density of the hulls and found 1.05 g cm^{-3} for the particle size of 840 μm. Besides, the later measured the thermal properties of soybean hulls, finding values of 4725 J kg^{-1} K^{-1}, 0.616 W m^{-1} K^{-1}, and 1.24 10^{-7} m^2 s^{-1} for the heat capacity, thermal conductivity and thermal diffusivity, respectively. Delignification of the material increased its thermal conductivity, which was associated with a higher movement of unbound water molecules. For cellans derived from soybean hulls (DONGOWSKI and EHWALD, 1999), particle size distribution showed a major fraction (97 %) in a range of 0.2-0.5 mm, for which the density was measured as 1.444 g mL^{-1} and surface area was 9.9 m^2 g^{-1}.

2.3.3 Bioreactors in solid-state fermentation and modeling of the process

Vessels for fermentation processes vary greatly in geometry and mode of operation and their main objective is to guarantee the appropriate environment for the development of the cells. In order to accomplish that, the main operational variables that may impact on growth are monitored whenever it is possible. Hence, modeling of the physicochemical and biological phenomena happening inside the reactor allows design and scale-up of better processes, prediction of process behavior, development of control strategies, and optimization of the operating conditions.

According to MITCHELL *et al.* (2006), there are many types of bioreactors for solid-state fermentation and they are classified in four groups with respect to their operation: static bioreactor with or without forced aeration through the bed and agitated beds with or without forced aeration through the bed. In all cases, the air that is supplied to the systems can have their temperature, humidity, and air flow controlled. The air, which contains water, is necessary not only to provide oxygen to the cells but also to remove CO_2 and heat from the bed. Drying ends up happening as water is both consumed by the microorganism and evaporated from the surface of the solid as heat is generated. Therefore, the authors state that axial and radial temperature gradients are inevitable and summarize the main phenomena inside the bioreactor as metabolic reactions that produce heat, heat conduction (which is less important in forcefully aerated reactors such as the packed bed) and convection, evaporation and convective mass transfer. Also, pressure drop tends to intensify as the microorganism grows and penetrate the solids and flow regime approximates to plug flow as a result of passing through the void part of the bed.

The modeling of the process comprehends two major groups of equations related

to transport phenomena and microbiological growth. The developments of modeling of these events have been separately reviewed by MITCHELL *et al.* (2003) and MITCHELL *et al.* (2004), respectively, but from those years on, other approaches have been reported. At that time, they reported on the main empirical equations used to describe microbial growth, such as the linear, exponential, logistic and two-phase equations. Though, from that time on, the exponential and logistic ones were the most applied, either purely or combined in two-phase models, as it is verified in Table 2.5.

The logistic equation is usually a better choice for a simple model once it better represents the behavior of cells growing in the solid matrix. Representation of the physiological state of cells can also be performed. Death kinetics may be included by adding a first-order decay term, as it is shown on the right side of Equation 2.10b, to differentiate viable and non-viable cells (MITCHELL *et al.*, 2004). One specific feature of the two-phase growth models (Equations 2.9 and 2.8)) is that both rate equations are evaluated at the same time and decision of which expression is going to be used for that moment is dependent on conditional statements.

Temperature dependence on the specific growth rate is not always taken as true, as it was assumed by FERNÁNDEZ-FERNÁNDEZ and PÉREZ-CORREA (2007) and DA SILVEIRA *et al.* (2014) in their modeling studies of SSF with *K. marxianus* and *G. fujikuroi*, respectively. In order to verify this, experimental evaluation is necessary. IKASARI *et al.* (1999) investigated in membrane cultures the effect of temperature on growth of *Rhizopus oligosporus* by imitating the typical temperature profiles found in solid-state fermentations through temperature shifts and used the two-phase model to understand the effect of temperature. The main results point out the importance of the response to temperature shift, as a considerable part of the hypha stopped growing. The authors also show the importance of this approach when compared to isothermal studies.

FANAEI and VAZIRI (2009) proposed that the cells state is important and described the parameter ϕ as the level of physiological factor that is related to past temperatures to which the microorganism has been submitted, representing the time it takes for a change in metabolism as a response to temperature changes (Equations 2.12a and 2.12b). The effect of temperature, in this case, is described by Arrhenius equations in parameters γ_S and γ_D.

The insertion of environmental effects such as temperature, water or physiological state is generally done by describing μ as a function of these variables. As it was mentioned above, the temperature dependence is usually accounted by Arrhenius-type formulations. These include the general formulation found in VILLADSEN *et al.* (2011)(Equation 2.13):

Table 2.5: Empirical growth equations used in models of solid-state fermentation. The table does not represent an exhaustive research of models.

Growth description	Empirical growth equations	Reference
Logistic growth	$\frac{\mathrm{d}b}{\mathrm{d}t} = \mu b \left(1 - \frac{b}{b_{max}}\right)$ (2.7)	BÜCK *et al.* (2015), CASCIATORI *et al.* (2016), DA SILVEIRA *et al.* (2014)
Two-phase growth	$\frac{\mathrm{d}b}{\mathrm{d}t} = \begin{cases} \mu b, & t < t_a, \\ \mu b L_{as} e^{-k_a(t-t_a)}, & t \geq t_a, \end{cases}$ (2.8)	HAMIDI-ESFAHANI *et al.* (2007), IKASARI *et al.* (1999)
	$\frac{\mathrm{d}b}{\mathrm{d}t} = \begin{cases} \mu b, & \mu b < \mu b \left(1 - \frac{b}{b_{max}}\right), \\ \mu b \left(1 - \frac{b}{b_{max}}\right), & \mu b \geq \mu b \left(1 - \frac{b}{b_{max}}\right) \end{cases}$ (2.9)	HAMIDI-ESFAHANI *et al.* (2007)
Physiological state	$\frac{\mathrm{d}b_T}{\mathrm{d}t} = \mu b_v$ (2.10a) $\frac{\mathrm{d}b_v}{\mathrm{d}t} = \mu b_v - k_D b_v$ (2.10b)	FERNÁNDEZ-FERNÁNDEZ and PÉREZ-CORREA (2007)
	$\frac{\mathrm{d}b_T}{\mathrm{d}t} = \mu b_v \left(1 - \frac{b_T}{b_{max}}\right)$ (2.11a) $\frac{\mathrm{d}b_v}{\mathrm{d}t} = \mu b_v \left(1 - \frac{b_T}{b_{max}}\right) - k_D b_v$ (2.11b)	MITCHELL *et al.* (2010)
	$\frac{\mathrm{d}b}{\mathrm{d}t} = \mu b \phi \left(1 - \frac{b}{b_{max}}\right)$ (2.12a) $\frac{\mathrm{d}\phi}{\mathrm{d}t} = \gamma_S \phi (1 - \phi^a) - \gamma_D \phi$ (2.12b)	FANAEI and VAZIRI (2009)

b is the cell mass, b_{max} is the maximum cell mass, b_T is the total cell mass, b_v is the viable cell mass,μ is the specific cell growth rate, ϕ is the physiological factor, γ_S and γ_D are the frequency factors for synthesis and denaturation of the physiological factor, k_D is the constant for the first order death decay, k_a is the first order decay of the fraction L_{as} of active segments within the deceleration phase of growth and t_a is the moment when this phase begins.

$$\mu_T = \frac{Ae^{(-E_A/R_gT)}}{1 + Be^{(-E_D/R_gT)}} \tag{2.13}$$

where the constants A and B are frequency factors and E_A and E_D are the energies for thermal activation and denaturation of internal components of cells, respectively, and adaptations can still be made. Another set of empirical equations proposed by SANGSURASAK and MITCHELL (1998) and further used by FANAEI and VAZIRI (2009) present a strategy to manipulate the sensitivity of the specific growth rate to temperature by changing the values of n_T. This parameter increases sensitivity as its value rise and impacts on how fast or slow the specific growth decreases. The following equations (2.14a, 2.14b, 2.14c) represent this:

$$\mu_T = \mu_{T_{opt}}, T \leq T_{opt} \tag{2.14a}$$

$$\mu_T = \frac{n_T + (T_{max} - T_{opt})}{T_{max} - T_{opt}} - \frac{\mu_{T_{opt}}(T_{max} - T)}{n_T + (T_{max} - T)}, T_{opt} \leq T \leq T_{max} \tag{2.14b}$$

$$\mu_T = 0, T \leq T_{max} \tag{2.14c}$$

where T_{opt} and $\mu_{T_{opt}}$ are the optimum values of temperature and specific growth rate, respectively. Finally, the growth dependence on water activity may be used if available data and water mass balances are applied in simulation studies. This was calculated by MITCHELL *et al.* (2010) and CASCIATORI *et al.* (2016) by Equation 2.15 and used to obtain a geometric mean value of μ (Equation 2.16).

$$\mu_W = D_0 e^{D_1 a_W^3 + D_2 a_W^2 + D_3 a_W + D_4} \tag{2.15}$$

$$\mu = \mu_{opt}\sqrt{\mu_T \mu_W} \tag{2.16}$$

where the constants D_0, D_1, D_2, D_3, and D_4 are related to the microorganism. Therefore, it is possible to relate both energy and mass balances to the biological behavior inside the reactor if the proper mathematical formulation is used. As the focus of this work is to develop models for fixed-bed bioreactors, attention will be focused in these reactors. A pseudo-homogeneous energy balance in a packed-bioreactor that includes evaporation as a mechanism for cooling was developed by SANGSURASAK and MITCHELL (1998) (Equation 2.17):

$$\begin{aligned}\rho_b C_{p_b}\frac{\partial T}{\partial t} + (\rho_a C_{p_a} + \rho_a f \Delta H_{vap}) v_z \frac{\partial T}{\partial z} = k_b \frac{\partial^2 T}{\partial z^2} + \frac{k_b}{r}\frac{\partial}{\partial r}\left(r\frac{\partial T}{\partial r}\right) \\ + \rho_s(1-\epsilon_0) Y_H \frac{\mathrm{d}b}{\mathrm{d}t}\end{aligned} \tag{2.17}$$

where, the subscripts a, b and s indicates the properties of the air, bed and solid, ΔH_{vap} is the enthalpy of water evaporation, C_p is the specific heat capacity, k is the

thermal conductivity, ρ is the density, f is the water carrying capacity, ϵ_0 is the bed porosity and Y_H is the heat yield. The second term on the left side is highlighted by the authors because it is an assumption that cooling by means of water evaporation makes air have a higher apparent heat capacity. They also used averagely weighted properties of the bed (Equations 2.18, 2.19, 2.20):

$$\rho_b = \epsilon_0 \rho_a + (1 - \epsilon_0)\rho_s \tag{2.18}$$

$$C_{p_b} = \epsilon_0 C_{p_a} + (1 - \epsilon_0)C_{p_s} \tag{2.19}$$

$$k_b = \epsilon_0 k_a + (1 - \epsilon_0)k_s \tag{2.20}$$

Other authors DA SILVEIRA *et al.* (2014), FANAEI and VAZIRI (2009) also include the properties of water in the calculation of heat capacity of the bed (Equation 2.21):

$$C_{p_b} = \frac{\epsilon_0 \rho_a (C_{p_a} + f\Delta H_{vap}) + (1 - \epsilon_0)\rho_s C_{p_s}}{\rho_b} \tag{2.21}$$

The initial conditions inside the reactor for cell concentration and temperature are assumed to be uniform throughout the bioreactor and boundary conditions for the problem studied by SANGSURASAK and MITCHELL (1998) are given by Equations 2.22a, 2.22b, 2.22c, and 2.22d. The first assumes that the temperature at the inlet of the reactor is equal to the inlet air temperature (T_{g_i}), the second is related to the absence of a temperature gradient at the reactor outlet, the third is related to the radial symmetry that imposes no gradient in the center of the bioreactor, and the fourth express the heat exchange in the wall, where T_∞ is the temperature of surroundings. The problem was solved by the orthogonal collocation method using Jacobi polynomials.

$$T_{z=0} = T_{g_i} \tag{2.22a}$$

$$\left(\frac{\partial T}{\partial z}\right)_{z=L} = 0 \tag{2.22b}$$

$$\left(\frac{\partial T}{\partial r}\right)_{r=0} = 0 \tag{2.22c}$$

$$\left(\frac{\partial T}{\partial r}\right)_{r=R} = \frac{Bi}{R}(T_\infty - T) \tag{2.22d}$$

If the reactor diameter is large enough, removal of heat by horizontal conduction

can be neglected and radial terms are excluded from the equation (MITCHELL *et al.*, 2003). FANAEI and VAZIRI (2009) compared the performance of two models on the prediction of temperature profiles relating growth to temperature by means of the physiological parameter, as it was aforementioned. One of the unidirectional models considered the existence of only the axial direction in a distributed model while the other so-called "lumped" did not consider the variation of temperature in the bed. In the last, a set of ordinary differential equations was resolved with a fourth order Runge-Kutta method while in the first the partial derivatives were approximated by equally spaced finite difference methods, having Equations 2.22a and 2.22b as boundary conditions. The expected conclusion that the distributed model had a better adjustment to data was attained.

In another approach, DA SILVEIRA *et al.* (2014) used the distributed model developed by (2009)FANAEI and VAZIRI (2009) without axial conduction and keeping the specific growth rate constant in a logistic growth model. The authors did maintain the water term in the balance and used the experimental data to analyze the model sensitivity and estimate μ, ρ, C_p, ϵ_0, and Y_H. The analysis revealed that the highest sensitivity was towards the heat yield and that evaporative cooling was more effective than increasing air flow rate.

Water balance is however of great importance and must be included in the models, once the amount that evaporates is considerable and normally not replenished (SANGSURASAK and MITCHELL, 1998). In recent developments, water and energy balances are already performed for solid-state fermentations with heterogeneous media. In this case, the balances are constructed for both the solid and gas phases and the connection between water and energy balances and the different phases occur mainly through the evaporative term.

In this sense, BÜCK *et al.* (2015) investigated the use of feedback controls schemes to regulate temperature and moisture content in a fixed-bed bioreactor by manipulation of the gas inlet variables and the jacket temperature. For that, the unidirectional model comprised only advection and two water and energy balance equations were used (Equations 2.23a, 2.23b, 2.23c, and 2.23d):

$$\rho_a \epsilon_0 \frac{\partial Y}{\partial t} + v_z \rho_a \frac{\partial Y}{\partial z} = \dot{\nu}(X) \beta a \rho_a \epsilon_0 (Y^* - Y) \tag{2.23a}$$

$$\frac{\partial SX}{\partial t} = -\dot{\nu}(X) \beta a \rho_a \epsilon_0 (Y^* - Y) + Y_w \frac{\partial Sb}{\partial t} \tag{2.23b}$$

$$\begin{aligned} \rho_a \epsilon_0 (C_{p_a} + Y C_{p_{vap}}) \frac{\partial T_g}{\partial t} + v_z \rho_a (C_{p_a} + Y C_{p_{vap}}) \frac{\partial T_g}{\partial z} = -ha(T_g - T_s) \\ + \Delta H_{vap}(T_s) \dot{\nu}(X) \beta a \rho_a \epsilon_0 (Y^* - Y) \end{aligned} \tag{2.23c}$$

$$(C_{p_s} + XC_{p_w})\frac{\partial ST_s}{\partial t} = ha(T_g - T_s) - \Delta H_{vap}(T_s)\dot{\nu}(X)\beta a\rho_a\epsilon_0(Y^* - Y) + Y_H\frac{\partial Sb}{\partial t} \tag{2.23d}$$

where the subscripts g and w represent gas and water, βa and ha are the mass and heat transfer coefficients, X is the moisture content and $\dot{\nu}(X)$ is the normalized drying rate. They also described the microbial growth by the logistic model and substrate (bed) biological degradation by Equation 2.24

$$\frac{\partial S}{\partial t} = Y_s\frac{\partial Sb}{\partial t} \tag{2.24}$$

and found that changing flow direction intermittently (air enters in the bioreactor by the "outlet") and proportional control of the jacket temperature would displace the peak temperature to the middle of the reactor and decrease its intensity.

CASCIATORI *et al.* (2016) included the radial coordinate to the preceding equations and additional transport phenomena such as heat conduction on the gas and the solid, diffusion of water in the gas and solid and drying (Equations 2.25a, 2.25b, 2.25c, and 2.25d):

$$\rho_a\epsilon_0\frac{\partial Y}{\partial t} + v_z\rho_a\frac{\partial Y}{\partial z} = \dot{\nu}(X)(X)\beta a\rho_a\epsilon_0(Y^* - Y) + \rho_a\epsilon_0 D_{g,z}\frac{\partial^2 Y}{\partial z^2} + \rho_a\epsilon_0 D_{g,r}\frac{1}{r}\frac{\partial}{\partial r}\left(r\frac{\partial Y}{\partial r}\right) \tag{2.25a}$$

$$\frac{\partial SX}{\partial t} = -\dot{\nu}(X)\beta a\rho_a\epsilon_0(Y^* - Y) + Y_w\frac{\partial Sb}{\partial t} + D_s S\frac{\partial^2 X}{\partial z^2} + D_s S\frac{1}{r}\frac{\partial}{\partial r}\left(r\frac{\partial X}{\partial r}\right) \tag{2.25b}$$

$$\rho_a\epsilon_0(C_{p_a} + YC_{p_{vap}})\frac{\partial T_g}{\partial t} + v_z\rho_a(C_{p_a} + YC_{p_{vap}})\frac{\partial T_g}{\partial z} = -ha(T_g - T_s) + \Delta H_{vap}(T_s)\dot{\nu}(X)\beta a\rho_a\epsilon_0(Y^* - Y) + \epsilon_0\lambda_{g,z}\frac{\partial^2 T_g}{\partial z^2} + \epsilon_0\Lambda_{g,r}\frac{1}{r}\frac{\partial}{\partial r}\left(r\frac{\partial T_g}{\partial r}\right) \tag{2.25c}$$

$$(C_{p_s} + XC_{p_w})\frac{\partial ST_s}{\partial t} = ha(T_g - T_s) - \Delta H_{vap}(T_s)\dot{\nu}(X)\beta a\rho_a\epsilon_0(Y^* - Y) + Y_H\frac{\partial Sb}{\partial t} + (1-\epsilon_0)\lambda_s\frac{\partial^2 T_s}{\partial z^2} + (1-\epsilon_0)\lambda_s\frac{1}{r}\frac{\partial}{\partial r}\left(r\frac{\partial T_s}{\partial r}\right) \tag{2.25d}$$

The boundary conditions to solve the problem were the same as those stated before, but it was also included mass boundary conditions. The discretization was

performed by applying the finite volume approach, resulting in ordinary differential equations. Initial conditions were also similar. Their results showed that in narrow fixed-bed bioreactors heat exchange by the wall is relevant and gas velocity and moisture content become important in the case of absence of wall transfer.

One alternative to solving the distributed problem with reduction of computational complexity has been validated by SAHIR *et al.* (2007) against the same original data that SANGSURASAK and MITCHELL (1998) used for a pseudo-homogeneous model. It was further tested by MITCHELL *et al.* (2010) for the study on mode operations for packed-bed bioreactors in a two-phase description of the system. Their idea is to simplify the distributed problem within the reactor approximating the bed column to n-tanks in series. Instead of the partial differential equations, this originates a set of ordinary differential equations describing heat and mass transfer.

Finally, it is noteworthy that regardless of the consideration of distributed problems or not, no work on mathematical description of SSF fermentation with *Y. lipolytica* was found.

Chapter 3

Characterization of the soybean hulls and lipases

This chapter covers new analytical methodologies and characterizations that were used in the thesis development. For that, this chapter was divided into two sections, comprising the soybean hulls and the lipases.

3.1 Soybean hull analysis

3.1.1 Introduction

Besides its chemical composition, the physical properties of the solids used in bioprocesses are critical for the development of models describing transport phenomena in bioreactors (DE CASTRO *et al.*, 2016). Among the physical properties of the solid, density, porosity, heat capacity and transport properties are relevant for process design and operation. However, their resultant shape and size distributions obtained after solid classification are also relevant for these physical properties (GUO *et al.*, 2012) used in (bio)processes development. Some authors have used dedicated equipment for shape determination, such as the CAMSIZER (CARDOSO *et al.*, 2013, OLIVEIRA *et al.*, 2015). For instance, TIEMERSMA *et al.* (2006) used a shape factor for spherical particles for the effective radial and axial dispersion coefficients calculation in packed-bed reactors used for autothermal production of hydrogen. CASCIATORI *et al.* (2016) considered cross and parallel flow for calculation of interfacial heat and mass transfer coefficients around the biomasses used in the simulation of packed-bed bioreactor. The authors previously determined the particle shape and measured their length and diameter. Therefore, the objective of this section is to measure some of these properties needed as inputs for the solid-state fermentation modeling and simulation.

3.1.2 Material and methods

Granulometric classification and chemical composition

Soybean hull (BSBIOS, Passo Fundo-RS, Brazil) was ground in a hammer mill (Tecnal) and kept frozen at -20 °C until use and the same lot was used during the thesis course. After thawing at room temperature, the material was classified with number 14 and 32 mesh sieves, corresponding to particle diameter (d_P) in the range of 0.5 mm $<d_P<$ 1.18 mm, and heat sterilized for 22 min at 120 °C. After this, the sterilized material was cooled to room temperature before previous utilization. For humidity quantification, at least 0.5 g of solid was dried until constant mass in a humidity analytical balance (Tecnal) at 105 °C. Soybean hull elemental analysis was performed using the Thermo ScientificTM Flash 2000 CHNS/O analyzer (ThermoFisher).

Size and shape

Bright-field microscopy (Eclipse E200, Nikon®) was performed and 165 images were acquired and recorded as RGB tiff files with 24 bits using the software Image-Pro Plus® 5.0 (Media Cybernetics, Inc.). Since the goal was to analyze the whole material and not the soybean hull cells, images were taken at 40x magnification. Size calibration was performed externally with a micrometer and a conversion factor (1.9277 μm pixel^{-1}) was used in the processing routine implemented in Matlab R2008a (The Mathworks, Natick, Mass.). The image analysis occurred according to the processing steps described in Figure 3.1.

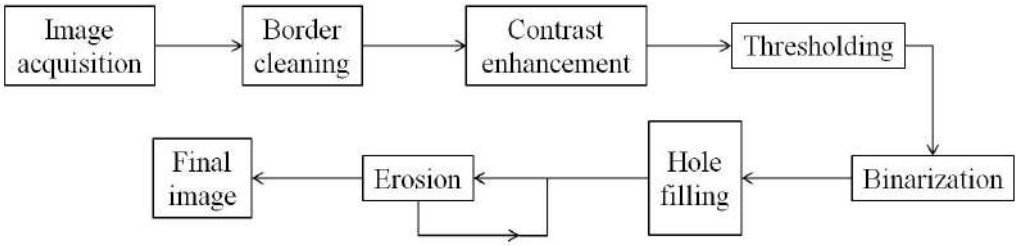

Figure 3.1: Steps of digital image analysis implemented on Matlab R2008a (The Mathworks, Natick, Mass.) used for soybean hull shape and size determination.

Erosion operations were performed to eliminate obvious artifacts generated during the processing. In these operations, the size range of the particles was used to aid in the process. Once the processing was done, the characteristic sizes (length, width and equivalent diameter) and shape factors (roundness and aspect ratio) of the objects were calculated with the following set of equations:

$$l = D_{Feret_{max}} \tag{3.1a}$$

$$w = D_{Feret_{min}} \tag{3.1b}$$

$$D_{eq} = 2\sqrt{\frac{A}{\pi}} \tag{3.1c}$$

$$Rd = \frac{4\pi A}{P^2} \tag{3.1d}$$

$$AR = \frac{D_{Feret_{max}}}{D_{Feret_{min}}} \tag{3.1e}$$

where $D_{Feret_{max}}$ and $D_{Feret_{min}}$ are the maximum and minimum Feret diameters, respectively, l is the length, w is the width, A is the projected area, P is the perimeter, D_{eq} is the equivalent diameter, Rd is the roundness and the AR is the aspect ratio. Additionally, the cumulative count of length, width and diameter were fit to the Rosin–Rammler–Bennett (RRB, Equation 3.2a), sigmoid (Equation 3.2b), and Gates–Gaudin–Schumann (GGS, Equation 3.2a)) models:

$$y = 1 - e^{\left(-\frac{s}{s_{63.2}}\right)^m} \tag{3.2a}$$

$$y = \frac{1}{1 + \left(\frac{s_{50}}{s}\right)^m} \tag{3.2b}$$

$$y = \left(\frac{s}{s_{100}}\right)^m \tag{3.2c}$$

where y is the cumulative count, s is the evaluated property, and m is a parameter. The subscript numbers indicate the value which corresponds to the percentage count in the cumulative distribution that is smaller than that size.

Density and porosity

Afterwards, the porosity of the solid material was measured according to the methodology used by DE CASTRO *et al.* (2016). It consists of gravimetric measurements of the solid material loaded in a 10-mL volumetric cylinder, which has its moisture content discounted and then provides an estimate of the dried bulk density (ρ_{ds}). Three types of packing were investigated for the measurement of densities and porosity. For the loose packing, the hulls were just poured into the cylinder, while the compact packing was obtained by tapping the solid and vibration packing was done with the aid of vortex at 3000 rpm, until no further change in volume was observed. The same procedure is conducted for the wet bulk density (ρ_{ws}), which requires water addition in the volumetric cylinder until all the material is wetted and the free water reaches the same height as the solid. After this, bed porosity (ϵ) is calculated with the Equation 3.3:

$$\epsilon_0 = 1 - \frac{\rho_{ds}}{\rho_{ws}} \tag{3.3}$$

3.1.3 Results

Digital image analysis

Important parameters for the development of heat and mass transfer models in reactors with solid particles can be measured by digital image analysis. In this work, two-dimensional image were acquired in bright-field microscopy, assuming the particle was at its most stable position. Visualization of some these images after processing with Matlab are shown in Figure 3.2.

Visual inspection of the images showed that a large amount of images were required (165 for 213 objects) to have a large number of objects for analysis, in contrast with yeast cells micrographs. Besides, border cleaning was also performed and eliminated some identified objects. Therefore, for a reliable analysis, the image acquisition step may become a laborious task. Despite the difference in luminosity throughout the micrographs, the routine was able to properly identify and separate the objects from the background, allowing the correct binarization while keeping the distinct features of the objects. However, at some cases the hulls were in contact, which led to a single object binarization. Although this might be primarily undesired, this contact between particles also happen in solid beds. Having this in mind, the soybean hulls properties were calculated. The cumulative distributions were plotted in Figure 3.3 and fitted to classic size distribution Equations (3.2a, 3.2b, and 3.2c). The parameters of the models are summarized in Table 3.1.

Table 3.1: Parameters for the cumulative distribution fit of length (l), width (w) and equivalent diameters (d_{eq}).

Model and	Characteristic dimension		
Parameters	w	l	d_{eq}
RRB			
m	5.59	4.18	-5.62
$s_{63.2}$	806.9	1335.4	992.2
R^2	0.87	0.88	0.84
Sigmoid			
m	-8.35	-6.18	8.47
s_{50}	729	1166	897
R^2	0.97	0.97	0.96
GGS			
m	3.94	2.94	-3.89
s_{100}	937	1631	1156
R^2	0.72	0.74	0.68

R^2:determination coefficient of the fitting.

Although the hulls used in this work were classified with sieves of 1.18 and 0.5 mm apertures, they presented rather disperse length distribution, varying in the range of 690 to 2480 μm, while the width was more concentrated in the range of 550 to

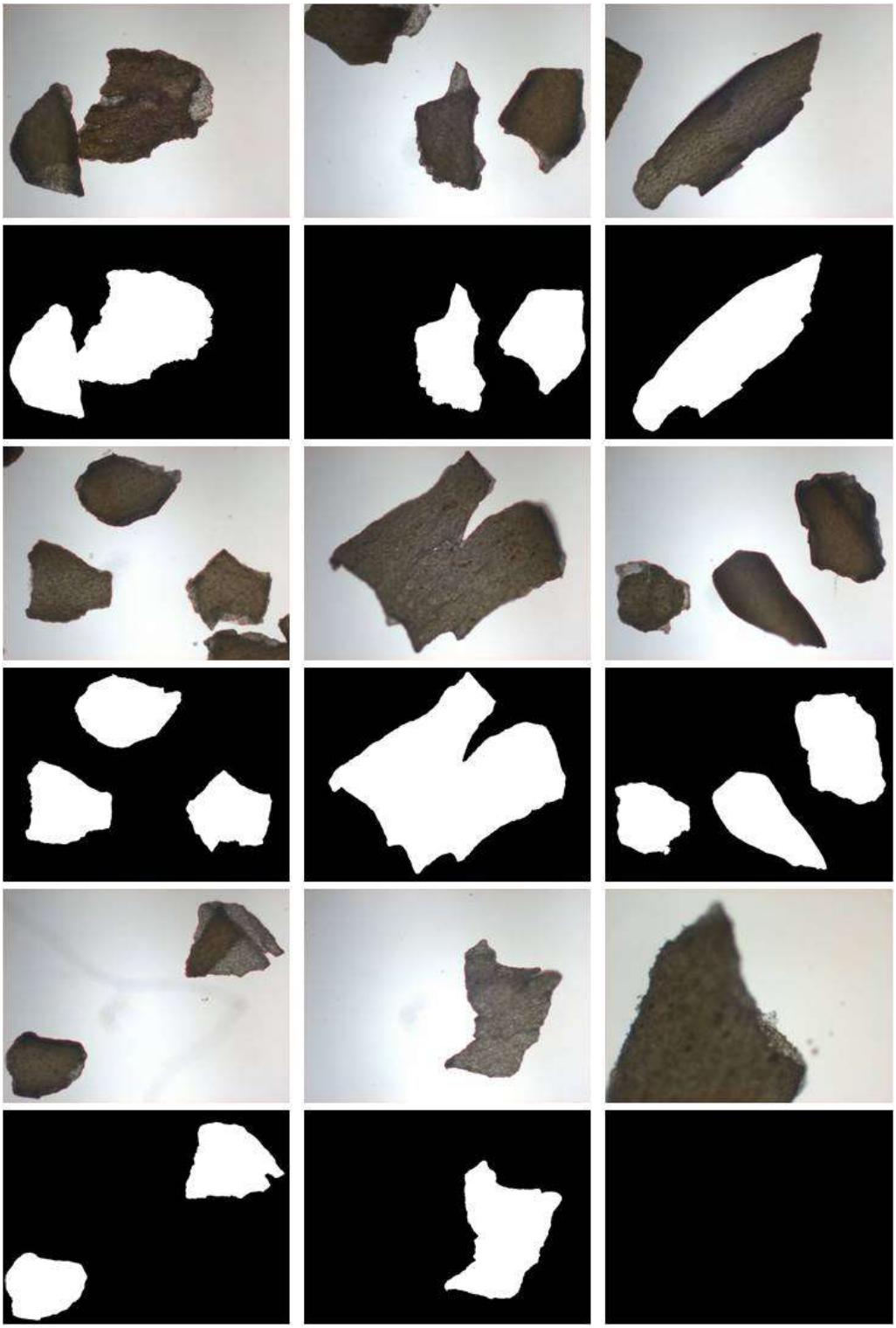

Figure 3.2: Digital images obtained by bright-filed optical microscopy at a total of 40 x magnification of soybean hulls after autoclave sterilization and their binary versions after automatic image processing.

850 μm. The equivalent diameter, which is influenced by these parameters, was closer to the distribution of the width, with a range of 650 to 1050 μm. Depending on the particle type and pretreatment, different size distributions are obtained. For

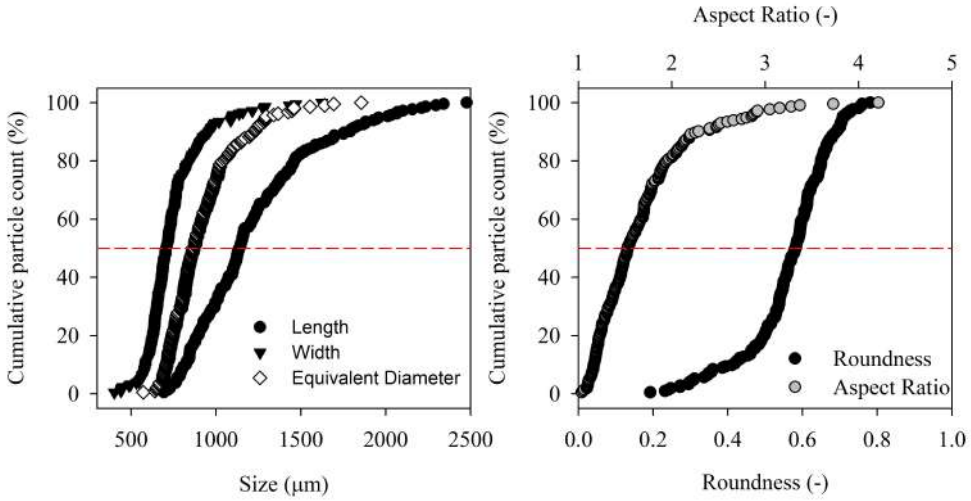

Figure 3.3: Cumulative distributions of length, width, equivalent diameter, aspect ratio and roundness of soybean hulls ($0.5<d_P<1.18$ mm) after heat sterilization in autoclave. The red dashed line indicates the cumulative value that accounts for 50 % of the counts.

example, GUO *et al.* (2012) characterized multiple biomasses (pine, beanstalk, rice straw and reed) and fitted the size distribution data of all biomasses together to a linear equation. DE CASTRO *et al.* (2016) had better fits using the sigmoid model for babassu, castor seed and sunflower cakes, and the RRB model for canola cake. Three models were used to describe the hulls size distribution and the best results (based on R^2 values) were found for the sigmoid model. In this case, the l_{50}, w_{50},and $d_{eq_{50}}$ values were equal to 1166, 729, and 897 μm, respectively.

The average diameter of the sieves used herein is 840 μm (or 768 μm, if the geometric mean is considered instead), somewhat similar to $d_{eq_{50}}$. CARDOSO *et al.* (2013) found l_{50} and w_{50} values of 1500 and 800 μm for the soybean hulls classified with 710-850 μm sieves, while OLIVEIRA *et al.* (2015) found 1500 and 760 μm with 710-850 μm sieves. The values for the width are close to the values calculated in this work, but it is relevant to mention that these authors measured this properties after analysis of much larger samples (several magnitude orders) and assumed that their data are consistent with the real values. GUO *et al.* (2012) also evaluated biomass samples with twice the value of object counts and the widths were in almost all cases in the range of granulometric sieving, while the lengths were not, and attributed this fact to the needle-like shape of the particles, which indicated that irregular particles may not be correctly classified with sieving. During sieving, the particles may align in the direction of smaller size, allowing them to pass through the apertures.

Figure 3.2 illustrates well the larger and narrower distribution of lengths and widths of the soybean hulls and their diverse forms. Despite that, the AR_{50} and Rd_{50} obtained by visual inspection of the red dashed line in Figure 3.3 were equal to

1.53 and 0.58, respectively. The roundness indicates that the degree of sharpness on the particle edges and the closer this value is to one, the more the projected image of the particle approximates to a circle. Our results were similar to those previously reported, while the AR_{50} was smaller (CARDOSO *et al.*, 2013, OLIVEIRA *et al.*, 2015), showing that the particles used in this work seemmed less elongated. However, it is not clear if this was due to the mathematical definition of AR applied, since these authors used the Martin diameter instead of the Feret one in the denominator, and once Martin diameter is generally smaller than Feret's (PEÇANHA, 2014), this would lead to larger values.

Physical and chemical characterization

Porosity is an important parameter to be determined for the success of microbial solid-state fermentations (DE CASTRO *et al.*, 2016, PITOL *et al.*, 2017). The packing technique used to form the bed structure during the use of biomasses is known to influence the physical properties, specially the bulk densities and porosity (CASCIATORI *et al.*, 2014, DE CASTRO *et al.*, 2016). Therefore, the bulk density and porosity measurements shown in Table 3.2 were evaluated according to three types of packing: loose, compact and vibration, as described elsewhere (CASCIATORI *et al.*, 2014).

Table 3.2: Bulk densities and porosity for different packing techniques of soybean hulls.

Packing technique	Bulk density (kg m^3)	Porosity (m^3_{void} m^{-3}_{bed})
Loose	265.60±11.58	0.725±0.004
Compact	308.37±9.61	Not measured*
Vibration	330.88±12.80	Not measured*

*Complete flooding of the samples was not achieved.

The lowest bulk density observed was obtained for the loose packing, with increasing values for the other packing techniques that apply more energy into the system, thus promoting the movement of the solid and accommodation and removal of air. Porosity measurements were assayed for all the types of packings, but as the bulk density increased, flooding of the system by slowly pouring water was not possible because air could not escape from the pores of the system, possibly due to its swelling capacity (MATIN *et al.*, 2013). The porosity value that was successfully measured herein was found to be smaller than those found by CASCIATORI *et al.* (2014) for sugarcane bagasse and higher than those of orange pulp and meal and wheat bran. However, for the mixture of sugarcane bagasse and wheat bran (7:3), at 80 % moisture content and loose packing, the porosity found was 0.746±0.010 m^3air m^{-3}bed. They also found an exponential decay dependence on

moisture content for the porosity, while the bulk density augmented.

Bulk densities in all cases were smaller than the value measured by CARDOSO *et al.* (2013) for soybean hulls, but in the same range of tobacco residue, sweet sorghum and fiber sorghum bagasses. Moreover, the values found herein are also similar to those obtained for castor seed cakes before packing (244.6±11.1 and 375.6±19.7 kg m^3, before and after packing, respectively) by DE CASTRO *et al.* (2016). Given the similarity to these other biomasses, the difference found for the hulls may be related to the methods used by CARDOSO *et al.* (2013), who first dried the soybean hulls at 105 °C and used them without prior sieving. This hypothesis is confirmed by these authors' analysis of true density before and after drying, specially for the bigger particles which were in a size range close the ones used herein.

DE CASTRO *et al.* (2016) attributed the low bulk density values and the high porosity to the damaged and channeled structure observed in scanning electron microscopy (SEM). In our optical microscopy study, the light intensity passing through the hulls in Figure 3.2 gets darker in some cases and may be from the superposition of hulls or from hulls with larger depth. Thus, it is possible that this superposition of one sheet of the hull over another may create this channeled structures that would increase the porosity, supported by the "flat" appearance that the particle presents.

The chemical composition of the hulls, assessed by the elemental analysis and moisture content determination, is shown in Table 3.3. The low nitrogen and sulfur mass percentages of the sample are consistent with the values expected for the majority of carbohydrate source and are in accordance with the ones measured by OLIVEIRA *et al.* (2015). The low protein content inferred from this analysis and corroborated with other data found in the literature (BRIJWANI and VADLANI, 2011, BRIJWANI *et al.*, 2010, LOMAN and JU, 2016, LÓPEZ *et al.*, 2018) pointed out a potential need for nitrogen supplementation upon use in solid-state fermentation. The low moisture content, close to the values of low water activity show in Figure 2.6 indicates that this raw material is not susceptible to natural microbial deterioration, based on classical water activity requirements.

Finally, as the values obtained in this section seems to correlate well with other reports, we concluded that the parameters which were not measured can be reliably outsourced from other studies.

Table 3.3: Elemental composition and moisture content of soybean hulls.

	Content (% m m^{-1})
Moisture	12.2±0.7
Element	
C	38.1±0.0
N	1.6±0.2
H	5.7±0.2
S	<0.3[a]
O	45.5±4.5

[a]Below detection level.

3.2 Lipase activity assays

3.2.1 Introduction

Several ways of assessing lipase reaction rates are available and have already been reviewed (BEISSON *et al.*, 2000, HASAN *et al.*, 2009). From the perspective of the molecular alterations happening at interfaces, techniques such as drop tensiometer combined with oil-water emulsion digestion are interesting (YAO *et al.*, 2013). However, to quickly assess substrate specificity or monitoring the bioprocess, this techniques may be inadequate.

The main procedures used while assaying *Y. lipolytica* lipases include: the end-point method of hydrolysis of triacylglycerols followed by titration of the released organic acids at constant pH (referred to as "lipolytic activity" through the text) (CAO *et al.*, 2017, DE SOUZA *et al.*, 2019, PEREIRA-MEIRELLES *et al.*, 1997, PIGNÈDE *et al.*, 2000, SALES *et al.*, 2020, SOUZA *et al.*, 2017); and the method of hydrolysis of 4-nitrophenyl fatty acid esters, which is a kinetic or end-point method wherein the product of the reaction 4-nitrophenol is quantified spectrophotometrically in the range of 405-410 nm (cited as "hydrolytic activity" herein) (BORDES *et al.*, 2010, IMANDI *et al.*, 2013a, LOPES *et al.*, 2016, PEREIRA-MEIRELLES *et al.*, 1997, SANTOS *et al.*, 2019).

The lipolytic method (with triacylglycerols) is continuous and can be automated and used with diverse substrates (HASAN *et al.*, 2009), though it has a limited sensitivity to 1 µmole of released fatty acid per minute and thus is not reliable for values smaller than 0.1 μmole min^{-1}. Besides, the final pH of the assay need to be above the pK_a of the fatty acid to guarantee its ionization and quantification (BEISSON *et al.*, 2000).

The hydrolytic method is not specific for lipases (esterases and proteases can hydrolyze them too). Moreover, lipases tend to act on primary esters bonds, while these esters are secondary, and in the case of p-nitrophenyl esters, it is recommended to use an inert micellar reagent to diminish spontaneous hydrolysis (BEISSON *et al.*,

2000). Some formulations propose the use of gum arabic (PALACIOS *et al.*, 2014, ŠIBALIĆ *et al.*, 2020), both gum arabic and Triton X-100 (KORDEL *et al.*, 1991, MASTIHUBA *et al.*, 2002) or ethylene glycol (HERNÁNDEZ-GARCÍA *et al.*, 2017) to dissolve the substrates. PALOMO *et al.* (2003) used 0.1 % Triton X-100 in their enzymatic assay to also avoid lipase aggregation, using 4-nitrophenyl butyrate or palmitate as substrates.

One last piece of information is that the $p\mathrm{K}_a$ of 4-nitrophenol is 7.15. Given the fact that there is an equilibrium between 4-nitrophenol and 4-nitrophenolate, in order to quantify the yellow product of the reaction at 405-410 nm, one should be careful enough to guarantee that no changes in pH values during the assays happen, since the molar extinction coefficient of phenolic solutions depends on the ionization state and, therefore, on pH (HASAN *et al.*, 2009). In this case, calibration curves should be performed for each pH. To exemplify this situation, Figure 3.4 shows the behavior of the absorption spectra of 4-nitrophenol at different pH values.

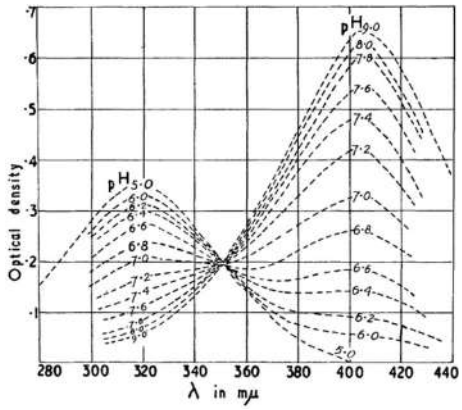

Figure 3.4: Absorption spectra for 4-nitrophenol solutions at different buffered solutions. The figure was withdrawn from BIGGS (1954).

The solution to this problem that has not been tackled so far (to the best of my knowledge) could be the quantification of the reaction product at the isosbestic point[1]. At this point, pH changes do not interfere in the absorbance of the reaction once it will be proportional to the sum of both species instead of one of them. Thus, true lipase activity would rather be assayed by the lipolytic method, but as a tool for accessing substrate specificity or for faster process monitoring, the hydrolytic procedure could be used. This logic was used in most studies of lipase production by *Yarrowia lipolytica*.

[1]The isosbestic point is the one represented by the wavelength where the optical density is equal at all pH values.

3.2.2 Material and methods

Enzyme extracts from solid-state fermentation of soybean meal supplemented with soybean oil with *Y. lipolytica* were kindly donated by the researcher Julio Sales, who produced it as described elsewhere (SALES *et al.*, 2020). Briefly, the samples were taken after 14 h of fermentation, extracted at 35 °C, with 50 mM phosphate buffer (solid-liquid ratio of 1 g:5 mL) at 200 rpm orbital shaker agitation, squeezed and centrifuged at 2000 g for 5 min. After this, the supernatant was frozen until further usage.

The enzymatic assay was then studied using the method of hydrolysis of 4-nitrophenyl dodecanoate using a Microtiter plate reader (SpectraMax M2e, Molecular Devices). Polystyrene microplates were used in the assay and at least one blank reaction (substitution of enzyme volume by buffer in one microplate well) was used at each round of measurements. After thawing the samples at room temperatures, the extract was 15-fold diluted with the same buffer used for extraction. The kinetic assay was performed by incubation of 20 μL of the enzyme solution at 37 °C for 5 min before addition of the 180 μL of substrate solution. This order was used to provide a better homogenization inside the well.

A study following the rationale of the surface dilution kinetic was conducted using the mixture of DMSO and Triton X-100 as "neutral dilutor". This was performed by fixing the bulk concentration of 4-nitrophenyl dodecanoate while varying the dilutor mixture. The mixtures followed the values in Table 3.4.

Table 3.4: Volume fraction of DMSO and Triton X-100 used in the enzyme assays development. The calculation was made on the basis of 20 μL stock substrate solution

$V_{TritonX-100}$	V_{DMSO}
100	0
095	5
80	20
50	50
20	80
10	90
5	95
2	98
1	99
0	1

A stock concentrated substrate solution (2.8 mM) was prepared by initially solubilizing the substrate in DMSO or Triton X-100 in microtubes. To achieve complete solubilization, a thermomixer (Eppendorf) was used to keep them at 37 °C. After this, the stock solutions were diluted in DMSO or Triton X-100 and transferred to

pre-heated conical tubes. Heating of the tubes was necessary once it was observed that cold tubes led to substrate adhesion on the wall. Next, the 50 mM phosphate buffer was added to the substrate to achieve the desired bulk substrate concentration. Also, the DMSO/Triton X-100 mixture was kept at a constant volume ratio of 1:100 (DMSO-Triton X-100/ phosphate buffer).

As the extinction coefficient of analytes in spectrophotometric techniques is highly dependent on the reaction conditions (ŠIBALIĆ *et al.*, 2020), it is worth mentioning that each mixture required a different calibration curve, since increasing amounts of detergent modify the signal measurement of the reaction product.

3.2.3 Results

In order to primarily decrease background solution interference in the enzymatic assay, different combinations of DMSO and Triton X-100 were used since the characteristic of the interfaces would also change. The solvent and detergent were used individually for comparison purposes. The results comprising background absorbance are shown in Figure 3.5.

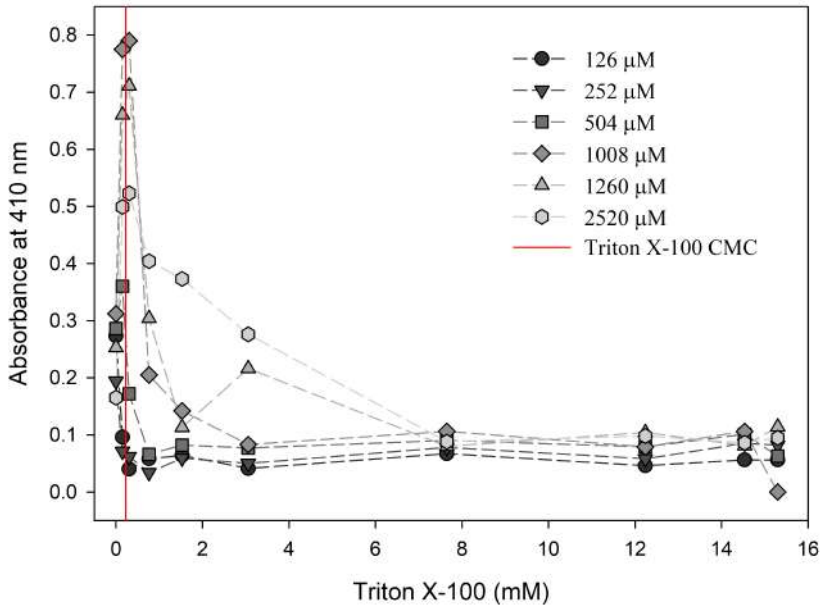

Figure 3.5: Absorbance of the blank (enzyme replaced by buffer) in the presence of the mixture of Triton X-100 (detergent/solvent) and DMSO. Different symbols were used to represent the studied *p*-nitrophenyl dodecanoate concentrations. CMC: critical micellar concentration.

According to the Figure 3.5, the final substrate preparation was either optically clear or opaque solutions, depending on the solvent/detergent mixture, as it is shown by the values of absorbance at 410 nm, which is typically used during enzymatic

assays. The values initially increased with the small addition of the detergent and then decreased and reached values of absorbance (410 nm) in the order of 0.1 for all substrate concentrations when Triton X-100 was used at 50 % v/v or higher percentage. For the three smaller bulk substrate concentrations, absorbance decayed promptly after the detergent CMC. This indicates that the detergent in higher concentrations is required to modify the whole substrate aggregation state. It is also likely that substrate aggregation occurs without the detergent, since the critical concentration for 4-nitrophenyl dodecanoate can be as low as 0.1 μM (GUTHRIE, 1972). In general, amphipathic substances having a single tail, such as fatty acids and detergentes such as Triton X-100, form spontaneous micelles above their CMCs without requiring sonication. Detergents are also used to form mixed micelles when added to a long-chain phospholipid vesicles. In this case, mixed micelles results in a less opaque solution, showing a decrease in light scattering (DEEMS, 2000). Thus it is possible that detergent inclusion results into phase transition to mixed micelles.

Following these findings, activity assays were conducted at the same substrate and Triton X-100/DMSO concentration, for which the results are found in Figure 3.6. The data plotted against Triton X-100 (Figure 3.6a) shows that lipase activity suffers a drastic reduction upon addition of the detergent, in the region before and around the CMC. The same finding was reported by BRÍGIDA (2010), which also observed some activation at 0.0005% Triton X-100. DE SOUZA *et al.* (2019) observed a decay in activity only in concentrations above the CMC using the lipolytic method with gum arabic. In smaller concentrations, lipase activity also suffers small interference from Tween-80 (another non-ionic surfactant) in gum arabic emulsions (YAO *et al.*, 2013). ALOULOU *et al.* (2007b) used purified Lip2p extract from SmF in the lipolytic assay without gum arabic (mechanically stabilized emulsion) and showed that activity could be measured only after the addition of sodium taurodeoxycholate, because lip2p of *Y. lipolytica* could be denatured in pure oil-water interface. This was also confirmed in another study with other detergents (ALOULOU *et al.*, 2007a), when the authors also evaluated Triton X-100 in concentrations that ranged from lower to higher than the CMC, showing a decay in activity with increasing detergent concentration. Therefore, the retention or activation of lipases in small concentrations of detergents should be related to a decrease in interfacial tension, which help in avoiding inactivation.

The drop in lipolytic activity can be related to the removal of substrate from the interface by tensoactive components. YAO *et al.* (2018) verified that the emulsion preparation method influence in the composition of the interface. Co-adsorption of Tween-80 and gum arabic or sequential adsorption of Tween-80 and gum arabic lead to an oil emulsion fastly covered by Tween-80 (it displaced the gum arabic used for stabilizing oil emulsions), while addition of Tween-80 to gum arabic stabilized emul-

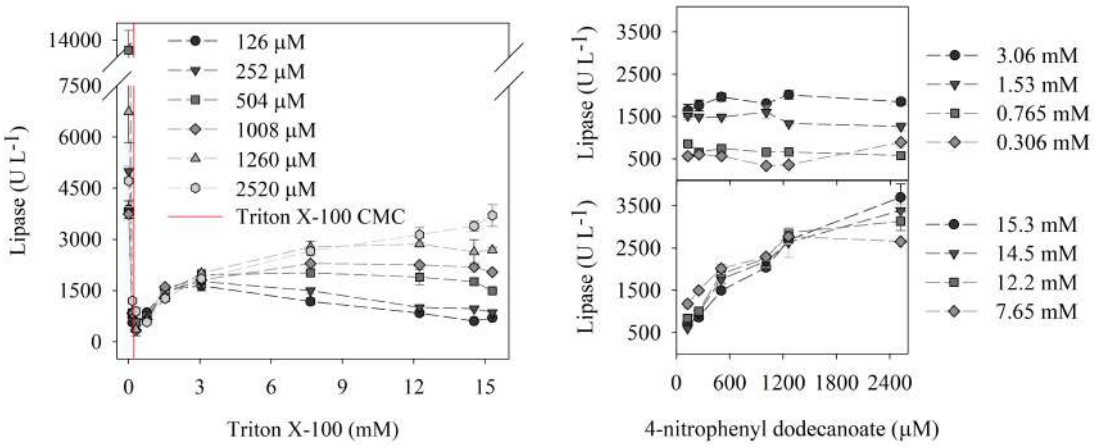

(a) (b)

Figure 3.6: Lipase activity in the presence of the mixture of Triton X-100 (detergent/solvent) and DMSO in various 4-nitrophenyl dodecanoate bulk concentrations. The data were plotted separately against the Triton X-100 (a) and bulk substrate (b) concentrates. In the second case, only the data from Triton X-100 above its critical micellar concentration (CMC = 0.23 mM) were plotted.

sion required more than 2 h for Tween-80 to fully adsorb. In high concentrations, it led to a reduction in both lipase adsorption rate and consequently the reaction rate (YAO *et al.*, 2018). Other possible reason for this can be the direct interaction of the enzyme with detergent micelles (YAO *et al.*, 2013). In our work, it is unlikely that free Triton X-100 caused the fast decay in activity in concentrations smaller than the CMC. Possibly, this is related to the smaller reactivity of the 4-nitrophenyl acyl esters after addition of Triton X-100 (BEISSON *et al.*, 2000).

For 4-nitrophenyl dodecanoate values smaller than 500 μM, the enzyme(s) seemed to be rather insensitive towards the detergent increase from 0.306 to 3.06 mM (already above the CMC) (Figure 3.6a). Nonetheless, at each detergent increase, activity reached a new higher plateau (Figure 3.6b), supporting the idea that substrate was not completely available in the micelles for hydrolysis and that in all cases, the substrate concentration in the micelles might have been equal. After 7.65 mM Triton X-100, activity diminished again, pointing possible inhibition effects. However, once the Triton X-100 concentration increases, the behavior changes. When large bulk substrate concentrations are used, a curve closer to the typical Michaelis-Menten is observed (Figure 3.6b), with differences in the maximum activities obtained for the substrate concentrations above 1000 mM. Despite that, these values are still smaller than those obtained in the system without Triton X-100 and in this sense, they are in accordance with the works previously mentioned.

BRÍGIDA (2010) used Michaelis-Menten parameters to describe lipase kinetic

behavior in SmF supernatant samples. In contrast, FRAGA *et al.* (2020) used the allosteric model and the Hill equation to describe CBLF samples. To gather more qualitative information, the classical Lineweaver-Burk plots were done and shown in Figure 3.7.

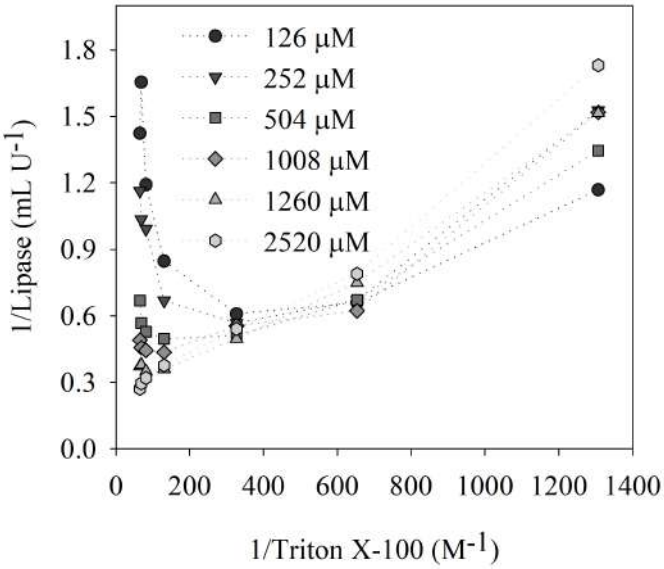

Figure 3.7: Lineweaver-Burk plots of lipase activity *versus* Triton X-100 concentration for various 4-nitrophenyl dodecanoate bulk concentrations.

The non-linear behavior observed in the plot for the low 4-nitrophenyl dodecanoate concentrations illustrated the deviation from the Michaelis-Menten behavior, mainly for small substrate concentrations. This deviation may occur from diverse reasons, including the presence of multiple enzyme forms or to different substrate interactions (activation, inhibition, multiple binding or cooperative effects) (PUNEKAR, 2018). Lip7p and Lip8p may be recovered from the cell wall with phosphate buffer washing (FICKERS *et al.*, 2005a), being a simple protocol like the one used for enzyme extraction in solid-state fermentation. However, as Triton X-100 is not a real substrate for the enzyme, it is possible that it interacts with them in a similar fashion, causing one of the substrate effects. It is known that cell wall proteins can be extracted with Triton X-100 (DEEMS, 2000). Possibly, the detergent in higher amount interacts in a non-specific manner with the enzyme, leading to this inhibitory effect (CARMAN *et al.*, 1995, YAO *et al.*, 2013). Thus it is more likely that detergent-enzyme interaction occurs, which would make this compound unsuitable as neutral diluent for surface dilution kinetic studies, at least in small ratios Triton X-100:substrate. Therefore, it is likely that Triton X-100 increases the amount of surfaces available for enzyme action given that this ratio is large enough.

Chapter 4

Production of lipase by *Y. lipolytica* by solid-state fermentation of soybean hulls

4.1 Preliminary experimental development

Initial experiments were conducted to provide knowledge about lipase production using the soybean hulls, which had not been used yet for this. At this stage, lipase activity quantification was performed using only DMSO as solvent for 4-nitrophenyl dodecanoate solubilization. Part of the results in this section were presented at the XXII National Bioprocesses Symposium (SINAFERM) / XIII Enzymatic Hydrolysis of Biomass Symposium (SHEB), in 2019.

4.1.1 Material and methods

Y. lipolytica pre-culture

Yarrowia lipolytica IMUFRJ 50682 strain, which was isolated from the Guanabara Bay in Rio de Janeiro, Brazil (Hagler e Mendonça-Hagler, 1981) and identified at the Federal University of Rio de Janeiro, was used for lipase production. Previously grown cells in YPD (Yeast Peptone Dextrose) medium were maintained frozen in glycerol solution (50%) at -50 °C and thawed by 28 °C heat shock, centrifuged and the supernatant was discarded. After this, cells were resuspended in liquid YPD medium and grown for 72 h at 28 °C and 160 rpm. YPD was composed of (in g L^{-1}): bactopeptone, 20; glucose, 20 and yeast extract, 10.

Solutions and reagents for protein analysis

Stock and extraction Buffer Stock buffer (200 mM potassium phosphate buffer, pH 7.0) was composed of 4.246 g of KH_2PO_4 and 8.5 g of K_2HPO_4 that was solubilized in distilled water to a final volume of 0.8 L and kept at room temperature until used. The extraction buffer (50 mM potassium phosphate buffer) is freshly prepared by diluting the stock phosphate buffer to a final concentration of 50 mM.

Lipase (hydrolytic) activity Just before starting the assay, 0.018 g of 4-nitrophenol dodecanoate (4-NPD, 321.41 g mol^{-1}, 98 %) is solubilized into 1 mL of dimethyl sulfoxide (DMSO) by vortexing. This solution was then diluted with extraction buffer reaching a final 4-NPD concentration of 0.55 mM.

Proteolytic activity 50 mM acetate buffer (pH 5.0) was prepared by solubilization of 2.395 g of sodium acetate in 200 mL of water, followed by mixing with 0.444 g of acetic acid (0.42 mL, 1.05 kg L^{-1}) and adjusting the final volume to 500 mL. Thus, it was used for preparing a 0.5 % m/V solution of azocasein, substrate of the proteolytic assay. 5 M potassium hydroxide (56.11 g mol^{-1}) was prepared by solubilization of 56.11 g in 200 mL of water. The trichloroacetic solution was prepared by solubilization of 15 g of it in 100 mL of water.

Protein quantification Stock bovine serum albumin solution (50 mg L^{-1}) was prepared by slowly diluting 1 mg of the protein in 15 mL of ultrapure water. After water was added until reaching the final volume of 20 mL and the solution was aliquoted in microtubes before storing at -20°C. The Coomassie Brilliant Blue G-250 reagent was prepared by first solubilizing 100 mg of the dye powder into 50 mL of ethanol (95 %) and then adding 100 mL of phosphoric acid (85 %). Then the volume of the solution was adjusted to 1 L by adding ultrapure water. This solution was then filtered and kept at 4°C until usage.

Fermentation

Precultured ovoid cells of *Yarrowia lipolytica* were sampled and absorbance was measured at 570 nm, which was then converted to cell concentration with a calibration curve. Cells were centrifuged at 3000 rpm for 15 min and then resuspended in a fixed spent medium volume and poured into the solid matrix (prepared as described in Chapter 3)), followed by a homogenization with a fork. Humidity was then adjusted with a solution containing the desired supplementation and the whole material was again homogenized with a fork. The appropriate volume of solution as it follows. The moisture content (MC) of the solid is defined as the ratio between the mass of

liquid (m_{liq}) and the wet mass of the sample (m_{ws}), which is the sum of of m_{liq} and the mass of the dry solid (m_{ds}) (Equation 4.1):

$$MC(\%) = \frac{100\ m_{liq}}{m_{ws}} \therefore MC = \frac{100\ m_{liq}}{(m_{liq} + m_{ds})} \tag{4.1}$$

After some algebraic manipulation, the previous equation can be written as a function of the mass of liquid (Equation 4.2):

$$m_{liq} = \frac{m_{ds} MC}{100 - MC} \therefore m_{liq} = \frac{m_{ws}(100 - MC_{sample})MC_{adj}}{100 - MC_{adj}} \tag{4.2}$$

where MC_{sample} is the actual moisture content of the sample and MC_{adj} is the desired moisture content after adjustment. The total mass of liquid is a sum of the supplementation solution ($m_{supplementation}$), the actual moisture content of the sample and the inoculum ($m_{inoculum}$) masses as it follows (Equation 4.3)

$$m_{liq} = m_{supplementation} + m_{ws}\ MC_{sample} + m_{inoculum} \tag{4.3}$$

Thus the mass of nutrient solution to be supplemented can be calculated once the mass of inoculum is fixed, which includes both the cells and the supernatant from the spent medium. In this study, the mass of inoculum and the nutrients to be supplemented varied according to the development of this work.

For the cultures in tray bioreactors, either 10 g (beaker) or 0.5 g (bottle) of soybean hull was utilized while 400 g of the same material was used in the packed-bed bioreactor (Figure 4.1). Table 4.1 summarizes the general features of bioreactors used for this work. Tray bioreactor experiments were conducted with air saturated environment at 28 °C. The same temperature was chosen for the fixed-bed bioreactor, but forced aeration was applied in this case. Sterile compressed air (filtered with 0.22 μm heat sterilized filter) at a gas flow of 5 L min^{-1} was sparged directly into the sterile water (previously autoclaved in the same conditions as the soybean hull) in order to become saturated and then supplied in the bottom of the bioreactor.

Table 4.1: Solid-state fermentation bioreactors used in this work.

Bioreactor	Material	Height (cm)	Loaded height (cm)	Diameter (cm)
Bottle	Glass	5.69	1	2.46
Beaker	Polypropylene	9.30	2	6.88
Packed-bed	Glass	36	28	10

The temperature was recorded with PT-100 thermocouples at 4 different heights (5.6, 11.6, 17.6 and 23.6 cm) and radii (1.32 and 4.09 cm) and samples of approximately 1.5 g were collected at 3 different heights (7, 14 and 21 cm) for quantification of cells and protein concentrations, lipase and protease activities, pH and humidity.

Figure 4.1: Fixed-bed bioreactors used for solid-state fermentation. In the center, the insulated packed-bed bioreactor with a vacuum-sealed jacket is filled with soybean hulls. The volumetric cylinder used to humidify the air before entering the bioreactor is shown in the right. A schematic drawing of the bioreactor system is also shown in Figure 4.7.

Extraction, pH and protein content determination

0.5 g of fermented material was aliquoted to measure humidity with a humidity analytical balance (Tecnal) in duplicate, while 0.25 g was aliquoted in duplicate for other analyses. Enzymes extraction was performed with 50 mM potassium phosphate buffer at 35 °C and 1000 rpm agitation in a thermomixer (Eppendorf) for 20 min. After extraction, the suspended material was submitted to centrifugation at 6000 rpm for 15 min and the supernatant was collected and frozen for quantification of total protein content, lipase, and protease activities. Cells were extracted following the same procedure, using water for extraction and eliminating the centrifugation step. pH was measured in cell extracts with a bench pHmeter.

Total protein quantification

Protein quantification from extracts was determined following the method of BRADFORD (1976) adapted to microtiter plates. A calibration curve ranging from 5 to 40 mg L^{-1} was prepared and applied to the plate (at least in duplicate) for every set of analyses performed. The procedure consists of mixing in each well 40 μL of the protein solution (either extracts or BSA standards) with 160 μL of the Coomassie

Brilliant Blue G-250 reagent and incubating the plate for 5 minutes at room temperature. Later, absorbance at 595 nm of the samples are registered by means of a microtiter plate reader (SpectraMax, Molecular Devices) and converted to concentration values according to the established calibration curve. Blank samples are prepared by replacing the samples with the extraction buffer.

Lipase (hydrolytic) activity quantification

Lipase activity from extracts was quantified by the method of 4-nitrophenyl dodecanoate hydrolysis with spectrophotometrical quantification of 4-nitrophenol at 410 nm. The assay was kinectly performed at 37 °C in a microtiter plate reader (SpectraMax, Molecular Devices) by mixing 20 μL of the sample with 180 μL of substrate solution. One activity unit was defined as the amount of enzyme capable of producing 1 μmol of 4-nitrophenol per minute in the assay conditions.

Protease activity quantification

Proteolytic activity from extracts was performed by the hydrolysis of the chromogenic substrate azocasein (CHARNEY and TOMARELLI, 1947). 100 µL of a 0.5 % m/V azocasein solution prepared in 50 mM acetate buffer (pH 5.0) was added to an equal volume of enzyme extract and incubated at 32 °C for 40 min with agitation. The reaction was stopped by addition of 100 μL of 15 % m/v trichloroacetic acid solution and samples were centrifuged at 3000 rpm for 15 min. 100 μL of supernatant from each sample and 100 μL of 5 M potassium hydroxide were then added into the 96-microtiter plate and absorbance at 428 nm was recorded in a microtiter plate reader (SpectraMax, Molecular Devices). One activity unit was defined as the amount of enzyme capable of producing a unitary increase in absorbance per minute.

Cell quantification

The cell content in the fermented biomass was indirectly quantified by means of the glucosamine assay proposed by AIDOO *et al.* (1981) with some modifications. 0.25 g of fermented material was hydrolyzed with 5 mL of 2.2 M HCl at 100 °C for two hours. A 2 mL sample of the hydrolysis product was titrated with 2.5 M NaOH using phenolphthalein solution until reaching the final point and then back-titrated with 1 % m/V $KHSO_4$. Following this, one part of the hydrolysis product was reacted with one part of acetylacetone solution in 0.25 M sodium carbonate (1:50 volumetric proportion) at 100 °C for 20 min in order to produce *N*-acetyl-glucosamine, which is then condensed and dehydrated with Ehrlich Reagent and ethanol (one and eight parts, respectively) at 65 °C for 10 min. Finally, absorbance at 530 nm was measured

and compared to a standard glucosamine calibration curve for the determination of glucosamine content. The standard glucosamine samples for calibration curve were submitted to both acetylation and condensation/dehydration reactions at the same conditions.

Preliminary assays in the adiabatic fixed-bed bioreactor

In order to understand and gain knowledge about the thermal behavior of the proposed process, cells were inoculated in soybean husks supplemented with soybean oil in the insulated packed-bed bioreactor(PBB), according to the procedure described in Section 4.1.1. At the same time, cells were inoculated in conventional tray bioreactor for comparison reasons.

Evaluation of supplementation strategies for increased lipase production

Aiming at increasing the lipase activity obtained, different nitrogen and carbon sources were tested. At a first moment, glucose solution and glucose/diammonium phosphate solution were investigated, maintaining soybean oil supplementation as a control in polypropylene beakers. All the supplementations were performed with stock solutions for a 1.5 % mass ratio of supplemented material to soybean hulls. Later, other carbon sources and nitrogen sources were separately tested in glass bottles, at the same mass ratio, including glucose, glycerol, soybean oil (control), urea, diammonium phosphate, and sodium nitrate. All the assays were performed in biological replicates.

Given the results, a central composite orthogonal rotational design (CCORD) was performed in order to test for possible interactions between nitrogen and carbon sources. Also, as humidity is important for the supply of water to sustain growth, this third variable was used to in this design. A set of seventeen fermentations was performed in glass bottles, according to Table 4.2, along with six additional center points fermentations in order to have a design which was both rotational and orthogonal. Statistical evaluation was performed using the software Statistica 7.0.

Table 4.2: Central composite orthogonal rotational design (CCORD) for evaluation of humidity, carbon and nitrogen sources for lipase production by *Yarrowia lipolytica*.

Variable	Experimental level				
(%g g^{-1})	-1.68	-1	0	+1	+1.68
Glucose	0.24	0.75	1.5	2.25	2.76
Diammonium phosphate	0.24	0.75	1.5	2.25	2.76
Moisture content	46.59	50	55	60	63.41

4.1.2 Results and discussion

Fermentation assays

As a way to gain experience in working with this type of bioreactor and to have an initial understanding of the behavior of *Y. lipolytica* cells in this system, a preliminary experiment with 1.5 % soybean oil supplementation was performed in the packed-bed and tray (beaker) bioreactor. The later served as control experiment. Given the fact that the fermented material has low density, in order to avoid holes gradually formed in solid matrix from sampling, samples were withdrawn only at predetermined times based on previous fermentations results not shown. Also, the thermocouples were adjusted to the specific positions that were used further for modeling (to the roots of Jacobi polynomials). The temperature data from the packed-bed can be observed in Figure 4.2, along with the data for enzyme production, pH and *N*-acetylglucosamine in Figure 4.3. Data from the tray is presented in Figure 4.4.

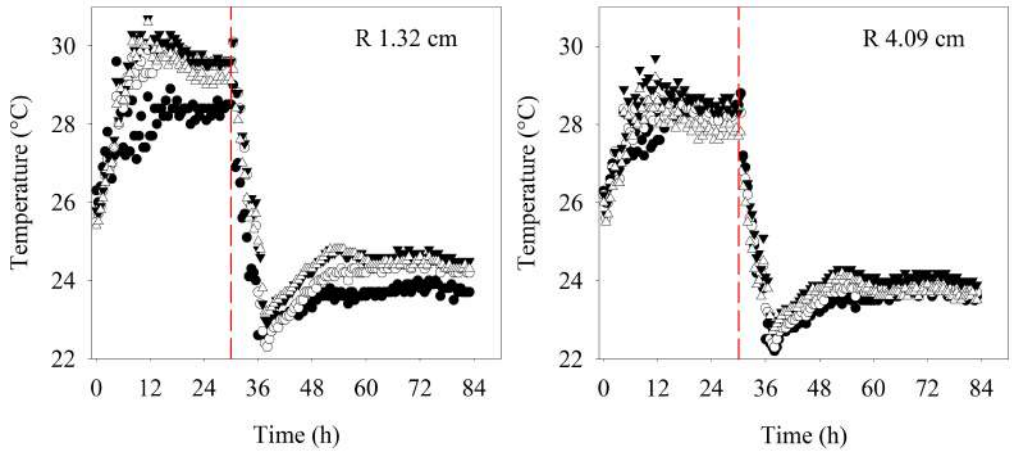

Figure 4.2: Temperature profiles measured at two different radii for fermentation of soybean hulls in insulated packed-bed bioreactors (PBB). Temperature measurement heights: 5.6 cm (filled circles), 11.6 cm (void circles), 17.6 cm (filled triangles) and 23.6 cm (void triangles)

The general thermal behavior was the same for all the measurements thermocouples. Temperature increased until approximately 12 h and then it was nearly constant until 30 hours, when the compressor had to be substituted for another one without a rotameter. Due to this substitution, the air was furnished at a stronger flow rate. The higher air velocity and consequently the increase in convective and evaporative heat removal provoked the decrease of the bed temperature, remaining then around 24 °C. The temperature did not rise as much, although it did increase more along the bed length. In the first height (5.6 cm), the temperature

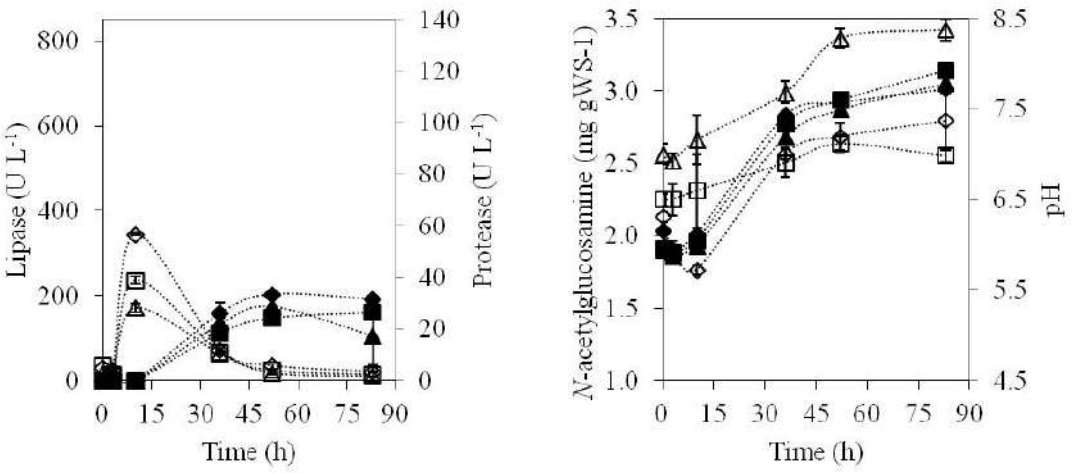

(a) (b)

Figure 4.3: Enzymes (a), *N*-acetylglucosamine and pH (b) profiles observed in packed-bed bioreactor fermentation of soybean hulls by *Yarrowia lipolytica* IMUFRJ 50682 for the heights 7 (diamond), 14 (square) and 21 (triangle) cm from the bottom of the bioreactor. Bars represent the standard deviations from measurements. Lipase and *N*-acetylglucosamine are represented by void marks, while protease and pH are shown as filled marks, respectively.

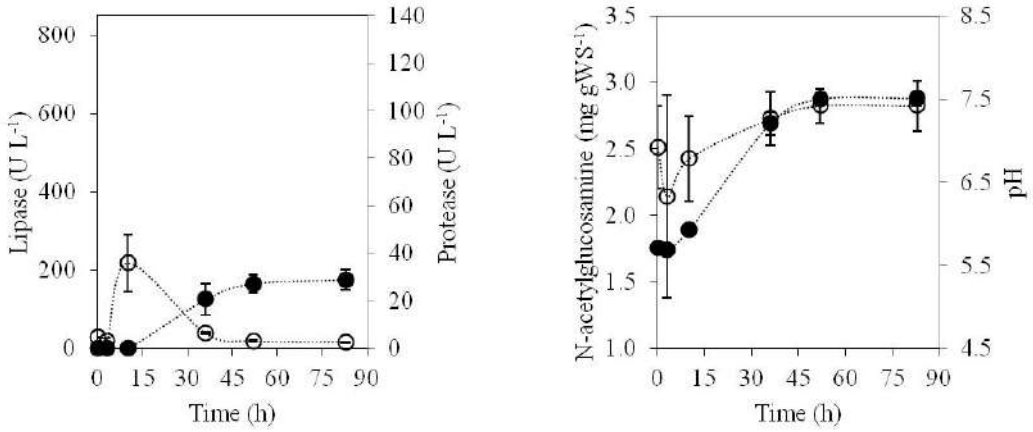

(a) (b)

Figure 4.4: Enzymes (a), *N*-acetylglucosamine and pH (b) profiles observed in tray (polyproylene beaker) bioreactor fermentation of soybean hulls by *Yarrowia lipolytica* IMUFRJ 50682.Bars represent the mean absolute deviation from two replicates. Lipase and *N*-acetylglucosamine are represented by void marks, while protease and pH are shown as filled marks, respectively.

did not surpass 30 °C, within the optimal temperature range for the cell, but for the other heights they reached or surpassed it. Despite the compressor exchange, the experiment was completed, and no macroscopic growth of cells was observed. *N*-acetylglucosamine measurements of the fermented material for the estimation of indirect cell growth were performed and confirmed that there was an increase of

only 35 % (approximately) in cells (Figure 4.3).

Interestingly, it is observed that temperature values never surpasses the value of 34 °C, which was reported to be the common temperature of survival of this yeast, as it was previously said before. However, AURIA *et al.* (1995) evaluated the influence of temperature on production of acid phosphatase in SmF by the strain NBIMCC 192 and found that the specific growth rate was the highest at 28 °C (around 0.23 h^{-1}), while at 36 °C the value was approximately 0.05 h^{-1}. At the highest temperature, cell growth was less pronounced.

Recently, while studying stress responses of *Yarrowia lipolytica*, RZECHONEK *et al.* (2018) observed that cells with a deletion of a gene responsible for cell signaling during stress events such as hyperosmotic environment grew fewer colonies at 35 °C then the non-deleted mutants. Also, both groups of cells grew less than at 30 °C and did not survive to 37 °C cultivation. All these observations together seem to make it very clear that after the optimal temperature of growth between 28 and 30 °C, cells have to survive stressful conditions and stop growth and adapt to the thermal that stress becomes important. KAWASSE *et al.* (2003) visualized morphological responses to thermally stressed cells, with increased hyphal length, which was also observed by RZECHONEK *et al.* (2018).

However, the cells also slightly grew in the tray (Figure 4.4b)), which indicates that temperature might not be totally responsible for this. The effect of temperature can not be excluded though, since the bed height is higher than those used for soybean meal with this yeast by other authors (DE SOUZA *et al.*, 2019, SALES *et al.*, 2020, SOUZA *et al.*, 2017).

Regarding enzymes production (Figure 4.3a), protease and lipase (hydrolytic) activities were measured and the profile observed was the same as those found for the tray (4.4a) and the ones reported by SOUZA *et al.* (2017), but using soybean meal as a solid matrix, though the authors obtained much higher lipase activities. Lipase production was higher in the height between the first and second set of thermocouples, possibly due to the maintenance of the appropriate temperature and peak activities were obtained at 10 h of fermentation. As the axial distance increased, lipase activity decreased (more than 50 %) and reached the same level as in the tray.

Protease production was also observed following lipase production and may be the possible reason for the lipase activity decay. However, differences through the bed were not as relevant as for the lipase production, once they were first detected from the moment the compressor had been exchanged on. This meant that temperature was stable at values where cells could produce protease without dealing with a thermal stressful. All these observations directed the research into the formulation of better supplementation to make it possible for cells to grow and produce higher

amounts of enzymes. When using lignocellulosic or fibrous materials for lipase production, supplementation or a mixture of solid matrices is advised (SALIHU *et al.*, 2012), especially because *Y. lipolytica* is not able to use these types of raw materials, as it was previously described.

Once it was verified that no macroscopic growth was occurring, which was also noticed for the tray, the next experiments focused on establishing a supplementation strategy to provide nutrients for growth. Once it is known that *Y. lipolytica* does express the enzymes required for lignocelluloses consumption or do it very poorly, other carbon and nitrogen sources were investigated. For this, fermentations with supplementation of soybean oil (control), glucose and a solution of glucose and diammonium phosphate were applied and desired responses were measured at 10 and 89 hours (Figure 4.5), in the expected moment of lipase production and of maximum growth and protease production.

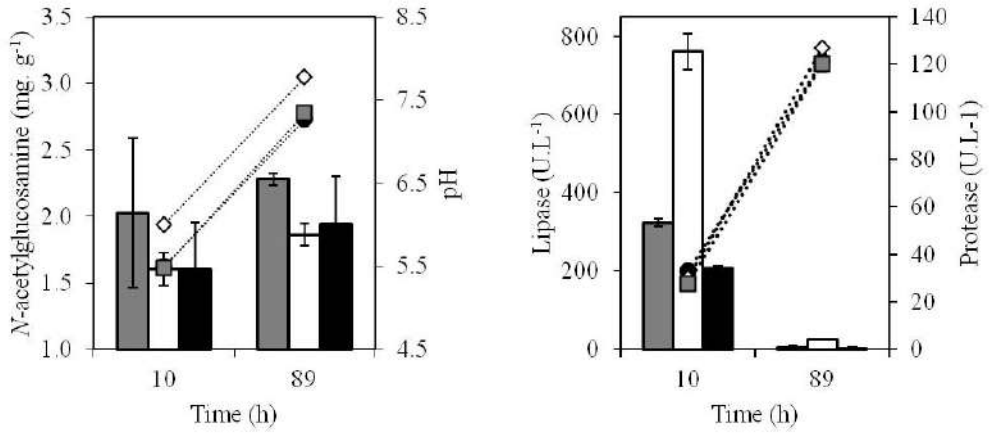

(a) (b)

Figure 4.5: *N*-acetylglucosamine content, pH (a), and enzyme (lipase and protease) activities (b) for tray bioreactor (polypropylene beakers) fermentation of soybean hulls with 1.5 % g g^{-1} glucose (white bars and squares), ammonium phosphate and glucose (gray bars and diamonds) and soybean oil (control, black bars and cross) by *Y. lipolytica* IMUFRJ 50682. Error bars represent the standard deviations from analytical measurements for the control, while in the other cases it represent the mean absolute deviation of two replicates.

Results from this assay have shown that still no cell development was attained, once there is no difference in glucosamine content for all the conditions (Figure 4.5a). Despite that, an increase of 2.2 and 0.93-fold in lipase production was observed with supplementation of glucose and both glucose and diammonium phosphate, respectively (Figure 4.5b). Accordingly, protease production was also enhanced by around 3.3-fold for both cases. pH increase (Figure 4.5a) for all the cases and passed the value of 6.5, from which *Y. lipolytica* is known to produce protease. Even though glucose seems to be repressive for lipase production, at least as it was

proposed by FICKERS *et al.* (2005b) for SmF, results for solid-state fermentation seem to be the opposite, as it was also observed for *P. restrictum* by DE AZEREDO *et al.* (2007). The authors conducted experiments in both submerged and solid systems and showed that this fungus is able to produce lipase even with glucose supplementation at a solid-state system, but not in submerged one.

To verify if this strain was able to produce better with other carbon and nitrogen sources, a new set of experiments were executed with the same ratio of supplementation as before, including glucose, glycerol, and soybean oil as carbon sources and urea, diammonium phosphate and sodium nitrate as nitrogen sources. The fermentations were performed in smaller scales (glass bottles) to avoid unnecessary consumption of the raw material. SANTOS *et al.* (2019) recently proposed that submerged culture miniaturization for this yeast strain is a valuable tool for developing lipase production and proposed direct scale up from this system to bench-scale reactors. Following this, "miniaturized" solid-state fermentations were performed. pH and lipase production results in this screening experiment are available in Figure 4.6. The fermentation was conducted for 21 hours with sampling every seven hours so the time of highest production and one sample before and after this moment would be verified.

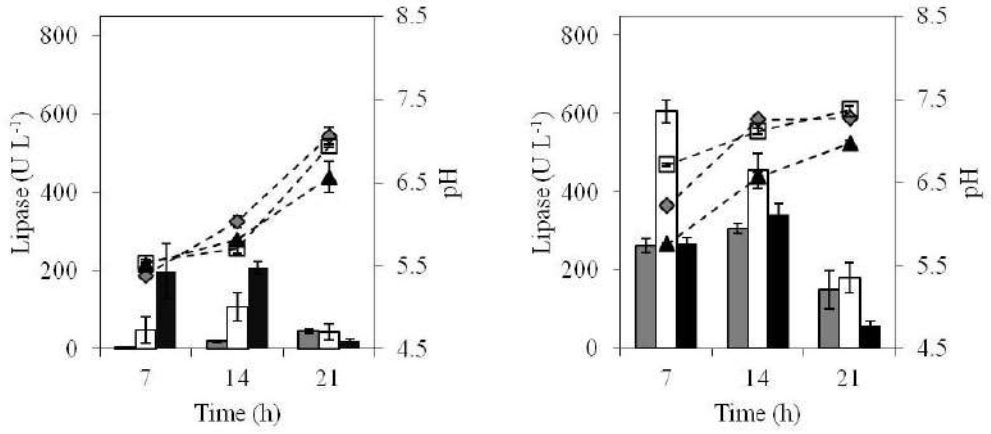

Figure 4.6: Lipase (hydrolytic) activity (bars) and pH for tray bioreactor (glass bottles) fermentation of soybean hulls with 1.5 % g g^{-1} supplementation of carbon (a) and nitrogen (b) sources, including glycerol (gray bars and diamonds), glucose (white bars and squares) and soybean oil (black bars and triangles), urea (gray bars and diamonds), diammonium phosphate (white bars and squares) and sodium nitrate (black bars and triangles) by *Y. lipolytica* IMUFRJ 50682. Error bars represent the standard deviations from measurements for three replicates.

The majority of evaluated conditions presented maximum lipase activity at 14 h of fermentation as it was previously expected, except for glycerol (Figure 4.6a) and diammonium phosphate (Figure 4.6b) supplementations. Glycerol has been re-

ported to be the more repressive carbon source for lipase production in SmF in the review by FICKERS *et al.* (2011) and the obtained data herein seem to support this hypothesis for solid-state fermentation. In this new system (glass bottle) soybean oil supplementation induced lipase production more than glucose (Figure 4.6a), in contradiction with the data obtained in plastic beakers. Nevertheless, results for oil supplementation in both systems appear to be compatible, but comparison remains impaired because sampling was performed at different times. Previous results for the fermentation in fixed-bed bioreactor Figure 4.3a have shown that lipase secretion seems to occur abruptly, given the differences in the values obtained for lipase activity data between 3 and 10 h of the process.

With respect to the nitrogen sources (Figure 4.6b), urea provided the least favorable conditions for lipase conditions, a result that is strongly in contrast to what was obtained for other *Y. lipolytica* strains (IMANDI and GARAPATI, 2007, IMANDI *et al.*, 2010c, 2013b), leading to the idea of a strain-specific behavior. After optimization of the levels of soybean oil supplementation, urea and moisture content with the same strain as the one used in the present, SOUZA *et al.* (2017) observed that urea supplementation was irrelevant for lipase production. Likewise, LOPES *et al.* (2016) had the same results when comparing urea and ammonium sulfate addition. In this case, sodium nitrate had a similar effect and diammonium phosphate was again the best nitrogen source. Besides that, lipase peaked at 7 h of fermentation with this supplement.

Although results from the single addition of carbon and nitrogen sources have indicated that soybean oil and diammonium phosphate seem to be the appropriate choice, lipase activity was still slightly smaller than when the combination of glucose and diammonium phosphate was tested. Given that synergetic effects between effectors have shown to be important for this yeast, as it was reviewed for morphological transition before, a CCORD was performed in the glass bottles. As for this system, only 0.5 g of raw material is used per trial, representing a 20-fold economy of soybean hulls when compared to the plastic beaker. As water becomes an important factor in the design of SSF, the synergistic effect was assessed for these three variables. Lipase production was used as a tool for rapid estimation of the best conditions for fermentation and the results are presented in Table 4.3.

The choice of the experimental region was made based on the previously acquired knowledge of the process and other results from the literature for the same strain (LOPES *et al.*, 2016, SOUZA *et al.*, 2017). The central point, chosen to assess the variability of the design, presented a mean value of 525.3 ± 61.4 U L^{-1} of hydrolytic activity (calculated from data of the trial 15 to 23) after 14 h of fermentation. When compared to the values obtained from single supplementation experiments Figure 4.6, at 14 h of fermentation, it seems that simultaneous nitrogen and carbon supple-

Table 4.3: Lipase activity obtained after 14 h of fermentation of soybeans hulls by *Y. lipolytica* IMUFRJ 50682 in glass bottles for a central composite orthogonal rotational experimental design. Values in parenthesis represent the coded variables used for analysis in the software Statistica 7.0.

Trial	Glucose (% m/m)	$(NH_4)_2PO_4$ (% m/m)	Moisture content (%)	Lipase (U L^{-1})
1	0.75 (−1)	0.75 (−1)	50 (−1)	750.5
2	0.75 (−1)	0.75 (−1)	60 (+1)	690.0
3	0.75 (−1)	2.25 (+1)	50 (−1)	790.7
4	0.75 (−1)	2.25 (+1)	60 (+1)	496.6
5	2.25 (+1)	0.75 (−1)	50 (−1)	369.4
6	2.25 (+1)	0.75 (−1)	60 (+1)	307.1
7	2.25 (+1)	2.25 (+1)	50 (−1)	671.4
8	2.25 (+1)	2.25 (+1)	60 (+1)	352.4
9	0.24 (−1.68)	1.5 (0)	55 (0)	809.7
10	2.76 (+1.68)	1.5 (0)	55 (0)	331.9
11	1.5 (0)	0.24 (−1.68)	55 (0)	476.7
12	1.5 (0)	2.76 (+1.68)	55 (0)	538.1
13	1.5 (0)	1.5 (0)	46.60 (−1.68)	640.4
14	1.5 (0)	1.5 (0)	63.41(+1.68)	393.5
15	1.5 (0)	1.5 (0)	55 (0)	652.1
16	1.5 (0)	1.5 (0)	55 (0)	572.9
17	1.5 (0)	1.5 (0)	55 (0)	478.6
18	1.5 (0)	1.5 (0)	55 (0)	557.5
19	1.5 (0)	1.5 (0)	55 (0)	524.0
20	1.5 (0)	1.5 (0)	55 (0)	472.5
21	1.5 (0)	1.5 (0)	55 (0)	526.8
22	1.5 (0)	1.5 (0)	55 (0)	467.8
23	1.5 (0)	1.5 (0)	55 (0)	475.8

mentation with these sources did not provide better conditions for lipase production than when only diammonium phosphate was added.

The analysis of these results was performed as described by CALADO and MONTGOMERY (2013). Analysis of variance (ANOVA) of the results has shown that only linear terms of the model, namely moisture content and carbon source, as well as interactions between nitrogen supplementation and carbon supplementation or moisture content, were significant at a confidence level of 95 %.

The generated model for the coded variables follows (Equation 4.4) and it was capable of explaining 89.5 % of the variance of results and the surface generated is a plane (at fixed values of nitrogen sources) that indicates that working with smaller values of moisture content and glucose addition is better.

$$Lipase = 536.8 - 134.1G - 84.3MC + 62.6GN - 61.3NMC \tag{4.4}$$

where G, MC, and N are the levels of glucose, moisture content and diammonium phosphate. However, the extraction process of these fermentations led to the recovery of different volumes of extract. This could be related to the moisture content adjustment step previous to the fermentation, as the solid matrix of the soybean hull is capable of absorbing a considerable amount of water. Thus, water retention can affect lipase recovery as the amount of free water to extract proteins would be smaller. MATIN *et al.* (2013) measured the water-holding capacity of soybean hull powder, without specifying its size range, and found values of 3.91 grams of water per gram of soybean hull powder.MUZILLA *et al.* (1989) measured water absorption for fine (0.84 mm, the closest to the value applied in this study), medium (1.65 mm) and coarse (2.36 mm) soybean hulls and concluded that water absorption increases with higher temperatures and particle diameters. The medium value obtained for water absorption at 25 °C was 4.1 g g^{-1}, somewhat similar to the ones observed by the previous authors.

CASCIATORI *et al.* (2014) have shown that sugarcane bagasse cells size (represented by the diameter) increase almost linearly. Other important properties such as bed porosity and bulk densities, also related to the expansion of the solid matrix by water absorption were also investigated for sugarcane bagasse, wheat bran and orange pulp and peel and the authors verified that within the moisture range for fermentations they may change exponentially depending on the analyzed property. Also, having these considerations in mind, careful regard towards moisture content as a variable in statistical designs must be made, focusing in the moisture content/volume of extraction relation. So far, the ratio of the volume of extraction to fermented mass is 5 mL g W.S.$^{-1}$. As an estimate, for fermentation with 55 % moisture content, 1 g of wet soybean hull could absorb around 37 % of the volume of water in the buffer. Therefore, working with smaller values of moisture content would lead to a higher water holding and lipases would be more concentrated as the volume of extractant effectively diminishes.

Besides, carbon supplementation with glucose seemed to be detrimental for lipase production. However, as the lipase production is repressed by glucose as previously mentioned by FICKERS *et al.* (2005b), the moment when lipase was secreted could have changed, thus affecting the results. Thus the supplementation at smaller quantities would accelerate the secretion process. One may conclude then that fixing the time for lipase extraction at 14 hours may have affected the model estimation process. Combining these ideas for the analysis of nitrogen supplementation, as moisture content has to be smaller (and have a negative sign in the coded model), both interactions seem to be beneficial for the increase of lipase production. As the model is linear, maximum activity within the range evaluated is achieved at minimal moisture content and maximum supplementations of carbon and nitrogen sources.

These conclusions suggest that an expansion in the range of supplementation is desired for better performance, as many authors investigated the range of 1 to 9 % carbon supplementation (mentioned in the literature review) for *Y. lipolytica*. VARGAS *et al.* (2008) also evaluated a wider range, between 1 and 8 % carbon source (glucose) concentration, for lipase production by *P. simplicissimum*. Since the results from the CCORD did not lead to a substantial increase of lipase production, different ranges of nutrient supplementation of complex and defined media were investigated.

4.2 Insights into media supplementation in solid-state fermentation of soybean hulls by *Yarrowia lipolytica*: impact on lipase production in tray and insulated packed-bed bioreactors

The results presented throughout this section were published in the Biochemical Engineering Journal (https://doi.org/10.1016/j.bej.2020.107866).

4.2.1 Abstract

Solid-state fermentation (SSF) with *Yarrowia lipolytica* requires appropriate medium supplementation and bioreactor configuration for efficient lipase production, which are related to the temperature profile due to the heat release by the metabolic activity and the heat removal mechanisms of the bioreactor. Thus, we evaluated supplementation with complex medium (CM) and defined medium (DM) for lipase production in tray and insulated packed-bed bioreactors (PBB), also assessing protease production. The media were composed of yeast extract (Y), bactopeptone (P) or diammonium phosphate (N), and glucose (D) or soybean oil (O). Lipase activities in tray bioreactors were, in general, higher in CM than in DM, reaching 32 U g^{-1} when supplemented with concentrated YPO medium. Supplementation with YPO in the PBB resulted in maximal temperatures of 35 °C, with axial and radial temperature differences of up to 5.3 °C and 2.1 °C, respectively. In this case, the PBB gave 58 % higher lipase yield than the tray, while in the presence of mixed-carbon source (YPDO), the yield was 47 % lower, suggesting that the carbon source is important for SSF scaling-up and the temperature increase was responsible for changes in the use of the soybean oil and in protease secretion by this yeast.

4.2.2 Introduction

Solid-state fermentation (SSF) has great potential for economic and sustainable production of organic acids, biosurfactants, flavors, pigments, biopolymers, and enzymes. The main characteristic of SSF is that the microorganism is in an environment closer to the natural one, where it can use the solid components as a nutrient source or as an inert support. Besides, this bioprocess is conducted with the near absence of free water (THOMAS *et al.*, 2013). In comparison with submerged fermentation (SmF), it presents some advantages, such as higher volumetric productivity reported in many studies, smaller chance of contamination, facilitated downstream processing (the product is more concentrated), and lower medium cost (ARORA *et al.*, 2018), which is mainly achieved with inexpensive, available agro-industrial residues (CASTILHO *et al.*, 2000).

Soybean seed processing generates various products (refined soybean oil, soybean protein concentrate, soybean isolate, and the soybean itself), and the hulls and the meal as by-products (DE PRETTO *et al.*, 2018). The hulls have lower commercial value due to the lower protein content (9-14 % by weight) and higher cellulose content (29-51 %) than the meal (50-52 % protein and 2-4 % cellulose) (LOMAN and JU, 2016). Besides, the hulls present high water holding capacity and low critical humidity point, being appropriate supports for SSF (JULIA *et al.*, 2016). The hulls have been used either solely (JULIA *et al.*, 2016) or in combination with wheat bran for cellulolytic enzyme production (BRIJWANI *et al.*, 2010) and in combination with orange peels for production of peptidase (LÓPEZ *et al.*, 2018). Additionally, the hulls also absorb a considerable amount of oil (2.77 – 4.25 g g^{-1} depending on the oil) (MATIN *et al.*, 2013), which is attractive for lipase production studies with oil supplementation.

Lipases (triacylglycerol acyl hydrolases, E.C. 3.1.1.3) find application in several industries. In the food industry, for instance, lipases are used as biocatalysts to produce flavors, structured lipids, or polyunsaturated-rich oils (MEUNCHAN *et al.*, 2015). Lipases produced by SSF using the yeast *Yarrowia lipolytica*, acting in a solid enzymatic preparation (lyophilized fermented solid) form, have been used for the removal of free fatty acids from acid oils (DA SILVA *et al.*, 2019) and the synthesis of esters for the food industry (DE SOUZA *et al.*, 2019). Lipase production by this yeast in SSF has been reported using agro-industrial residues (LOPES *et al.*, 2016, MOFTAH *et al.*, 2013, UR REHMAN *et al.*, 2014), including those from the soybean industry (mainly soybean meal) (FARIAS *et al.*, 2014, IMANDI *et al.*, 2010a,c, 2013a, SOUZA *et al.*, 2017, UR REHMAN *et al.*, 2014), but not with the use of soybean hulls. In all the cases, supplementation with carbon or nitrogen sources was necessary for improved production with this yeast. This requirement for nutrient

supplementation can be attributed to the fact that wild strains of *Y. lipolytica* do not hydrolyze some raw materials, such as xylan, cellulose, hemicelluloses, or consume some monomeric sugars like xylose, arabinose, rhamnose, and galactose. The lack of ability to consume these substrates is due to the absence (or deficient expression) of genes encoding for the corresponding metabolic enzymes (LEDESMA-AMARO and NICAUD, 2016). Therefore, finding the adequate combination of solid matrix and supplementation is one of the challenges to use *Y. lipolytica* for lipase production in SSF.

This GRAS (Generally Regarded As Safe) yeast (GROENEWALD *et al.*, 2014) secretes considerable amounts of enzymes (lipases and proteases) (NICAUD, 2012). Genetic regulation of lipase expression in this strain is not fully understood, mainly due to the diversity of lipases and the influence of medium composition in their production, location (bounded to the cell wall, intra or extracellular), secretion, and activity. However, lipase regulation responds mainly to some external stimuli (FICKERS *et al.*, 2011). Regulation of LIP2 expression, the gene coding for the main extracellular lipase (Lip2p), involves cell responses to glucose, which represses lipase production (FICKERS *et al.*, 2005b), to triacylglycerol molecules, which in turn activate the SOA (specific for oleic acid) genes and other mechanisms for free fatty acid consumption (DESFOUGÈRES *et al.*, 2010). Complex nitrogen formulations, such as peptone and tryptone, also seem to upregulate lipase production (TURKI *et al.*, 2009). Thus, lipase regulation depends on the medium formulation.

Heat is produced according to the type of substrate used in the medium. For instance, VOLESKY *et al.* (2007) measured the heat yield of *Y. lipolytica* cells grown with glucose, n-dodecane, or hexadecane in SmF. The yield in the presence of hydrophobic substrates was higher (69-87 %) than that for glucose. In SSF, the heat transfer mechanisms (such as conduction, forced aeration, water evaporation, and thermal diffusion) are mainly related to the bioreactor configuration and peaks of temperature occur due to the difficulty of heat removal (DA SILVEIRA *et al.*, 2014, MITCHELL *et al.*, 2003). Therefore, the bioreactor configuration and the type of substrate (supplemented or found in the solid matrix) used for cell growth or product induction determine the temperature reached in the bioreactor.

Tray fermentations with low bed loading are usually conducted prior to bench-top bioreactor evaluation to achieve an appropriate medium formulation while aiming at fast and cheaper process development. However, as the primary form of heat removal from the bed in trays is by conduction followed by convection, the scale-up requires high surface area due to the bed height limitation. In contrast, the use of packed-bed bioreactor with forced aeration presents advantages, since advective and evaporative heat transfer are favored (ARORA *et al.*, 2018). This strategy has recently been tested at pilot-scale for lipase production by *Rhizopus microsporus*

(PITOL *et al.*, 2017). Successful scale-up from 15 g to 15 kg was possible due to the small metabolic heat production by the fungus (26 W kg^{-1}) and the combination of solid substrates (wheat bran and sugar cane) that provided high porosity and avoided bed compaction.

Despite the history of studies for lipase production by *Y. lipolytica* in tray bioreactors, no study further evaluated it in a forcefully aerated packed-bed bioreactor nor monitored the temperature profile during the process. Although soybean meal was used before, lipase activity decay was observed in tray SSF of this agro-industrial residue with *Y. lipolytica* (FARIAS *et al.*, 2014, SOUZA *et al.*, 2017), *Penicillium simplicissimum* (VARGAS *et al.*, 2008) or *P. verrucosum* (KEMPKA *et al.*, 2008). Besides, as a result of the consumption of the solid matrix, the bed may lose its structure and hinder the performance of packed-bed bioreactors. Thus, soybean hulls were tested in tray and PBB to overcome these issues. Therefore, the objective of this work was to explore the potentiality of lipase production and responses of the yeast *Y. lipolytica* IMUFRJ 50682 in SSF of soybean hulls, evaluating complex and defined media formulations for supplementation along with possible implications of medium choice in tray and insulated packed-bed bioreactor cultivation.

4.2.3 Material and methods

Microorganism and pre-culture conditions

Yarrowia lipolytica IMUFRJ 50682 strain, which was isolated from the Guanabara Bay in Rio de Janeiro, Brazil (HAGLER and MENDONÇA-HAGLER, 1981), and identified at the Federal University of Rio de Janeiro, was used for lipase production. Previously grown cells in the YPD medium were maintained frozen in glycerol solution (50%) at -50 °C and thawed by heat shock at 28 °C, centrifuged, and the supernatant was discarded. After this, cells were resuspended in YPD medium and grown for 72 h at 28 °C and 160 rpm. The composition of this medium (in g L^{-1}) was: yeast extract (Y), 10; bactopeptone (P), 20; glucose (D), 20.

Soybean hull preparation and soybean oil elemental analysis

Soybean hull (kindly provided by the biodiesel industry BSBios, Passo Fundo, Brazil) was ground in a hammer mill (Tecnal) and kept frozen at -20 °C until further use. After thawing at room temperature, the material was sieved to keep the particle diameter (d_P) in the range of 0.5 mm $< d_P <$ 1.18 mm and heat sterilized for 22 min at 120 °C. After this, the sterilized material was cooled to room temperature before previous utilization. Soybean oil elemental analysis was performed using the Thermo ScientificTM Flash 2000 CHNS/O analyzer (ThermoFisher).

Fermentation

Pre-cultured ovoid cells of *Yarrowia lipolytica* were sampled, centrifuged at 3000 rpm for 15 min, resuspended in a fixed spent medium volume from the pre-culture flask and poured into the solid matrix, followed by homogenization with a fork. Humidity was then adjusted to 55 % by homogenization with a solution containing the desired supplementation (Table 4.4). In this study, the mass of inoculum was equivalent to either 0.71 mg g^{-1} in complex media or 0.50 mg g^{-1} in defined media.

Table 4.4: Assay conditions for complex and defined media formulation for lipase production by *Yarrowia lipolytica*.

Medium	Inoculum size (% mg g^{-1})	Composition (% g g^{-1})				
		Glucose	Soybean Oil	Diammonium Phosphate	Yeast Extract	Bacto peptone
YPD	0.71	1.762	-	-	0.8810	1.762
YPD 5x	0.71	8.810	-	-	4.405	8.810
YPDO	0.71	4.405	4.405	-	4.405	8.810
YPO	0.71	-	8.810	-	4.405	8.810
YPD10x	0.50	17.62	-	-	8.810	17.62
DN	0.50	1.762	-	1.762	-	-
DN 5x	0.50	8.81	-	8.810	-	-
DON 5x	0.50	4.405	4.405	8.810	-	-
DN 10x	0.71	17.62	-	17.62	-	-

Supplementation of soybean oil (1.5 % m/m) was previously reported for lipase production by the same yeast strain in SSF of soybean meal (SOUZA *et al.*, 2017). Based on the concentration of the standard YPD medium, which is commonly used for *Y. lipolytica* cultivation (BARTH and GAILLARDIN, 1996), different nitrogen and carbon sources were tested in the present work. Complex (YPD based) and defined media containing glucose, soybean oil (O), and diammonium phosphate (N) formulation were evaluated. In addition, concentrated media were also tested since the range of nutrient supplementation described in the literature (IMANDI *et al.*, 2010a,c, 2013a) can reach higher mass percentages (1-9 % m/m). The mass percentage of each added substance was calculated and is shown in Table 4.4. The assays in trays were performed as fermentation duplicates, and the results were presented as the average ± mean absolute deviation (MAD). MAD was calculated as $|x_1 - x_2|/2$, with x_1 and x_2 being the values measured in each fermentation replicate.

For the experiments in tray bioreactors, 0.5 g of soybean hull was utilized in small glass bottles, while 400 g of the same material was used in the packed-bed bioreactor (PBB) (Figure 4.7), which was insulated with a vacuum-sealed jacket at the side walls (it simulates conditions where heat removal by side walls is ineffective, such as

those in scaled-up packed-beds). Table 4.5 summarizes the general features of the vessels used for this work. Tray bioreactor experiments were conducted with an air-saturated environment at 28 °C in a fermentation chamber (Tecnal) (DE SOUZA *et al.*, 2019, FARIAS *et al.*, 2014, SOUZA *et al.*, 2017). For the PBB, the room air temperature was set at 26.5 °C. Forced aeration was applied in this case with sterile compressed air (filtered with 0.22 μm heat sterilized filter) at a gas flow of 5 L min^{-1}. The gas was sparged directly into sterile water, where a sintered metallic filter was used to reduce bubble diameter and increase mass transfer. The gas phase with increased water content was then supplied at the bottom of the bioreactor. Bed temperature was recorded at four different heights (5.6, 11.6, 17.6 and 23.6 cm from the bottom), and two different radii (1.32 and 4.09 cm).

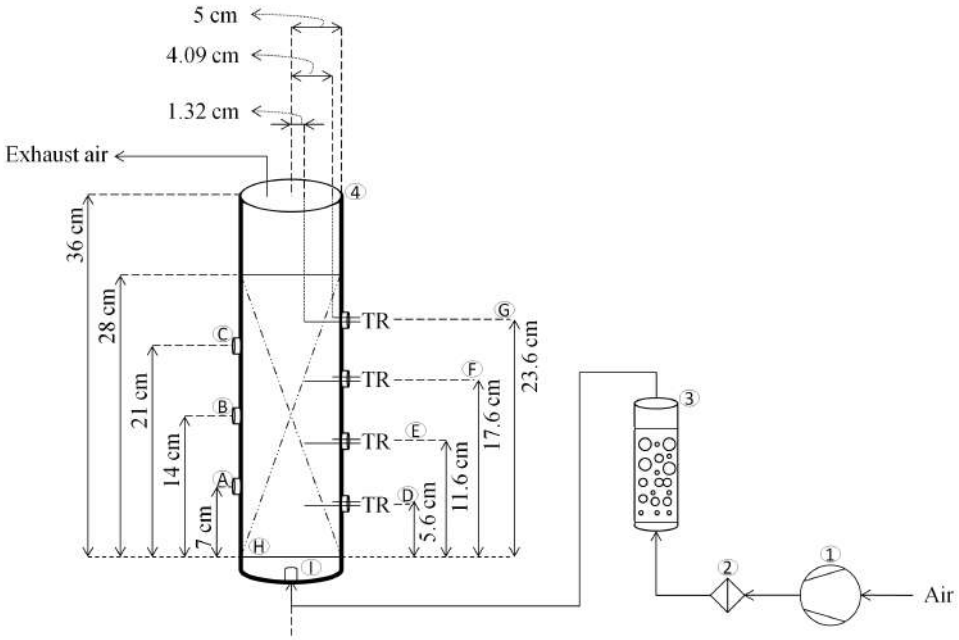

Figure 4.7: Schematic representation of the insulated packed-bed bioreactor. Insulated side walls are represented by thick lines. 1: air compressor; 2: air sterilization filter; 3: water saturation column; 4: bioreactor. A — C: sampling ports; D — G: temperature sensors; H: metal mesh support for the solids; I: air distributor.

Table 4.5: General design characteristics of solid-state fermentation bioreactors.

Bioreactor	Tray	Insulated packed-bed
Material	Glass	Glass
Height (cm)	5.7	36
Loaded height (cm)	1.0	28
Diameter (cm)	2.5	10

Sampling and enzyme extraction

For the tray experiments, all the fermented material in each flask was used for enzyme extraction. In PBB, excessive sampling may create cavities in the bed and thus affecting the gas flow pattern inside the bed. Therefore, samples of approximately 1 g were collected at 3 different ports (7, 14, and 21 cm height from the bottom of the bioreactor), which were sufficient for the enzyme extraction and estimation of the moisture content, without compromising the bed structure. The fermented material was aliquoted (0.20—0.25 g on wet basis) and frozen before further extraction. Enzymes extraction was performed with 50 mM potassium phosphate buffer (pH 7.0, 5 mL g^{-1}) at 35 °C and 1000 rpm agitation in a thermomixer (Eppendorf) for 20 min. After extraction, the suspended material was centrifuged at 6000 rpm for 15 min, and the supernatant was collected for quantification of lipase and protease activities.

Analytical methods

Lipase activity Lipase activity from extracts was quantified using the method of 4-nitrophenyl dodecanoate hydrolysis, which consists of the quantification of the hydrolysis product 4-nitrophenol spectrophotometrically at 410 nm. The substrate was solubilized in both 1 mL of dimethyl sulfoxide (DMSO) and Triton X-100, separately by vortexing. Prior to use, 10 μL of each solution was pipetted, vortexed, and then phosphate buffer was added (1980 μL), forming a clear solution that was maintained at 37 °C. The assay was monitored at 37 °C in a microtiter plate reader (SpectraMax, Molecular Devices) for 10 minutes. Samples (20 μL) were incubated in the microtiter plate for five minutes, and the reaction was started by the addition of 180 μL of substrate solution (1.5 mM). One activity unit was defined as the amount of enzyme capable of producing 1 μmol of 4-nitrophenol per minute in the assay conditions. Lipase productivity (Q_{Lip}, U L^{-1} h^{-1}) was calculated with the equation $Q_{lip} = Lip/t_f$, where t_f is the fermentation time when maximum lipase activity (Lip) was measured. Conversion of the productivity into mass basis (U $g^{-1}h^{-1}$) was done by multiplying it by $V_{extraxtion}/(1-MC)$, where $V_{extraction}$ is the volume of extraction per wet mass of solids, and MC is the sample moisture content. Moisture content was measured as described elsewhere (SOUZA *et al.*, 2017). For the tray bioreactor, the initial moisture content was used in the calculation, while the measured moisture content at each sampling time was used for the PBB.

Protease activity Proteolytic activity was estimated by the hydrolysis of the chromogenic substrate azocasein (CHARNEY and TOMARELLI, 1947). 100 μL of a 0.5 % m/v azocasein solution prepared in 50 mM acetate buffer (pH 5.0) was

added to an equal volume of enzyme extract and incubated at 32 °C for 40 min with agitation. The reaction was stopped by addition of 100 μL of 15 % m/v trichloroacetic acid solution, and samples were centrifuged at 3000 rpm for 15 min. 100 μL of supernatant from each sample and 100 μL of 5 M potassium hydroxide were then added into the 96-microtiter plate and absorbance at 428 nm was recorded in a microtiter plate reader (SpectraMax, Molecular Devices). One activity unit was defined as the amount of enzyme capable of producing a unitary increase in absorbance per minute.

pH measurement pH was monitored using a bench pHmeter after following the enzyme extraction protocol previously described with modifications. In this procedure, distilled water was used instead of the buffer, and centrifugation was not performed before measurement.

4.2.4 Results and discussion

Preliminary assays in tray bioreactor

Common nutrients investigated in previous reports of lipase production by *Y. lipolytica* in SSF in tray bioreactors (FARIAS *et al.*, 2014, IMANDI *et al.*, 2010a,c, 2013a, MOFTAH *et al.*, 2013, SOUZA *et al.*, 2017, UR REHMAN *et al.*, 2014) are nitrogen (soybean meal, yeast extract, peptone, casein, malt extract, urea, $NH_4H_2PO_4$, $(NH_4)_2SO_4$, NH_4Cl, NH_4NO_3, and $NaNO_3$) and carbon sources (soybean oil, glucose, sucrose, fructose, starch, lactose, and maltose). However, each strain presented a specific response to the combination of solid residues and supplementation used. In this sense, we investigated the use of the soybean hulls with different supplemented media (described in Table 4.4) in the tray bioreactor to identify the most promising medium for further experiments in the PBB. Since this yeast secretes acid (AXP) and alkaline (AEP) extracellular proteases depending on the medium pH (GLOVER *et al.*, 1997) and protein degradation (including lipase) results in matrix alkalinization (RIGO *et al.*, 2010), pH and proteolytic activity were also monitored. Results for both complex and defined media evaluation in trays are presented in Figure 4.8.

Lipase production in complex media Based on the medium used herein for inoculum preparation of *Y. lipolytica* cells, lipase production was first tested in complex media containing glucose (D), yeast extract (Y), and bactopeptone (P) (Figure 4.8.a and b) within soybean hulls. Lipase activity (Figure 4.8a) peaked at 585 U L^{-1} at 12 h in YPD and 320 U L^{-1} at 24 h in YPD 5x. In YPD, the production time agrees reasonably with the ones reported by SOUZA *et al.* (2017) and FARIAS *et al.* (2014), who cultivated the same *Y. lipolytica* strain in soybean meal. However, these

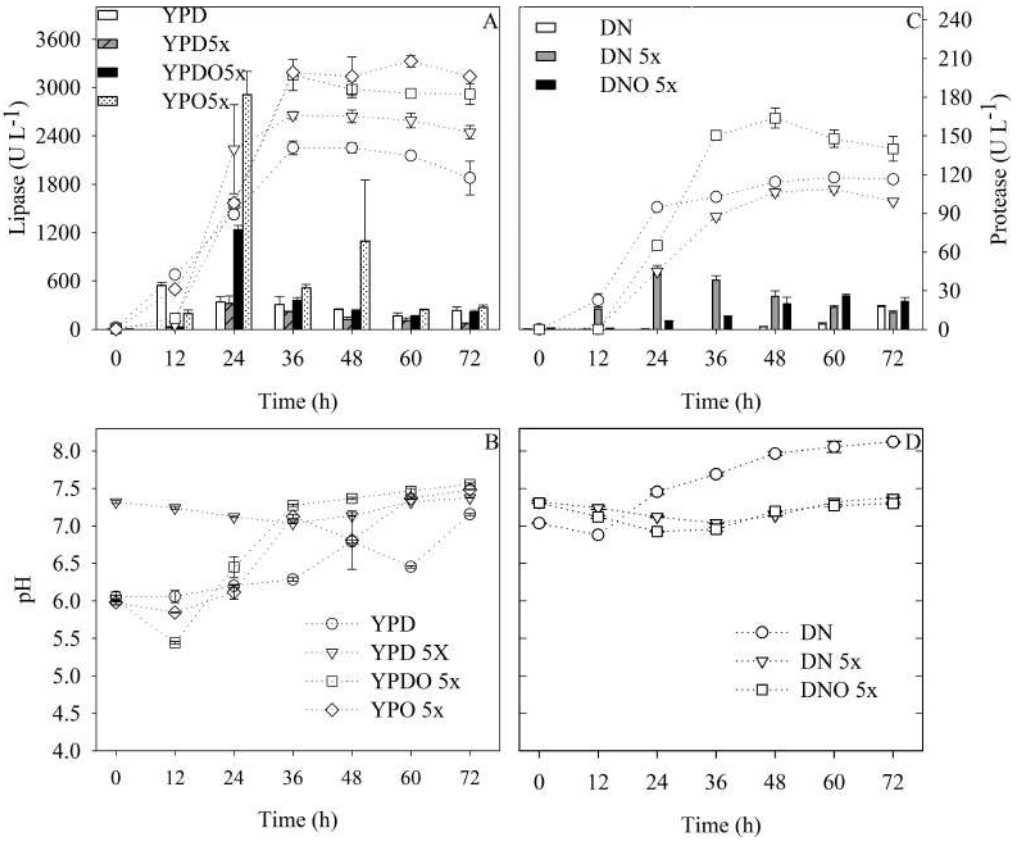

Figure 4.8: Lipase (bars) and protease (marks) activity (A, C) and pH (marks) (B, D) profiles for fermentation of soybean hulls supplemented with different complex (left column) and defined (right column) medium in tray bioreactors. Data are related to the preliminary assays (Section3.1) and are presented as average ± mean absolute deviations obtained from two fermentation replicates. Standard deviations from all analyses are smaller than 15 %.

authors induced lipase production with soybean oil and soybean sludge, respectively, and obtained higher activities than those of YPD and YPD 5x used in this work. SASSI *et al.* (2016) observed that mixtures of oleic acid with glucose (40:60 glucose:oleic acid in C-mol basis) increased mRNA induction under the regulation of lipase (Lip2) promoter in SmF. The mixture also resulted in higher induction than with oleic acid alone. Therefore, we used soybean oil (which also contains oleic acid) in our study to increase lipase activity following this strategy of partial or complete substitution of glucose in the concentrated versions of the complex media. The mixture (YPDO 5x) resulted in a 3.9-fold increase in lipase activity at 24 h, while soybean oil alone (YPO 5x) gave a higher increase (9-fold). Thus, our results indicate that soybean oil used solely or together with glucose in complex media is beneficial for lipase production.

Although lipase activity increased with the addition of soybean oil, it did not remain stable until the end of the fermentation. Instead, lipase activity decayed in all media. Protease maximal activity was reached in 36 h and was higher in

soybean oil-based media than that for YPD-based media. pH was above 6 for most of the fermentation time in all cases. Thus, it is most likely that protease activity is related to AEP. GLOVER *et al.* (1997) studied AEP and AXP expression in samples from *Y.lipolytica* SmF with pH ranging from 3.5 to 7.5 and barely detected AXP by Western Blotting. In contrast, the authors detected AEP in all samples. Since lipase is less resistant towards serine proteases (ALOULOU *et al.*, 2013), such as AEP, this can explain the concomitant decay in lipase activity, with an increase in pH and protease secretion.

Lipase production in defined media In previous SSF works, IMANDI *et al.* (2010a,c, 2013a) found improved lipase production by *Y. lipolytica* using glucose and urea. For the strain used in this work, urea was detrimental in soybean meal (SOUZA *et al.*, 2017) and did not allow lipase to accumulate until the end of fermentation in a mixture of two-phase olive mill waste and wheat bran (LOPES *et al.*, 2016). Based on this, the combination of a different nitrogen source (diammonium phosphate) with glucose and soybean oil was evaluated in media without adding the yeast extract and bactopeptone.

Lipase activity (Figure 4.8c) in the defined medium (DN) was smaller than the values obtained with the YPD media (Figure 4.8a). Protease production profiles had the same general pattern in these two media but with a slower increase (maximum at 48 h), reaching values around 120 U L^{-1} by the end of fermentation, these values being equal to or lower than those observed in YPD media. Lipase production was largely delayed compared to the complex media, having its maximum activity at 72 h. The concentrated medium (DN 5x) led to an increase in maximum lipase activity, with delayed and smaller protease activity, which could be the reason for the increase in lipase activity. Partial substitution of glucose by soybean oil (DNO 5x) did not result in higher lipase activity. The protease activity was further stimulated, similar to what can be observed for YPDO 5x and YPO 5x media (Figure 4.8a). The maximal lipolytic activity occurred earlier at 60 hours, with a sustained value until the end of the process.

Diammonium phosphate supplementation led to pH values (Figure 4.8d) above 7.0 in all the fermentations with defined media. The pH drop for DN medium was prolonged in DN 5x and DNO 5x media as a consequence of higher ammonium ions supplementation and, therefore, a longer ammonium consumption time, in agreement with the delay in protease production after the nitrogen source depletion. As protease production was slower in DN 5x, lipase activity also decreased less abruptly. At 24 h, lipase activity was higher, and protease activity was smaller in DN 5x than in YPD 5x. Thus, it is not possible to attribute the inferior lipase production in the concentrated defined media to the lack of yeast extract and peptone. Instead,

since *Y. lipolytica* growth diminishes in pH above 7.0 (BARTH and GAILLARDIN, 1996), it is likely that pH affected growth and, consequently, lipase production in YPD 5x, as pH adjustment was not done before inoculation in this work. Since successful SSF at acidic pH (initial value in the range of 5.5 to 6.5) with Y. lipolytica was possible with solid residues other than soybean hulls (LOPES *et al.*, 2016, SOUZA *et al.*, 2017) and pH control during fermentation can be difficult in SSF (RIGO *et al.*, 2010), this problem can be further tackled with the use of buffered or pH-adjusted media.

Lipase production in insulated packed-bed bioreactor

General remarks on process monitoring Given that higher lipase production in the previous assays was achieved with the concentrated complex media supplementation, these media were chosen for further tests in tray and insulated PBB. However, the less concentrated versions of these media were used for a shorter (24 h) bioreactor operating time (Figure 4.9). This strategy allowed more detailed monitoring of enzyme activities with regular 3-hour sampling without damage to the PBB bed structure. The decrease in sampling interval for these experiments provided valuable information regarding the wide variation of lipase and protease amounts between samples. As an example, lipase activities increased at least 5-fold from 9 to 12 h for the tray and PBB systems (Figure 4.9a), reaching maximal values in 15 h, indicating that detailed monitoring of the process is necessary to accurately determine the harvesting time before the lipolytic activity decays by the action of proteases.

The time to reach the maximum lipase activity was again close to the one reported by SOUZA *et al.* (2017) (14 h in their study), in tray bioreactor. The authors estimated cell concentration indirectly by quantification of *N*-acetylglucosamine, and the results showed no growth within the first 4 h of fermentation. In this sense, heat production would be relatively small during this lag phase. In our experiments, we calculated the average temperature at 4 h in the PBB experiments with the measurements from all the thermocouples, and in fact, they were close to the temperature of 28 °C used in trays (27.7 ± 0.2 °C, 27.6 ± 0.2 °C and 28.2 ± 0.2 °C for the YPD, YPDO, and YPO media, respectively). Therefore, the temperature of 26.5 °C set for the room air allowed a comparison between the two bioreactor configurations. The time to reach maximal lipase activity (Figure4.9a, b, and c) in both bioreactors occurred 6 h after the time at which the temperature peaked (Figure 4.9d, e, and f) in the PBB for all media. In general, pH and protease activity values for each medium showed the same tendency of increase after 9 h, although they continue to rise until the end of fermentation. This fact, along with the apparent correlation between maximum lipase secretion and temperature, indicates

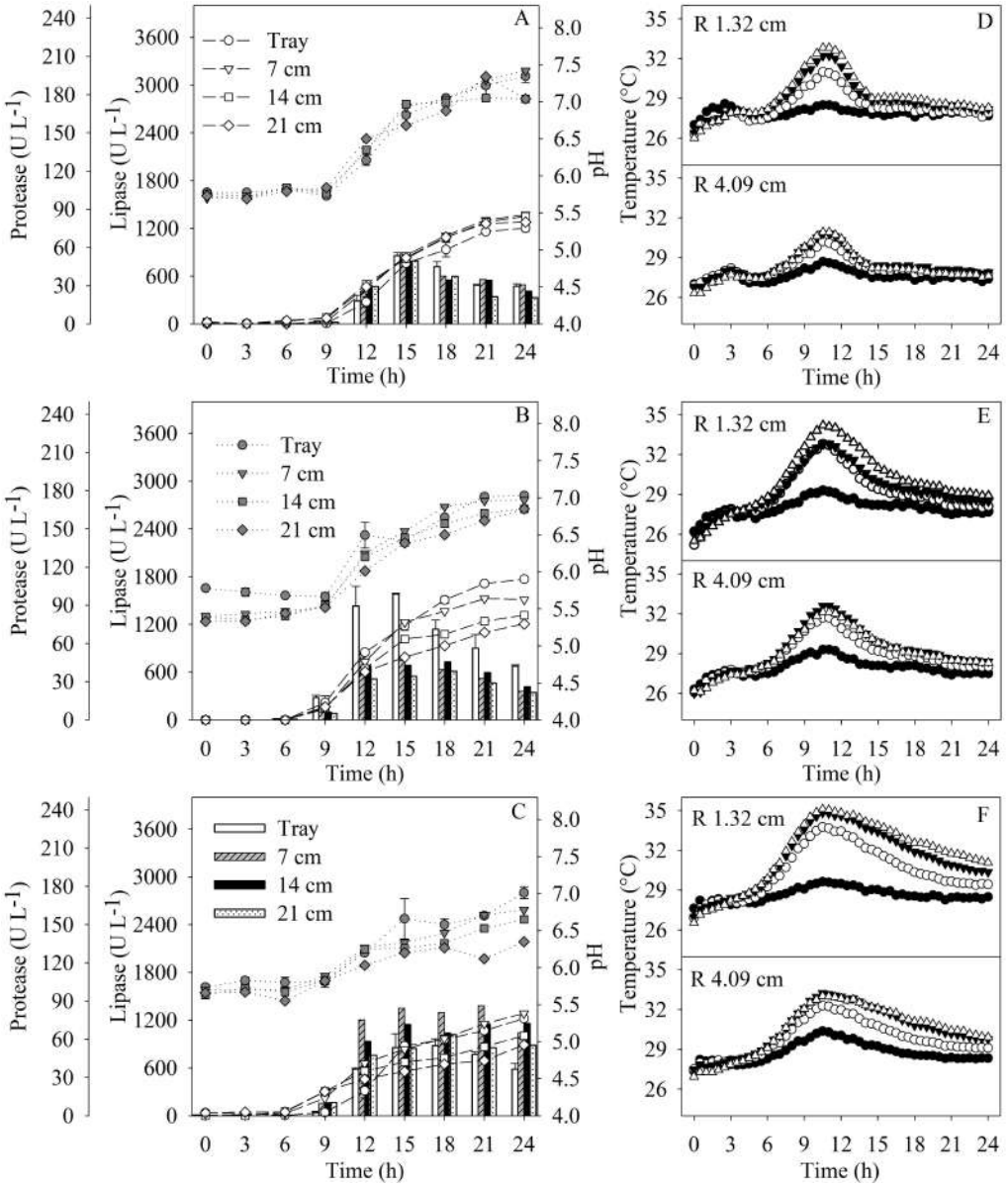

Figure 4.9: Lipase (bars), protease (void marks), pH (grey marks) (A, B, and C) and temperature profiles measured at two different radii (D,E, and F) for fermentation of soybean hulls in tray and insulated packed-bed bioreactors (PBB) supplemented with different complex medium (YPD: A and D; YPDO: B and E; YPO: C and F). Tray data are presented as average ± mean absolute deviations from two fermentation replicates. Standard deviations from all analyses are smaller than 15 %. Temperature measurement heights: 5.6 cm (filled circles), 11.6 cm (void circles), 17.6 cm (filled triangles) and 23.6 cm (void triangles).

that temperature monitoring is a promising strategy for adequate harvesting time determination in lipase production by *Y. lipolytica*, which directly influences the bioprocess productivity. However, this should not be regarded as a general rule. In the case of PBB operation without significant temperature increase, such as the one reported by PITOL *et al.* (2017), oxygen uptake rates would be more suitable for this purpose.

Fermentation in tray versus insulated packed-bed bioreactor The time-dependent behavior of enzymatic activities and pH for the YPD medium (Figure 4.9a) was similar in both systems. However, concerning soybean oil partial (Figure 4.9b) or complete (Figure 4.9c) substitution, a slightly slower increase in pH and protease activity is verified, with greater effect as the oil amount and the PBB height increases. To summarize the different responses obtained in studying media formulations, lipase productivity, lipase-to-protease ratio, and the yield of lipase production related to initial carbon mass were calculated and are shown in Table 4.6.

Table 4.6: Responses obtained for the fermentation of soybean hulls supplemented with either complex or defined media

Bioreactor	Medium	Maximum Lipase (kU L^{-1})	Protease* (U L^{-1})	Q^*_{LIP} (U $L^{-1}h^{-1}$)	Lipase / Protease Ratio*	$Y^{**,a}_{Lip/C}$ (kU $L^{-1}g^{-1}$)
Packed-bed	YPD	0.879	53.8	58.6	16.3	125
	YPDO	0.834	45.7	69.5	18.3	80.9
	YPO	1.35	52.3	90.1	25.8	99.6
Tray	YPD	0.857	47.5	57.1	18.0	122
	YPDO	1.58	73.9	105	21.4	153
	YPO	0.856	54.7	57.1	15.6	63.1
	YPD 5x	0.320	140	13.3	2.29	9.09
	YPDO 5x	1.24	97.4	51.5	12.7	24.0
	YPO 5x	2.91	98.1	121	29.7	42.9
	DN	0.255	116	3.54	2.19	36.2
	DN 5x	0.684	44.9	28.5	15.2	19.4
	DON 5x	0.374	148	6.24	2.53	7.26

*Q_{LIP}: Lipase productivity;**Calculated at the point of maximum lipase activity;^{a}: calculated from initial total carbon content based on elemental analysis of soybean oil.(Y): Yeast extract; (P): Bactopeptone; (D) Glucose; (O) Soybean oil; (N) Diammonium phosphate.

YPDO/tray and YPO/PBB combinations led to the best performance indicators, with contradictory results found for lipase production. Concerning the YPDO medium, lipase to protease ratio for the insulated PBB attained 85 % of the value found in the tray, while the maximum lipase activity and yield corresponded to only 53 % of those from the tray. Moreover, the lipase to protease ratio was comparable with the ones for YPD systems. In contrast, YPO supplementation resulted in a 58 % increase in lipase production in the PBB, even though it is still less pronounced than the one obtained with the YPDO medium in the tray bioreactor. The production profile for YPO/tray was also similar to the one in YPD/tray, but with a lower yield. The enhanced yield and lipase-to-protease ratio obtained in YPDO fermentation in tray showed that the obtained lipase activity could not be reached

using only soybean oil in tray bioreactor. The glucose-to-soybean oil carbon ratio used in this work was 34:66, which is close to the one proposed by SASSI *et al.* (2016) for maximal lipase induction in SmF fermentations with glucose and oleic acid. Thus, this observation of improved results with mixed co-substrate in the tray is consistent with the idea that neither the carbon source for growth nor the inducer should be used alone for lipase production by this yeast.

Time-dependent temperature profiles and effects in the insulated PBB KAWASSE *et al.* (2003) have shown an increase in the yield of *Y. lipolytica* biomass in relation to glucose under thermal stress in SmF. Other temperature-related effects on citric acid production and morphology of this yeast were also reviewed recently by TIMOUMI *et al.* (2018). The authors showed a decrease in citric acid production rate when cells were cultivated outside the optimum temperature and the enhancement in yeast-mycelial transition when cells undergo heat shock. Therefore, the impact over lipase production found for the PBB cultivation (in YPDO and YPO media) might be, to some degree, related to the temperature increase.

The highest temperature in the PBB experiments (Figure 4.9 d, e and f, and Figure 4.10) was around 35 °C, which is superior to the upper-temperature limit (34 °C) reported for growth of most Yarrowia lipolytica strains (BARTH and GAILLARDIN, 1996). Pronounced axial temperature gradients were attained between 9 and 15 h of fermentation. The temperature differences relative to the lower set of thermocouples (5.6 cm) ranged from 4.5 to 5.5 °C at the inner radius (1.32 cm) and 2.4 to 3.5 °C at the more external radius (4.09 cm). The three upper sections of the bioreactor also showed radial temperature gradients (hotter closer to the central axis of the bioreactor), suggesting that although the PBB was insulated, thermal exchange with side walls still occurred, probably due to an imperfect vacuum-sealed jacket. Non-uniform flow due to wall effect is unlikely to occur due to the high column/particle diameter ratio, above 85. The radial temperature difference varied from 1 to 2 °C, especially when lipase secretion started (between 9 and 12 hours), and the temperature had already reached 30 °C. At this value, the specific growth rate of some *Y. lipolytica* strains decreases in SmF (KARASU-YALCIN *et al.*, 2010, VASILEVA-TONKOVA *et al.*, 1996). For the three superior heights, this temperature was reached before 9 h of fermentation with oil supplementation (partial/complete substitution) and after 10.5 h for YPD cultivation. After 11 h, the temperature in the bioreactor started to decay in all the eight measurement points for all tested media, because cells were no longer in high metabolic activity, leading to a smaller heat production rate in comparison with the heat removal by the forceful aeration. The decrease in metabolic activity could be indirectly verified by the pH and protease profiles observed in both types of bioreactors, denoted by

an increase after 9 h. Closer to the bed base, the temperature did not surpass 30 °C for the three evaluated media, within the usual range for *Y. lipolytica* cultivation.

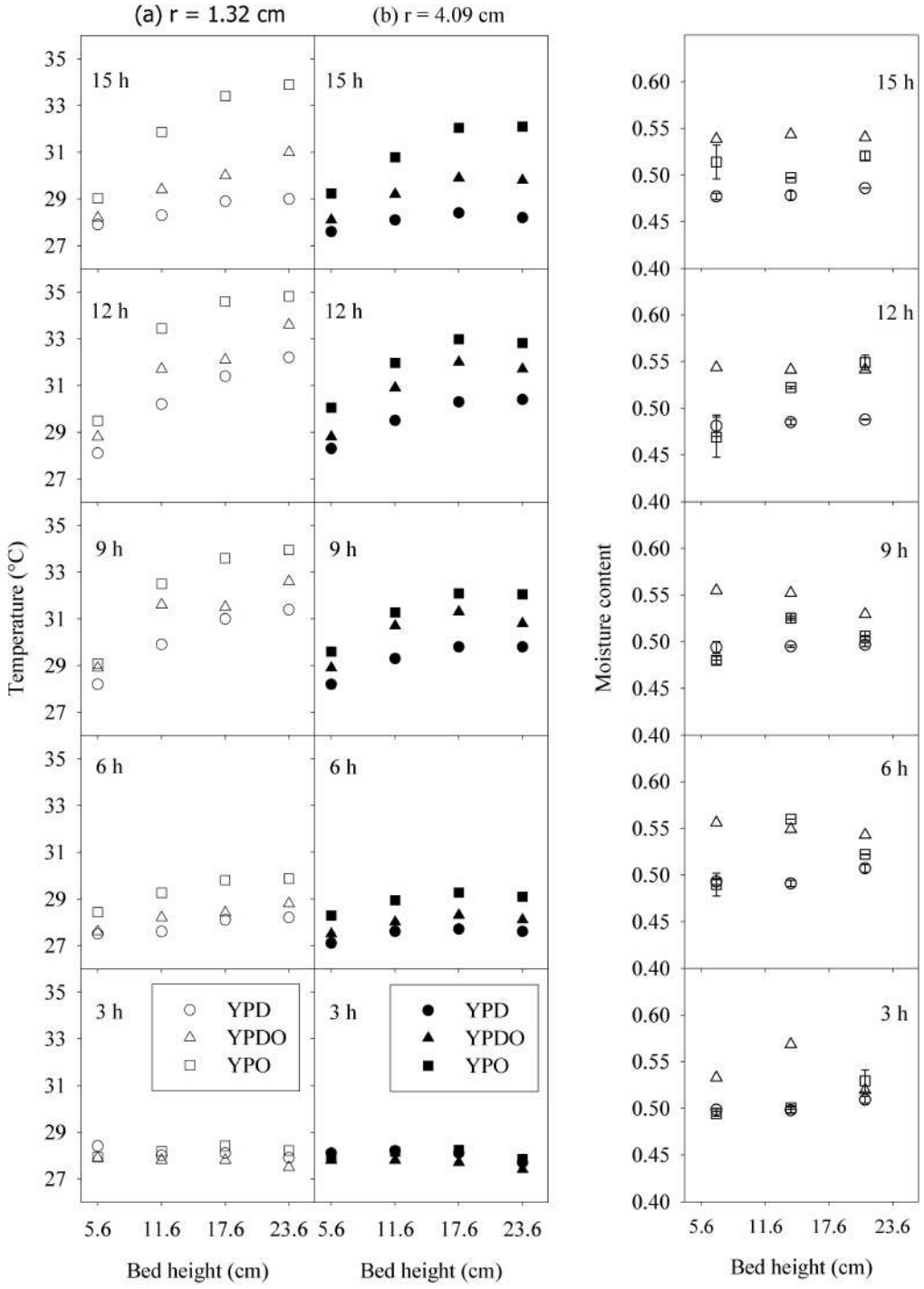

Figure 4.10: Figure 4. Axial temperature (monitored at two radii) and moisture profiles (measured after solid sampling) for fermentation of soybean hulls in insulated packed-bed bioreactors supplemented with different complex medium at various moments of the bioprocess.

For the fermentation with soybean oil in the PBB, the temperature remained above 32 °C at the more external radii and two upper heights for 2 h or more. This

value has been reported to be a restrictive temperature for protein secretion for some *Y. lipolytica* strains grown in YPD (TITORENKO and RACHUBINSKI, 1998), i.e., AEP secretion rate drastically decreases after exposure to this temperature for 2 h, without loss of AEP stability (measured with immunoprecipitation). Thus, as this temperature was reached in the PBB, this impairment on secretion can be verified by the smaller protease activity detected in YPDO and YPO (at the 14 and 21 cm sampling ports) in comparison with samples from the tray fermentation and the lower sampling port of the PBB. Therefore, lipase activity in the upper axial positions was more stable in YPDO and YPO. Furthermore, it was equal or higher in the PBB than in the tray for the YPO medium.

Although smaller protease activity was favorable to the maintenance of lipase activity with the increased temperature in the PBB, the temperature might also have affected carbon source assimilation. A comparison of the lipase yield in the PBB with the tray shows an opposite tendency for YPDO and YPO. In YPDO, as the temperature increased, cells may have used soybean oil, at least partially, for maintenance activities instead of using it only for product induction and cell growth. Heat shock at 37 °C in SmF completely stopped cell growth of the same strain used in this work (KAWASSE *et al.*, 2003). Thus, although the temperature did not rise as much, it is likely that the increased temperatures in PBB were sufficient to cause metabolic changes. TA *et al.* (2012) showed that *Y. lipolytica* cells grown with lipids are more resistant to heat shock than those grown on glucose. Besides, they verified that lipid bodies are induced in higher amounts in YPO than in YPD. Thus, a hypothesis that could be raised is that the oil was accumulated inside the cells as lipid bodies. In this sense, superior production in the PBB could be obtained in YPO because more soybean oil is available to the cells helping with the thermal burden. Therefore, lipase production through this strategy could benefit from the heat accumulation, once enough carbon source is supplemented for growth, enzyme induction and its accumulation due to the thermal stress.

Spatial temperature and moisture content profiles Regarding the spatial temperature profiles (Figure 4.10), as the temperature closer to the column wall (r = 4.09 cm) was systematically lower than the inner radial temperature (r = 1.32 cm) for all heights and all media, and also due to the high column/particle diameter ratio and the random packing for every experiment, we can discard the wall effect to explain the differences in radial temperature shown in this figure. Therefore, the hypothesis of unequal air flow distribution at the base of the bed may be discarded. Also, no large void spaces that could act as preferential flow paths and no bed deformation were visually noticed during the experiments. Bed deformation (mainly shrinking) and channeling are common drawbacks for packed-bed bioreac-

tor scale-up (ARORA *et al.*, 2018). CASTRO *et al.* (2015) used babassu cake as substrate for hydrolases production with Aspergillus oryzae in PBB and observed that the temperature peaked at 72 and 48 h in the lower and upper bed halves, respectively. They attributed this time difference in the temperature peaks to the blockage of the solid matrix and, consequently, to smaller gas velocity in the upper portion of the bioreactor. As the temperature peaks observed in the present work happened nearly at the same time for all media, and based on the above comments about the radial temperature, there is no indication that air flow patterns might have influenced the obtained axial temperature profiles. As expected for an exothermic process with energy transport due to the air flow, the axial temperature presented an increasing profile from the bottom to the top of the column.

Axial moisture content profiles shown in Figure 4.10 indicate that moisture content remained rather uniform for the YPD medium during the high metabolic activity period. In addition, the moisture content in oil-supplemented fermentations seems to remain equal or higher than that for YPD. Drying was not intense, which can be attributed to the use of a low gas flow rate. The superficial air herein used (0.01 m s^{-1}) was smaller than the values used by PITOL *et al.* (2017) (0.06 m s^{-1}) and CASTRO *et al.* (2015) (0.02 m s^{-1}), who also did not observe drying of the bed, at least for the same fermentation time considered in the present work. Besides, as the emulsified media were added to the soybean hulls, the oil may have helped in preventing water evaporation by changing effective transport coefficients for water.

Comparison with other lipase production processes in SSF

Bioprocess productivities using other fungi, *Y. lipolytica* and soybean residues are compared in Table 4.7, along with some other residues used for lipase production by *Y. lipolytica*. The use of *Y. lipolytica* IMUFRJ 50682 with soybean meal has proven to be superior, but there is still space for further improvements when supplementing soybean hulls, which are already being addressed by our group. Ultimately, the strain herein used showed similar or superior performances in both tray and PBB when compared to other *Y. lipolytica* strains and some fungi (*Aspergillus* and *Thermomucor*), for which production time was nearly 3-fold shorter. Also, a 46 % productivity increase was observed in the YPO fermentation scale-up from 0.5 g in the tray to 400 g in the PBB, which represents an 800-fold increase in the mass of solids. Faster processes are of high relevance since time-consuming ones tend to increase bioreactor sizes and hence capital investment (CASTILHO *et al.*, 2000, CASTRO *et al.*, 2015).

Table 4.7: Compilation of main results for lipase production by solid-state fermentation.

Strain	Substrate and supplementation	Bioreactor and conditions	Q^*_{LIP} (U g^{-1} h^{-1})	Reference
Y. lipolytica CECT 1240 (ATCC 18942)	Triturated nut with 2 % glucose, 2 % urea, and mineral and vitamin solution	Tray, 30 °C, 90 % moisture, 264 h	0.3	(DOMÍNGUEZ *et al.*, 2003)
P.simplicissimum	Soybean meal	Tray, 27.5 °C, 55 % moisture, 80 h, 0.25<d_P<0.42 mm	0.4	(VARGAS *et al.*, 2008)
P. verrucusum	Soybean bran	Tray, 27,5 °C, 55 % moisture, 48 h 0.35<d_P<1.0 mm	0.8	(KEMPKA *et al.*, 2008)
Penicillium P58, P74	Soybean meal with 1 % oil and 3 % urea	Tray, 27 °C, 55 % moisture, 48 h, 0.5<d_P<1 mm	3.1	(RIGO *et al.*, 2010)
Penicillium sp.	Soybean meal	Tray, 27 °C, 55 % moisture, 48 h, 1.0<d_P<2.0 mm	3.9	VARDANEGA *et al.* (2010)
Aspergillus sp.	Soybean bran	Tray, 30 °C, 80 % moisture, 96 h	0.6	(FLEURI *et al.*, 2014)
Thermomucor indicae seudaticae N31	Soybean bran	Tray, 45 °C, 72 h	0.1	(FERRAREZI *et al.*, 2014)
Y. lipolytica NCIM 3589	Mustard oil cake with salt solution, 1.5 % urea, and 7 % glucose	Tray, 30 °C, 50 % moisture, 96 h	0.6	IMANDI *et al.* (2013a)
C. lipolytica NRRL Y-1095	Soybean meal	Tray, 30 °C, 1.5 mm, 72 h	4.10-3	(UR REHMAN *et al.*, 2014)

Strain	Substrate and supplementation	Bioreactor and conditions	Q^*_{LIP}(U g^{-1} h^{-1})	Reference
Y. lipolytica IMUFRJ 50682	Soybean meal with soybean sludge (4% m/m)	Tray, 28 °C, 58 % moisture, 14 h, $d_P \leq 1.18$ mm	9.9	(FARIAS *et al.*, 2014)
	Soybean meal with 1.5 % oil	Tray, 28 °C, 55 % moisture, 14 h, $d_P \leq 1.18$ mm	6.7	SOUZA *et al.* (2017)
	Soybean hulls with YPDO	Tray, 28 °C, 55 % moisture, 15 h, $0.5 < d_P < 1.18$ mm	1.2**	This work
	Soybean hulls with YPO	Packed-bed bioreactor, 28 °C, 55 % moisture, 15 h, $0.5 < d_P < 1.18$ mm	0.9	

d_P: particle diameter obtained by sieving; Q_{LIP}: Lipase productivity;*:g: grams of dry substrate;

**: calculated assuming constant moisture contentof 55 %. (Y): Yeast extract; (P): Bactopeptone; (D) Glucose; (O) Soybean oil.

4.2.5 Conclusions

Supplementation strategies, along with process conduction in the tray and insulated packed-bed bioreactors, have been tested to gather information regarding the behavior of the yeast *Yarrowia lipolytica* when growing on soybean hulls. When comparing concentrated defined medium (DM), all the responses show a decrease in performance when glucose was partially replaced by soybean oil. However, complex medium (CM) presented the opposite tendency, with better results for glucose substitution. pH played an important role in DM and YPD 5x, as experiments above pH 7.0 resulted in reduced lipase production, needing a preliminary pH adjustment step. Despite these limitations, the results obtained for CM confirmed their superiority for the induction of lipases.

More importantly, this work revealed that, in insulated packed-bed bioreactor supplemented with complex media, the temperature might serve as an indirect indicator of harvesting time for lipase production. Meanwhile, the temperature may influence protease production and also improve lipase stability. As this fact was only perceived in media with soybean oil, we showed the relevance of synergistic effects arising from different bioreactor types and medium supplementations. Furthermore, the PBB process with YPO media showed promising productivity, indicating that optimization strategies might increase even more this bioprocess performance.

Chapter 5

Thermal and growth modeling of lipase production in insulated packed bed bioreactor with *Yarrowia lipolytica*

Heat and mass balance equations that mathematically describe solid-state fermentations have been used for many years, with increasing level of phenomenological description. However, for application in the process engineering, this tool needs to be validated with experimental data from bioreactors (FANAEI and VAZIRI, 2009).

These bioreactors are commonly classified in two groups: static or agitated (MITCHELL *et al.*, 2003). For instance, FIGUEROA-MONTERO *et al.* (2011) have shown that forceful aeration in static trays improved the global heat transfer by more than 60 %, while mass transfer increased by 210 %. In packed beds, where the air flows through the bed, DA SILVEIRA *et al.* (2014) verified that the volumetric air flow rate increase *per se* is not the main responsible for heat removal, as evaporation impacts more on the temperature than the effect of air convection. Water removal by excessive evaporation may impair growth if the water activity at the solid is outside of the range for the microorganism.

Although the yeast *Y. lipolytica* has been cultivated in trays since 2003, all the studies focused on media supplementation and valorization of biomass. Little or no knowledge of thermal and water dependencies on growth in solid state fermentation are available. Besides, the modeling approach for better process comprehension has not been tackled yet. Therefore, as a tool to evaluate the production of lipase by this yeast, heat and mass transport equations were used in simulation studies using the software EMSO.

5.1 Mathematical model description

The model recently proposed by CASCIATORI *et al.* (2016) (Equations 2.25a, 2.25b, 2.25c, and 2.25d) was chosen to described the proposed process assuming its main hypothesis. However, some adaptations were done for this yeast. In this case, it was assumed that the yeast is not able to consume the residue due to its major lignocellulotic composition. Thus, the derivatives for the soybean hulls consumption were simplified and the model became (Equations 5.1, 5.2, 5.3,and 5.4).

$$\rho_a\epsilon_0\frac{\partial Y}{\partial t} + v_z\rho_a\frac{\partial Y}{\partial z} = \dot{\nu}(X)\beta a\rho_a\epsilon_0(Y^* - Y) + \rho_a\epsilon_0 D_{g,z}\frac{\partial^2 Y}{\partial z^2} + \rho_a\epsilon_0 D_{g,r}\frac{1}{r}\frac{\partial}{\partial r}\left(r\frac{\partial Y}{\partial r}\right) \tag{5.1}$$

$$S\frac{\partial X}{\partial t} = -\dot{\nu}(X)\beta a\rho_a\epsilon_0(Y^* - Y) + Y_w S\frac{\partial b}{\partial t} + D_s S\frac{\partial^2 X}{\partial z^2} + D_s S\frac{1}{r}\frac{\partial}{\partial r}\left(r\frac{\partial Y}{\partial r}\right) \tag{5.2}$$

$$\begin{aligned}\rho_a\epsilon_0(C_{p_a} + YC_{p_{vap}})\frac{\partial T_g}{\partial t} + v_z\rho_a(C_{p_a} + YC_{p_{vap}})\frac{\partial T_g}{\partial z} = -ha(T_g - T_s)\\ +\Delta H_{vap}(T_s)\dot{\nu}(X)\beta a\rho_a\epsilon_0(Y^* - Y) + \epsilon_0\lambda_{g,z}\frac{\partial^2 T_g}{\partial z^2} + \epsilon_0\Lambda_{g,r}\frac{1}{r}\frac{\partial}{\partial r}\left(r\frac{\partial T_g}{\partial r}\right)\end{aligned} \tag{5.3}$$

$$\begin{aligned}(C_{p_s} + XC_{p_w})S\frac{\partial T_s}{\partial t} = ha(T_g - T_s) - \Delta H_{vap}(T_s)\dot{\nu}(X)\beta a\rho_a\epsilon_0(Y^* - Y) +\\ Y_H S\frac{\partial b}{\partial t} + (1-\epsilon_0)\lambda_s\frac{\partial^2 T_s}{\partial z^2} + \epsilon_0\lambda_s\frac{1}{r}\frac{\partial}{\partial r}\left(r\frac{\partial T_s}{\partial r}\right)\end{aligned} \tag{5.4}$$

In this work, dimensionless spatial coordinates were used, which implied the variables exchange of the form $\overline{z} = z/L$ and $\overline{r} = (r/R)^2$ (taking advantage of the radial symmetry). Thus, it required the following derivative equalities to be obeyed (Equations 5.5 and 5.6:

$$\frac{\partial \bullet}{\partial z} = \frac{1}{L}\frac{\partial \bullet}{\partial \overline{z}} \tag{5.5}$$

$$\frac{\partial \bullet}{\partial r} = \frac{2\overline{r}^{1/2}}{R}\frac{\partial \bullet}{\partial \overline{r}} \tag{5.6}$$

Therefore, by applying Equations 5.5 and 5.6 into Equations 5.1, 5.2, 5.3,and 5.4, they became

$$\rho_a\epsilon_0\frac{\partial Y}{\partial t}+\frac{v_z\rho_a}{L}\frac{\partial Y}{\partial \overline{z}}=\dot{\nu}(X)\beta a\rho_a\epsilon_0(Y^*-Y)+\frac{\rho_a\epsilon_0 D_{g,z}}{L^2}\frac{\partial^2 Y}{\partial \overline{z}^2}+\frac{4\rho_a\epsilon_0 D_{g,r}}{R^2}\frac{1}{\overline{r}}\frac{\partial}{\partial \overline{r}}\left(\overline{r}\frac{\partial Y}{\partial \overline{r}}\right) \tag{5.7}$$

$$S\frac{\partial X}{\partial t}=-\dot{\nu}(X)\beta a\rho_a\epsilon_0(Y^*-Y)+Y_wS\frac{\partial b}{\partial t}+\frac{D_s}{L^2}S\frac{\partial^2 X}{\partial \overline{z}^2}+4\frac{D_sS}{R^2}\frac{1}{\overline{r}}\frac{\partial}{\partial \overline{r}}\left(\overline{r}\frac{\partial Y}{\partial \overline{r}}\right) \tag{5.8}$$

$$\begin{aligned}\rho_a\epsilon_0(C_{p_a}+YC_{p_{vap}})\frac{\partial T_g}{\partial t}+\frac{v_z\rho_a(C_{p_a}+YC_{p_{vap}})}{L}\frac{\partial T_g}{\partial \overline{z}}=-ha(T_g-T_s)\\ +\Delta H_{vap}(T_s)\dot{\nu}(X)\beta a\rho_a\epsilon_0(Y^*-Y)+\frac{\epsilon_0\lambda_{g,z}}{L^2}\frac{\partial^2 T_g}{\partial \overline{z}^2}+\frac{4\epsilon_0\Lambda_{g,r}}{R^2}\frac{1}{\overline{r}}\frac{\partial}{\partial \overline{r}}\left(\overline{r}\frac{\partial T_g}{\partial \overline{r}}\right)\end{aligned} \tag{5.9}$$

$$\begin{aligned}(C_{p_s}+XC_{p_w})S\frac{\partial T_s}{\partial t}=ha(T_g-T_s)-\Delta H_{vap}(T_s)\dot{\nu}(X)\beta a\rho_a\epsilon_0(Y^*-Y)+\\ Y_HS\frac{\partial b}{\partial t}+\frac{(1-\epsilon_0)\lambda_s}{L^2}\frac{\partial^2 T_s}{\partial \overline{z}^2}+\frac{4(1-\epsilon_0)\lambda_s}{R^2}\frac{1}{\overline{r}}\frac{\partial}{\partial \overline{r}}\left(\overline{r}\frac{\partial T_s}{\partial \overline{r}}\right)\end{aligned} \tag{5.10}$$

As a result of these manipulations, the boundary conditions were also modified (Equations 5.7—5.10). Due to radial symmetry, the derivative at the center of the bioreactor was only required to be finite in the new coordinate system.

Inlet

$$\left(\frac{\partial X}{\partial \overline{z}}\right)_{\overline{z}=0}=\left(\frac{\partial T_s}{\partial \overline{z}}\right)_{\overline{z}=0}=0;T_g=T_{g_0};Y=Y_0 \tag{5.11}$$

outlet

$$\left(\frac{\partial X}{\partial \overline{z}}\right)_{\overline{z}=1}=\left(\frac{\partial T_s}{\partial \overline{z}}\right)_{\overline{z}=1}=\left(\frac{\partial T_g}{\partial \overline{z}}\right)_{\overline{z}=1}=\left(\frac{\partial Y}{\partial \overline{z}}\right)_{\overline{z}=1}=0; \tag{5.12}$$

Center

$$\left(\frac{\partial X}{\partial \overline{r}}\right)_{\overline{r}=0}=\rightarrow finite \tag{5.13a}$$

$$\left(\frac{\partial T_s}{\partial \overline{r}}\right)_{\overline{r}=0}=\rightarrow finite \tag{5.13b}$$

$$\left(\frac{\partial T_g}{\partial \overline{r}}\right)_{\overline{r}=0}=\rightarrow finite \tag{5.13c}$$

$$\left(\frac{\partial Y}{\partial \overline{r}}\right)_{\overline{r}=0}\rightarrow finite; \tag{5.13d}$$

Wall

$$\begin{aligned} \left(\frac{\partial X}{\partial \overline{r}}\right)_{\overline{r}=1} &= \left(\frac{\partial Y}{\partial \overline{r}}\right)_{\overline{r}=1} = 0; \\ -\frac{2\overline{r}^{1/2}\Lambda_{g,r}}{R}\left(\frac{\partial T_g}{\partial \overline{r}}\right)_{\overline{r}=1} &= \alpha_{wall}(T_{g_{\overline{r}}} - T_{wall}); \\ -\frac{2\overline{r}^{1/2}\lambda_s}{R}\left(\frac{\partial T_s}{\partial \overline{r}}\right)_{\overline{r}=1} &= \alpha_{wall}(T_{s_{\overline{r}}} - T_{wall}); \end{aligned} \tag{5.14}$$

Y. lipolytica growth on the soybean hulls was described by the logistic growth equation, with $\mu_{g_{opt}}$ based on the *N*-acetylglucosamine data from SOUZA *et al.* (2017), while lipase production was assumed to be growth associated. The temperature dependence was represented by Equation 2.13, with parameters estimated from SmF data of acid phosphatase production by this yeast (VASILEVA-TONKOVA *et al.*, 1996). Although water activity dependence is usually included when mass balances are applied (CASCIATORI *et al.*, 2016, MARQUES *et al.*, 2006), it was excluded in this study since no data was found for this yeast.

The gas heat (λ and Λ) and mass (D) dispersion coefficients in the axial and radial directions (z and r subscripts, respectively) were calculated using the core unit cell model, which allowed the determination of the reduced dispersion coefficients by Equation 5.15(NEUBRONNER *et al.*, 2010) under the hypothesis of plug flow, constant porosity and particle diameter much smaller than the bioreactor radius.

$$f_{deform} = f_{shape}\left(\frac{1-\epsilon_0}{\epsilon_0}\right)^{10/9} \tag{5.15a}$$

$$N = 1 - \frac{f_{deform}}{k_p}, k_p = \frac{\lambda_s}{\lambda_g} \tag{5.15b}$$

$$k_c = \frac{2}{N}\left(\frac{f_{deform}}{N^2}\frac{k_p - 1}{k_p} ln \frac{k_p}{f_{deform}} - \frac{f_{deform}+1}{2} - \frac{f_{deform}-1}{N}\right) \tag{5.15c}$$

$$\Lambda_{red} = 1 - \sqrt{1-\epsilon_0} + k_c\sqrt{1-\epsilon_0} \tag{5.15d}$$

$$D_{red} = 1 - \sqrt{1-\epsilon_0} \tag{5.15e}$$

where f_{shape} is a particle shape factor (1.25 for spheres, 1.4 for Raschig rings or broken particles), f_{deform} is a deformation factor and λ is the heat dispersion coefficient of the fluid (gas) or the particle. Equation 5.15e is obtained as a special case by making $\lambda_p = 0$ (under heat-mass transfer analogy). The molecular Péclet numbers were calculated (Equations 5.16a and 5.16b) and later used to determine the effective heat and mass transfer coefficients (Equation 5.17):

$$Pe_{0_m} = \frac{v_z d_P}{D_g} \tag{5.16a}$$

$$Pe_{0_T} = \frac{v_z \rho_a (C_{p_a} + Y_0 C_{p_{vap}}) d_P}{\lambda_g} \tag{5.16b}$$

$$\lambda_{g,z} = \lambda_g (\Lambda_{red} + \frac{Pe_{0_T}}{2}) \tag{5.17a}$$

$$\Lambda_{g,r} = \lambda_g (\Lambda_{red} + \frac{Pe_{0_T}}{8}) \tag{5.17b}$$

$$D_{g,z} = D_g (D_{red} + \frac{Pe_{0_m}}{2}) \tag{5.17c}$$

$$D_{g,r} = D_g (D_{red} + \frac{Pe_{0_m}}{8}) \tag{5.17d}$$

The Reynolds number of the particle (Re_p) was calculated using the equivalent diameter as the characteristic length. Empirical correlations for flow around spheres were used to determine the Nusselt (Nu , Equations 5.18b (ACRIVOS and TAYLOR, 1962) and 5.18c (FINLAYSON and OLSON, 1987)) and Sherwood (Sh) numbers based on the heat and mass transfer analogy ($Sh = Nu$). The interfacial area (a) was calculated and multiplied by the heat (h) and mass (β) transfer coefficients at the interface to obtain the volumetric transfer coefficients (CASCIATORI *et al.*, 2016).

$$Re_p = \frac{v_z d_P}{\nu_{air}} \tag{5.18a}$$

$$Nu = 2 + \frac{Pe_{0_T}}{2} + \frac{Pe_{0_T}^2 ln Pe_{0_T}}{4} + 0.03404 Pe_{0_T}^2 + \frac{Pe_{0_T}^3 ln Pe_{0_T}}{16}, Re_p < 1 \tag{5.18b}$$

$$Nu = 2 + \frac{0.45 Pe_{0_T}^{4/3} Re_p^{0.11}}{0.9 Pe_{0_T}^{1/3} Re_p^{0.11} + 0.5 Pe_{0_T}}, Re_p \geq 1 \tag{5.18c}$$

$$h = \frac{\lambda_g Nu}{d_P} \tag{5.18d}$$

$$\beta = \frac{D_g Sh}{d_P} \tag{5.18e}$$

$$a = \frac{6(1 - \epsilon_0)}{d_P} \tag{5.18f}$$

The coefficient for heat transfer between the wall and the gas was initially estimated using an empirical correlation described in Equation 5.19 (LI and FINLAYSON, 1977):

$$\alpha_{wall} = \frac{0.17 Re_p^{0.79} \lambda_{g,m}}{d_P} \tag{5.19}$$

The saturation moisture content and the water activity of the gas phase were calculated as described by CASCIATORI *et al.* (2016), using the saturation vapor pressure calculated with the Antoine Equation. Finally, the parameter and initial variable values used for the simulations are shown in Table 5.1.

Table 5.1: Parameters used for the simulation of *Y. lipolytica* growth, temperature . and lipase production in solid-state fermentation of soybean hulls.

Parameter	Definition	Unit	Value	Ref. or source
Microbial parameters				
μ_{opt}	Optimum specifc growth rate	h^{-1}	0.239	Estimated from SOUZA *et al.* (2017)
E_A	Activation energy	kJ mol^{-1}	34.96	Estimated from VASILEVA-TONKOVA *et al.* (1996)
E_D	Denaturation activation energy	kJ mol^{-1}	549.89	Estimated from VASILEVA-TONKOVA *et al.* (1996)
A	Frequency factor	—	1.19×10^{6}	Estimated from VASILEVA-TONKOVA *et al.* (1996)
B	Frequency factor	—	5.06×10^{93}	Estimated from VASILEVA-TONKOVA *et al.* (1996)
Y_w	Water yield	kg_{H_2O} kg^{-1}	0.3	CASCIATORI *et al.* (2016)
Y_q	Heat yield	J kg^{-1}	1.47×10^{7}	VOLESKY *et al.* (2007)
$Y_{B/Glu}$	Biomass yield on glucose	kg_B $kg^{-1}_{glucose}$	0.32	VOLESKY *et al.* (2007)
b_{max}	Maximum cell concentration	g kg^{-1}	6.3584	Calculated from $Y_{B/Glu}$
$Y_{P/B}$	Lipase yield on biomass	U L^{-1}	1.77×10^{5}	Calculated from $Y_{B/Glu}$ and b_{max}
Design and operating parameters				
a_{w_0}	Inlet water activity	—	0.85	CASCIATORI *et al.* (2016)
L	Bioreactor lenght	cm	28	

Parameter	Definition	Unit	Value	Ref. or source
r	Bioreactor radius	cm	5	
v_z	Superficial gas velocity	m s^{-1}	0.0106	
Substrate and bed properties				
ν_{air}	Air viscosity	m^2s^{-1}	15.93×10^{-6}	
ρ_a	Air density	kg m^{-3}	1.1614	
$C_{p_{vap}}$	Vapor heat capacity	J $kg^{-1}K^{-1}$	1872	
C_{p_a}	Air heat capacity	J $kg^{-1}K^{-1}$	1007	
P	Pressure	Pa	101325	
ϵ_0	Porosity	—	0.725	
d_P	Particle diameter	mm	0.897	
ΔH_{vap}	Water heat of vaporization	J kg^{-1}	2414300	
C_{p_w}	Water specific heat	J $kg^{-1}K^{-1}$	4179	
C_{p_s}	Solid specifc heat	J $kg^{-1}K^{-1}$	4725	MUZILLA *et al.* (1991)
R_g	Universal gas constant	J $mol^{-1}K^{-1}$	8.314	
ρ_s	Solid density	g cm^{-3}	1.05	MUZILLA *et al.* (1991)
Initial dependent variables				
b_0	Initial cell concentration	g kg^{-1}	0.71	
S	Solids concentration	kg m^3	162.08	
T_{g_i}	Inlet gas temperature	K	299.5	
T_{s_0}	Solid initial temperature	K	T_{g_i}	
T_{g0}	Gas initial temperature	K	T_{g_i}	
Transport properties				
D_g	Water molecular diffusivity in the air	m^2s^{-1}	2.5×10^{-6}	
D_s	Water dispersion coefficient in the solid	m^2s^{-1}	1.5×10^{-10}	CASCIATORI *et al.* (2016)
λ_g	Molecular thermal conductivity of the air	J $s^{-1}m^{-2}K^{-1}$	0.0263	
λ_s	Solid-state stagnant thermal conductivity	J $s^{-1}m^{-2}K^{-1}$	0.616	MUZILLA *et al.* (1991)
$\dot{\nu}(X)$	Normalized drying rate	—	1	CASCIATORI *et al.* (2016)
h	Interfacial heat transfer coefficient	J $s^{-1}m^{-2}K^{-1}$	64.0	

Parameter	Definition	Unit	Value	Ref. or source
β	Interfacial mass transfer coefficient	m s^{-1}	6.08×10^{-2}	

5.1.1 Model simulation

The proposed set of equations was implemented in the software EMSO (Environment for Modeling, Simulation and Optimization (SOARES and SECCHI, 2003). In order to solve the partial derivatives, the polynomial approximation using orthogonal collocation was used using the available plugin OCFEM. The method consists of approximating the variable by a polynomial such that the approximation residue is zero at the collocation points. In this case, collocation points are the roots of the Jacobi polynomials, defined by its degree of the polynomial (n), and the exponents n_1 and n_2 of the weight function (Equation 5.20)

$$w(x) = x^{n_2}(1-x)^{n_1} \tag{5.20}$$

Due to the radial symmetry of the problem, the best value of n_2 for the radial polynomial is zero. The other values of n_1 (for both the radial and axial polynomials) and n_2 (for the axial polynomial) were set to 0. In the simulations, after mesh refinement analysis, the number of internal axial and radial collocation points was set to 10 and 4, respectively.

5.1.2 Sensitivity Analysis and Parameter Estimation

A sensitivity analysis was performed to verify parameter influence on process variables according to Equation 5.21a. The derivatives were calculated using a central difference approximation, which were later normalized, as shown in Equation 5.21b:

$$s_{i,j,t} = \frac{\partial \psi_{j,t}}{\partial p_i} \approx \frac{\Delta \psi_{j,t}}{\Delta p_i} = \frac{\psi_{j,t}(p_i+\xi_i) - \psi_{j,t}(p_i-\xi_i)}{2\xi_i} \tag{5.21a}$$

$$s^*_{i,j,t} = \frac{\psi_{j,t}(p_i+\xi_i) - \psi_{j,t}(p_i-\xi_i)}{2\xi_i}\frac{p_i}{\psi_{j,t}(p_i)} \tag{5.21b}$$

where $s_{i,j,t}$ is the sensitivity of the j-th calulated process variable ($\psi_{j,t}$) calculated at the time t to the i-th parameter (p_i), based on a ξ_i parameter variation, and $s^*_{i,j,t}$ is the normalized sensitivity. In this evaluation, a ±5 % parameter variation was employed. After the sensitivity analysis, parameter estimation was done using the least squares objective function (F_{obj}), as described by Equation 5.22.

$$F_{obj} = \sum_t \sum_j (\psi_{j,t} - \tilde{\psi}_{j,t})^2 \tag{5.22}$$

where $\tilde{\psi}_{j,t}$ are the experimental values of the j-th variable (solid temperature and moisture content along the bed) and t_j-th experimental temporal point. The experimental data were based on the insulated PBB temperature values obtained during fermentation with YPD medium, as described in Chapter 4. The flexible polyhedron method was used for direct search of desired parameters. The temperature experimental data were obtained in 4 axial positions and two radii. The thermocouples used for experimentation were positioned radially to match the orthogonal collocation points, facilitating the estimation process. In the axial case, the calculated data were previously interpolated to match the orthogonal collocation points.

5.2 Results

5.2.1 Base case simulation

The use of heat and mass balance equations in simulation of solid-state fermentation processes is of great relevance for a better design and comprehension of the ongoing relevant phenomena. Therefore, a base case simulation was done to verify the model performance considering the 24-hour period of the acquired experimental data.

Simulation with the base case parameters was done and it was not successful initially. The program was unable to complete the integration steps without reaching the maximum allowed temperature values (which were set to 60 °C). A careful investigation of the parameters revealed that the values obtained for the mass interface transfer coefficient ($\beta = 6.08 \times 10^{-2}$ m s^{-1}) had a profound impact on the simulation. It is noteworthy mentioning that the experimental solid moisture content had little change during the fermentation time, thus evaporation might have occurred with low intensity. To modify this behavior in the mass balance equations, a test was performed using the water dispersion coefficient (D_s) instead of the molecular diffusivity of water in the air ($D_{g,m}$)to calculate the β value using Equation 5.18e. The new value of β was $3.65{\times}10^{-7}$ m s^{-1} and the main results are presented in Figure 5.1.

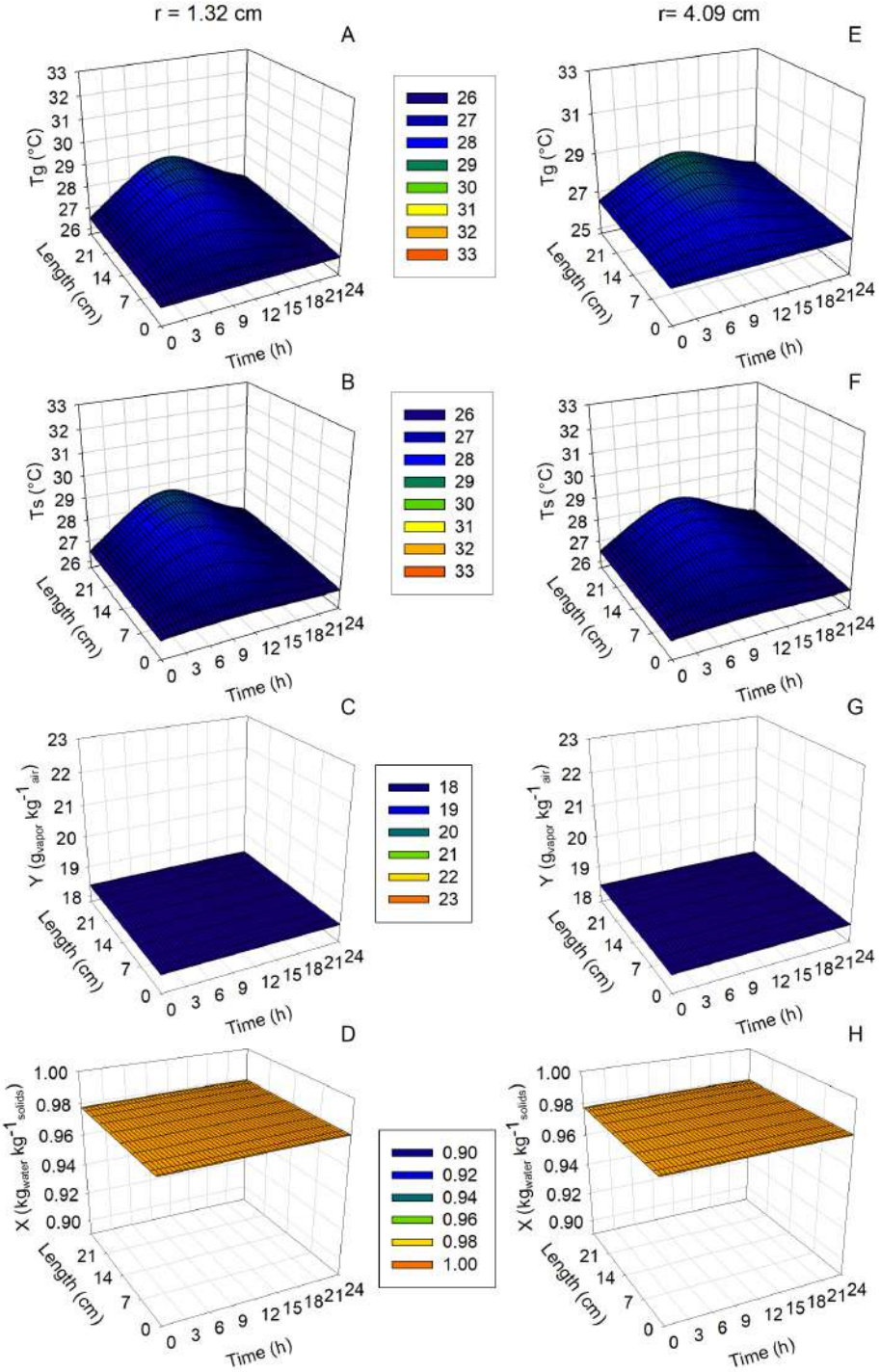

Figure 5.1: Gas (A,B) and solid (C,D) temperatures, gas (E,F) and solid (G,H) moisture content for the base case at different radii.

Regarding the temperature peaks, they were less intense than the experimental ones, but they were timely consistent with experimental. No difference in gas and solid phases temperatures were observed in both radii (1.32 and 4.09 cm). The solid moisture content remained nearly constant throughout the simulation time, as desired. These results indicated that change in an interfacial-related parameter could be the reason for this poor result, especially if one considers that this parameter is multiplied by the specific area, which is bigger for spherical particles than for cylindrical objects, for instance.

The Nu correlations used in this first simulation (Equations 5.18b and 5.18c) were developed for single particle heat and mass transfer evaluation at low Pe values. However, MARTIN (1978) compiled data from various works on estimation of these interfacial transfer coefficients which deviate from the asymptotic value at low Pe values (when $Pe \rightarrow 0$, $Nu \rightarrow 2$ for spherical particles). From his work, it was possible to verify that the Nusselt number estimated herein (for $Pe = 0.44$) might have been grossly different, leading to h and β overestimation, since the values for Nu were smaller. To investigate this, new simulations using $Nu = 0.0001$ and $D_{g,m}$ for β estimation were performed. The values for h and β were 2.93×10^{-3} J s^{-1}m^{-2}K^{-1} and 2.787×10^{-6} m s^{-1}, respectively, and the results are shown in Figure 5.2.

The moisture profiles showed little variation, which is expected in a process where water removal by evaporation is not expressive. The new temperature profiles presented the same characteristics, with noticeable differences at the solid temperatures, leading to temperature profiles closer to experimental values. Temperatures did not surpass 30 °C, being within the usual cultivation temperature for *Y. lipolytica*, thus growth is not supposed to be hindered. No radial and axial differences for both phases were observed (less than 1 °C), while in comparison with the previous simulation, solid phase temperatures were up to 3 °C higher than in gas phase for the peak values. CASCIATORI *et al.* (2016) evaluated the effect of radial heat removal by manipulating the bioreactor radius and keeping the gas superficial velocity proportional, showing that non-negligible gradients may occurs for lower L/D ratios. In the present study, the L/D ratio is low enough so that this effect could happen in the system, causing a radial gradient, as also evidenced by the experimental data. The axial gradients that were characteristic in the base case simulation disappeared, possibly as a result of the low Nu value.

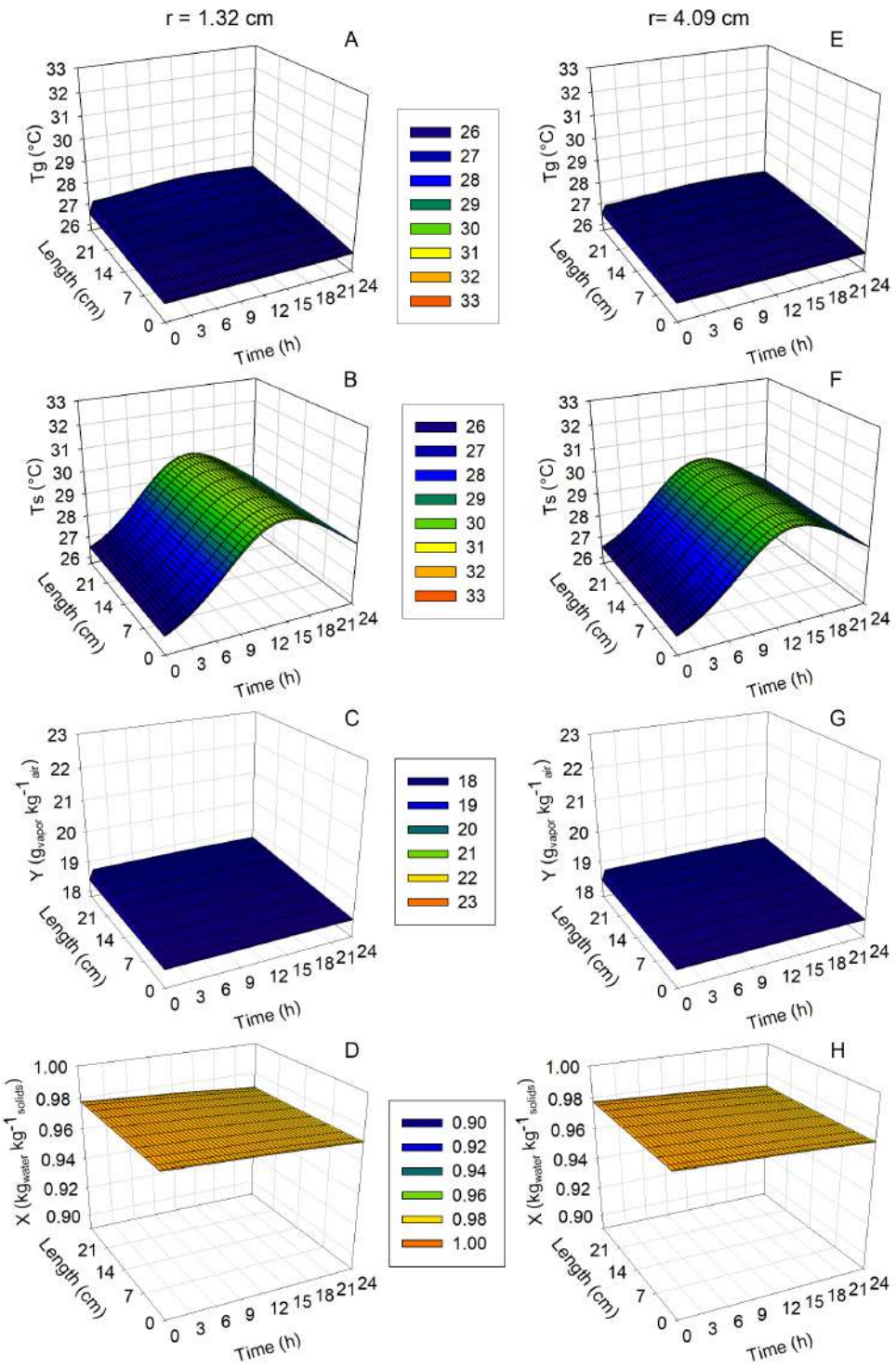

Figure 5.2: Gas (A,B) and solid (C,D) temperatures, gas (E,F) and solid (G,H) moisture content for $Nu = 0.0001$ at different radii.

5.2.2 Sensitivity analysis and parameter estimation

Although the predicted behaviors were somewhat closer to acquired data, this indicated that further improvements were needed in the model. Parameter estimation requires the delimitation of a viable search region for the parameters. Besides, the knowledge of the most influential parameters is fundamental when choosing the ones to estimate. Apart from the already mentioned motives to verify Nu influence, other physical properties were evaluated (ϵ_0, a_{w0}, and α_{wall}) due to diverse reasons: despite the insulation, a radial gradient was observed and therefore a correlation was used to calculate α_{wall} as an initial guess, knowing that it was not valid for the simulated bioprocess; the water activity in the gas phase was not measured, but it was assumed to be high enough, since a sintered metallic filter was used in the experiments for increased mass transfer in a column prior to gas injection in the bioreactor; and the porosity is known to modify as a function of the moisture content of the solid (CASCIATORI *et al.*, 2015). Therefore, the porosity measurement described in Chapter 3 may not be completely valid in the process conditions, but it serve as an initial guess. For these reasons, a normalized sensitivity analysis based on the previous simulation with $Nu = 0.0001$ was done and the results are shown in the form of heat map in Figure 5.3.

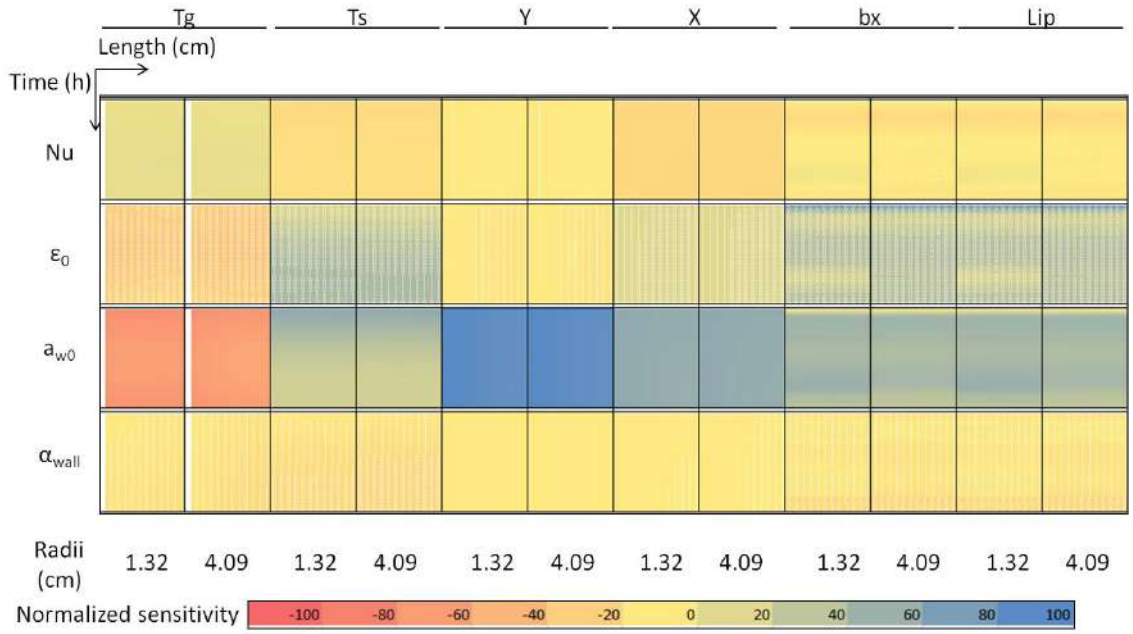

Figure 5.3: Heat map for the normalized sensitivity of different variables towards the physical parameters Nu, ϵ_0, a_{w0}, and α_{wall} at different radii for the simulation of lipase production by *Y. lipolytica*. Tg: gas temperature; Ts: solid temperature; Y: vapor content in the air; X: water content in the solids; bx: cell content in the solids; Lip: extractable lipase.

The rate of evaporation and its associated heat transfer are dependent on Nu,

ϵ_0, and a_{w0}, thus it is expected that these parameters have major influence on the predicted behaviors. From Figure 5.3, it is evidenced that a_{w0} has the biggest influence among the evaluated variables, with higher intensity for those related to the gas phase, as expected. The porosity of the bed influences more the gas and solid temperatures, which also impact on cell responses. Although Nu and α_{wall} are directly connected to heat removal in the bed, these promote less influence on the system. At such low flow conditions, convective heat transfer is not a dominant mechanism, leading to a system where dispersion becomes increasingly relevant, as it can also be inferred from the Pe value. Besides, the combination of low gas superficial velocity with an insulated bioreactor tends to consistently decrease the role of wall heat transfer in heat removal from the bed.

The impact of these physical properties on cell growth and lipase production were also explored and a_{w0} had the biggest influence. Although no water activity dependence was used to describe the specific growth rate (μ), the water activity directly influences the amount of heat removed from the solids, so an indirect influence on the solid temperature led to this response.

Next, a preliminary parameter estimation was executed for Nu and a_{w0}. For this, Y_{xs} was changed to 0.6, since the yields observed for this strain in SmF were higher than the value used before. Besides, the original ϵ_0 was used as it was measured experimentally. α_{wall} was not estimated because the search method always led this parameter to the frontier of the search region after numerous tries. Thus, its value was still calculated with Equation 5.19. The results obtained after estimation are shown on Figures 5.4 and 5.5. The experimental data along with their corresponding values obtained were also shown in Figure 5.6.

Nu and a_{w0} estimated values were $3.96\times10^{-4}\pm7.33\times10^{-5}$ and 0.97 ± 6.06, with levels of significance of 0.99 and 0.28, respectively. The low level of significance for the initial water activity could suggest that it was not relevant for the model, although it was not removed from it. The correlation between parameters was moderate (-0.67), indicating a compensatory effect that could lead to the low evaporation rates observed indirectly by moisture content values in Figures 5.4 D and H. The low Nu value may be an indication that any sort of malflow distribution might have indeed occurred, which is emphasized when working with low Pe conditions. MARTIN (1978) proposed that the irregular porosity distribution along the cross section area of the reactor may induce areas of by-pass, where local porosity values differ considerably from the average value, and, as function of this by-pass proportion, effective Nu values could be calculated.

In relation to the physical variables presented in Figure 5.4, it became evident that temperature measurements in both phases were different, although in the same phase there was only minor differences in the profile. In the solid phase, where the

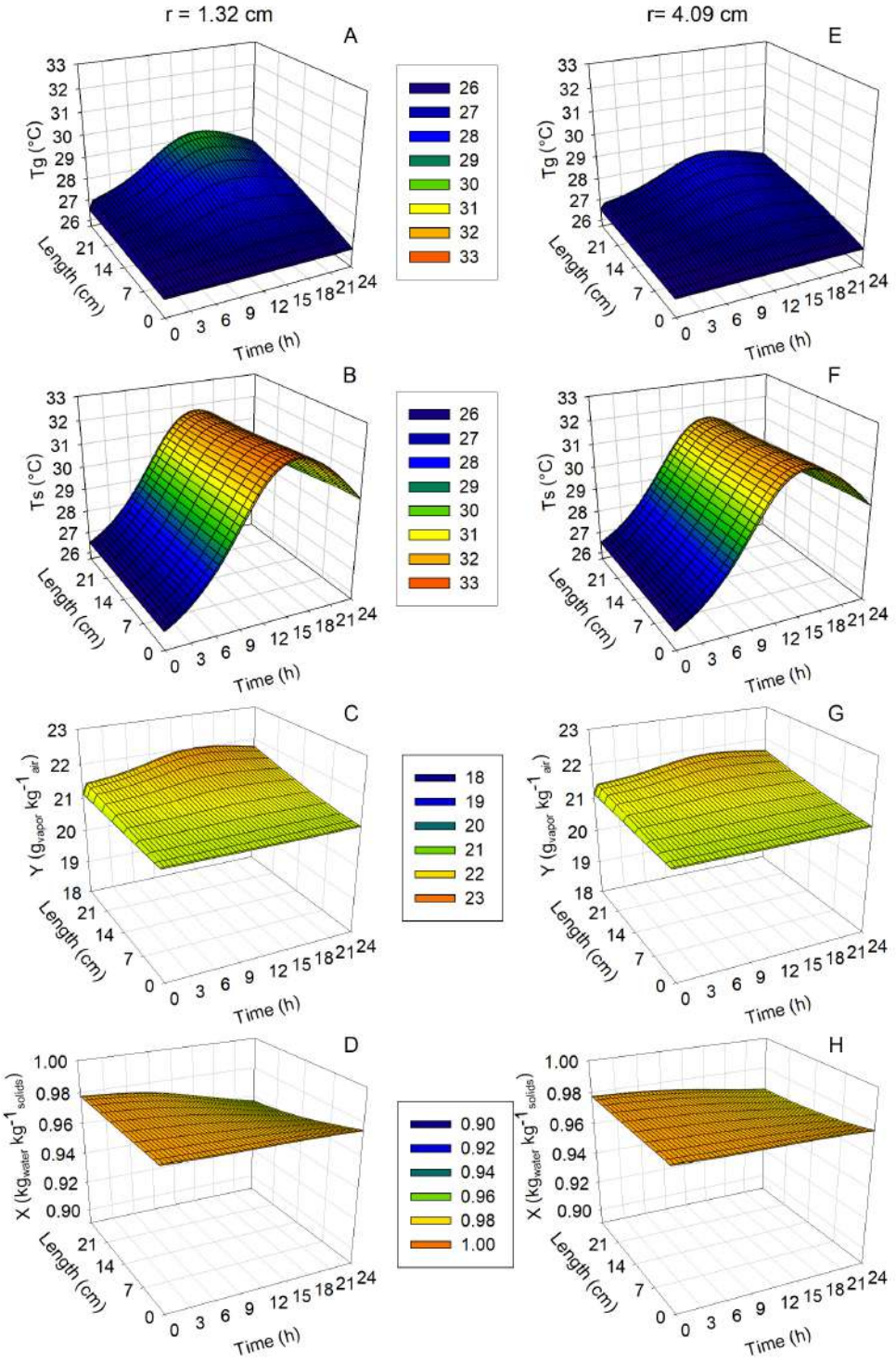

Figure 5.4: Gas (A, B) and solid (C, D) temperatures, gas (E,F) and solid (G, H) moisture content after parameter estimation at different radii.

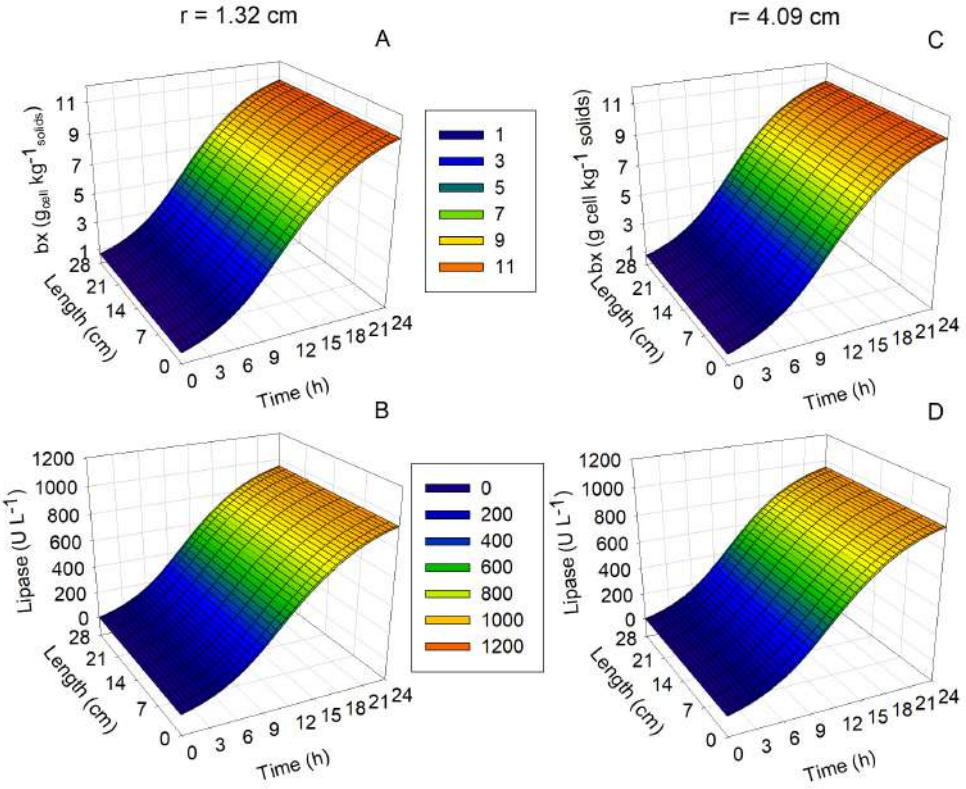

Figure 5.5: Cell (A, C) and Lipase (B, D) calculated values after parameter estimation at different radii.

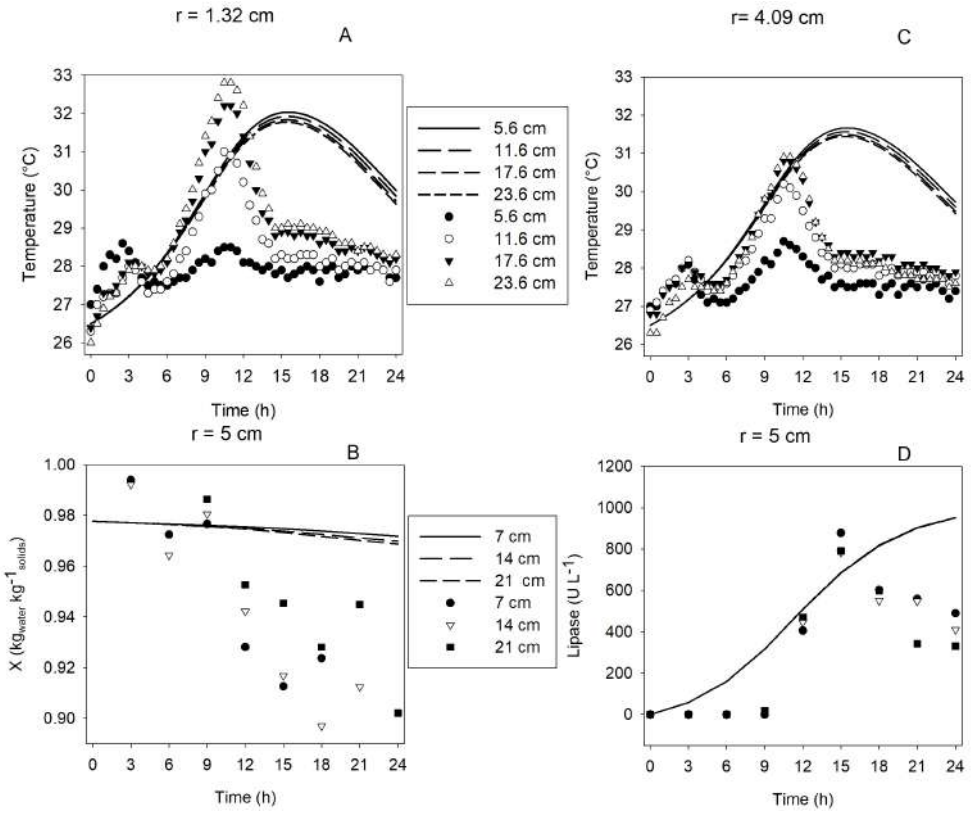

Figure 5.6: Temperature (A,C), solid moisture content (B) and lipase (D) data from experiments (symbols) and the model (lines).

yeast cells are found, the temperature reached nearly 32 °C at 15 h, which represent a 6-hour delay from the experimental peak value (Figure 5.6 A, C). The solid profiles showed no relevant axial profiles, while this was a little more pronounced for the gas phase, as it was expected for the moving phase. The gas phase in the portion of the reactor closer to the center has a slightly higher temperature value than in the other radial position, evidencing a small radial difference. This tendency was also observed for the vapor content values. Although the temperatures had risen considerably more with the new values for the estimated parameters, water evaporation was not intense, both for the experimental and predicted values (Figure 5.6 B), which may be attributed to the low air superficial velocity and the high water activity of the inlet gas stream resulting from the air bubbling in the column prior to entering in the bottom of the bioreactor.

When it concerns the cells and lipase production (Figure 5.5), no apparent differences were found when comparing data from both radii (1.32 and 4.09 cm), in accordance with the absence of differences in the solid temperatures (Figure 5.4 B, F). The exponential phase end is strictly connected to the peak temperatures, where lipase production also start to slow down. The maximum experimental lipase activity (Figure 5.6 D) was 879 U L^{-1}, obtained at 15 h of fermentation, similar to the value predicted by the model. However, the model values kept rising until the end of the process, in contrast with fermentation data, which indicates that the proteases produced by *Y. lipolytica* could be included in the model to account for this difference.

Despite the different fermentation types, data from SmF has been proven to be useful for initial guesses of parameter values to use in the model. Typical values for μ_{max} for *Yarrowia lipolytica* grown with YPD medium with reduced peptone are in the order of 0.3 h^{-1} (SANTOS *et al.*, 2019), higher than the value used herein. This could be critical for the successful parameter estimation given that the cell metabolism is the heat source in the bioreactor. Thus, the delay in peak temperatures are likely to be a consequence of the slow growth. DA SILVEIRA *et al.* (2014) modeled the SSF for the yeast *K. marxianus* and estimated μ to be 0.86 h^{-1}, much higher than the values regularly used for filamentous fungi, showing that high specific growth rates can indeed occur in SSF.

Finally, a major difference can be observed from the temperature profiles after the peak times. Since the experimental data showed that the temperature decay happened quickly, this cannot be predicted with the logistic equation used to describe cell growth. This kinetic model is known to represent in a simple manner the lag and transition from exponential to stationary growth phases MITCHELL *et al.* (2004). Therefore, the exponential kinetic expression could be used instead to represent this stop in heat generation.

Chapter 6

Conclusions and perspectives

This work proposed the use of soybean hulls as inexpensive solid residue for valorization by means of lipase production in a solid-state fermentation process using the non-conventional yeast *Y. lipolytica*. For this, experimental and computational research was conducted towards methodological developments, experimental data acquisition and mathematical modeling.

The study of a new methodology for lipase activity quantification was performed. In the developed enzymatic assay, Triton X-100 quantity above the critical micellar concentration was shown to be appropriate for use, despite the diverse effect commonly reported. This was only possible when a sufficiently large amount of substrate was also used in the kinetic assays.

Partial characterization of the soybean hulls was executed. The chemical composition was similar to that found in the literature. A digital image processing routine implemented in Matlab was used for the size characterization, along with density and porosity measurements, which allowed their later use in the simulation studies.

An investigation of supplementation media was conducted to lead to higher enzyme production by this yeast. Both defined and complex media were tested in either tray or insulated packed-bed bioreactors. In general, complex media supplementation provided higher lipase production. Comparison of collected data from both types of bioreactor indicated that the temperature increase in the insulated PBB may have influenced the protease and lipase production temporal profiles, specially in soybean oil-containing media.

Simulations were performed with thermal and mass balance equations. The model was satisfactory at predicting the maximum temperatures reached in the bioreactor. The values used for the Nusselt number for estimation of heat and mass interfacial coefficients were crucial for the model performance. The value used was much smaller than the values for single sphere, in accordance with other values found for packed beds. Finally, the kinetic description of lipase production as a growth associated product was performed, for which the values were similar to those

experimentally observed.

6.1 Suggestions for future work

- Investigation of lipase kinetic mechanisms in Triton X-100 rich reaction media, including the determination of surface limit concentrations for substrates in mixed Triton X-100/substrate micelles;
- Identification of alkaline and acid proteases produced by the yeast during the process to propose strategies to circumvent lipase activity decay;
- Experimental measurements of porosity, density, heat and mass transfer properties for the soybean hulls at varied moisture and soybean oil content values;
- Experimental measurements of offstream gases (CO_2 and O_2) for indirect cell quantification;
- Experimental investigation of other process conditions leading to higher Péclet numbers (increased air velocity or particle diameter) for a more robust parameter estimation process;
- Inclusion of protease production and lipase decay by action of proteases; inclusion of a thermal activity decay expression for enzyme description;
- Inclusion of the Nu correlation proposed by MARTIN (1978) and evaluate the performance of the model;
- Optimization of lipase production using the studied models and experimental validation;
- Model evaluation for the cases where soybean oil is used in the supplementation media.

References

ACRIVOS, A., TAYLOR, T. D., 1962, "Heat and mass transfer from single spheres in stokes flow", *Physics of Fluids*, v. 5, n. 4, pp. 387–394. ISSN: 10706631. doi: 10.1063/1.1706630.

AIDOO, K. E., HENDRY, R., WOOD, B., 1981, "Estimation of Fungal Growth in a Solid State Fermentation System", *European Journal of Applied Microbiology and Biotechnology*, v. 12, pp. 6–9.

ALOULOU, A., PUCCINELLI, D., DE CARO, A., et al., 2007a, "A comparative study on two fungal lipases from Thermomyces lanuginosus and Yarrowia lipolytica shows the combined effects of detergents and pH on lipase adsorption and activity", *Biochimica et Biophysica Acta (BBA) - Molecular and Cell Biology of Lipids*, v. 1771, n. 12 (dec), pp. 1446–1456. ISSN: 13881981. doi: 10.1016/j.bbalip.2007.10.006.

ALOULOU, A., RODRIGUEZ, J. A., PUCCINELLI, D., et al., 2007b, "Purification and biochemical characterization of the LIP2 lipase from Yarrowia lipolytica", *Biochimica et Biophysica Acta (BBA) - Molecular and Cell Biology of Lipids*, v. 1771, n. 2 (feb), pp. 228–237. ISSN: 13881981. doi: 10.1016/j.bbalip.2006.12.006.

ALOULOU, A., BÉNAROUCHE, A., PUCCINELLI, D., et al., 2013, "Biochemical and structural characterization of non-glycosylated Yarrowia lipolytica LIP2 lipase", *European Journal of Lipid Science and Technology*, v. 115, n. 4, pp. 429–441. ISSN: 14387697. doi: 10.1002/ejlt.201200440.

ANTOLOVIĆ, V., MARINOVIĆ, M., FILIĆ, V., et al., 2014, "A simple optical configuration for cell tracking by dark-field microscopy", *Journal of Microbiological Methods*, v. 104 (sep), pp. 9–11. ISSN: 01677012. doi: 10.1016/j.mimet.2014.06.006.

ARBIGE, M. V., SHETTY, J. K., CHOTANI, G. K., 2019, "Industrial Enzymology: The Next Chapter", *Trends in Biotechnology*, v. 37, n. 12 (dec), pp. 1355–1366. ISSN: 01677799. doi: 10.1016/j.tibtech.2019.09.010.

ARORA, S., RANI, R., GHOSH, S., 2018, "Bioreactors in solid state fermentation technology: Design, applications and engineering aspects", *Journal of Biotechnology*, v. 269 (mar), pp. 16–34. ISSN: 01681656. doi: 10.1016/j.jbiotec.2018.01.010.

AUGUSTYNIAK, W., BRZEZINSKA, A. A., PIJNING, T., et al., 2012, "Biophysical characterization of mutants of Bacillus subtilis lipase evolved for thermostability: Factors contributing to increased activity retention", *Protein Science*, v. 21, n. 4 (apr), pp. 487–497. ISSN: 09618368. doi: 10.1002/pro.2031.

AURIA, R., ORTIZ, I., VILLEGAS, E., et al., 1995, "Influence of Growth and High Mold Concentration on the Pressure-Drop in Solid-State Fermentations", *Process Biochemistry*, v. 30, n. 8, pp. 751–756.

AVIARA, N. A., 2020, "Moisture Sorption Isotherms and Isotherm Model Performance Evaluation for Food and Agricultural Products". In: Kyzas, G., Lazaridis, N. (Eds.), *Sorption in 2020s*, v. 32, IntechOpen, pp. 137–144, mar. doi: 10.5772/intechopen.87996.

AVIARA, N., AJIBOLA, O., ONI, S., 2004, "Sorption Equilibrium and Thermodynamic Characteristics of Soya Bean", *Biosystems Engineering*, v. 87, n. 2 (feb), pp. 179–190. ISSN: 15375110. doi: 10.1016/j.biosystemseng.2003.11.006.

BARNAY-VERDIER, S., BOISRAMÉ, A., BECKERICH, J.-M., 2004, "Identification and characterization of two α-1,6-mannosyltransferases, Anl1p and Och1p, in the yeast Yarrowia lipolytica", *Microbiology*, v. 150, n. 7 (jul), pp. 2185–2195. ISSN: 1350-0872. doi: 10.1099/mic.0.26887-0.

Barth, G. (Ed.), 2013a, *Yarrowia lipolytica*, v. 24, *Microbiology Monographs*. Berlin, Heidelberg, Springer Berlin Heidelberg. ISBN: 978-3-642-38319-9. doi: 10.1007/978-3-642-38320-5.

Barth, G. (Ed.), 2013b, *Yarrowia lipolytica*, v. 25, *Microbiology Monographs*. Berlin, Heidelberg, Springer Berlin Heidelberg. ISBN: 978-3-642-38582-7. doi: 10.1007/978-3-642-38583-4.

BARTH, G., GAILLARDIN, C., 1996, "Yarrowia lipolytica". In: Wolf, K. (Ed.), *Nonconventional Yeasts in Biotechnology*, Springer Berlin Heidelberg, cap. 10, pp. 313–388, Berlin, Heidelberg. doi: 10.1007/978-3-642-79856-6_10.

BEISSON, F., TISS, A., RIVIÈRE, C., et al., 2000, "Methods for lipase detection and assay: a critical review", *European Journal of Lipid Science and Technology*, v. 102, n. 2 (feb), pp. 133–153. ISSN: 1438-7697. doi: 10.1002/(SICI)1438-9312(200002)102:2<133::AID-EJLT133>3.0.CO;2-X.

BERG, O. G., CAJAL, Y., BUTTERFOSS, G. L., et al., 1998, "Interfacial Activation of Triglyceride Lipase from Thermomyces (Humicola) lanuginosa : Kinetic Parameters and a Basis for Control of the Lid †", *Biochemistry*, v. 37, n. 19 (may), pp. 6615–6627. ISSN: 0006-2960. doi: 10.1021/bi972998p.

BIGGS, A. I., 1954, "A spectrophotometric determination of the dissociation constants of p-nitrophenol and papaverine", *Transactions of the Faraday Society*, v. 50, pp. 800. ISSN: 0014-7672. doi: 10.1039/tf9545000800.

BORDES, F., BARBE, S., ESCALIER, P., et al., 2010, "Exploring the Conformational States and Rearrangements of Yarrowia lipolytica Lipase", *Biophysical Journal*, v. 99, n. 7 (oct), pp. 2225–2234. ISSN: 00063495. doi: 10.1016/j.bpj.2010.07.040.

BOTELHO, A., PENHA, A., FRAGA, J., et al., 2020, "Yarrowia lipolytica Adhesion and Immobilization onto Residual Plastics", *Polymers*, v. 12, n. 3 (mar), pp. 649. ISSN: 2073-4360. doi: 10.3390/polym12030649.

BOTELLA, C., HERNANDEZ, J. E., WEBB, C., 2019, "Dry weight model, capacitance and metabolic data as indicators of fungal biomass growth in solid state fermentation", *Food and Bioproducts Processing*, v. 114 (mar), pp. 144–153. ISSN: 09603085. doi: 10.1016/j.fbp.2018.12.002.

BRADFORD, M. M., 1976, "A rapid and sensitive method for the quantitation of microgram quantities of protein utilizing the principle of protein-dye binding", *Analytical Biochemistry*, v. 72, n. 1-2, pp. 248–254. ISSN: 10960309. doi: 10.1016/0003-2697(76)90527-3.

BRAGA, A., MESQUITA, D., AMARAL, A., et al., 2015, "Aroma production by Yarrowia lipolytica in airlift and stirred tank bioreactors: Differences in yeast metabolism and morphology", *Biochemical Engineering Journal*, v. 93 (jan), pp. 55–62. ISSN: 1369703X. doi: 10.1016/j.bej.2014.09.006.

BRAGA, A., MESQUITA, D., AMARAL, A., et al., 2016, "Quantitative image analysis as a tool for Yarrowia lipolytica dimorphic growth evaluation in different culture media", *Journal of Biotechnology*, v. 217 (jan), pp. 22–30. ISSN: 01681656. doi: 10.1016/j.jbiotec.2015.10.023.

BRÍGIDA, A. I. S., 2010, *Imobilização De Lipases Utilizando Fibra Da Casca De Coco Verde Como Suporte Para Aplicações Industriais*. D.sc. thesis, Universidade Federal do Rio de Janeiro.

BRIJWANI, K., VADLANI, P. V., 2011, "Cellulolytic Enzymes Production via Solid-State Fermentation: Effect of Pretreatment Methods on Physicochemical Characteristics of Substrate", *Enzyme Research*, v. 2011, n. 1 (jun), pp. 1–10. ISSN: 2090-0414. doi: 10.4061/2011/860134.

BRIJWANI, K., OBEROI, H. S., VADLANI, P. V., 2010, "Production of a cellulolytic enzyme system in mixed-culture solid-state fermentation of soybean hulls supplemented with wheat bran", *Process Biochemistry*, v. 45, n. 1 (jan), pp. 120–128. ISSN: 13595113. doi: 10.1016/j.procbio.2009.08.015.

BÜCK, A., CASCIATORI, F., THOMÉO, J., et al., 2015, "Model-based Control of Enzyme Yield in Solid-state Fermentation", *Procedia Engineering*, v. 102, pp. 362–371. ISSN: 18777058. doi: 10.1016/j.proeng.2015.01.163.

BURGEMEISTER, S., NATTKEMPER, T., NOLL, T., et al., 2010, "CellViCAM—Cell viability classification for animal cell cultures using dark field micrographs", *Journal of Biotechnology*, v. 149, n. 4 (sep), pp. 310–316. ISSN: 01681656. doi: 10.1016/j.jbiotec.2010.07.020.

CALADO, V., MONTGOMERY, D. C., 2013, *Planejamento de Experimentos usando Statistica*. Rio de janeiro, E-papers Serviços Editoriais. ISBN: 85-87922-83-1.

CAO, H., JIANG, Y., ZHANG, H., et al., 2017, "Enhancement of methanol resistance of Yarrowia lipolytica lipase 2 using β-cyclodextrin as an additive: Insights from experiments and molecular dynamics simulation", *Enzyme and Microbial Technology*, v. 96 (jan), pp. 157–162. ISSN: 01410229. doi: 10.1016/j.enzmictec.2016.10.007.

CARDOSO, C., OLIVEIRA, T., SANTANA JUNIOR, J., et al., 2013, "Physical characterization of sweet sorghum bagasse, tobacco residue, soy hull and fiber sorghum bagasse particles: Density, particle size and shape distributions", *Powder Technology*, v. 245 (sep), pp. 105–114. ISSN: 00325910. doi: 10.1016/j.powtec.2013.04.029.

CARMAN, G. M., DEEMS, R. A., DENNIS, E. A., 1995, "Lipid signaling enzymes and surface dilution kinetics", *Journal of Biological Chemistry*, v. 270, n. 32, pp. 18711–18714. ISSN: 00219258. doi: 10.1074/jbc.270.32.18711.

CASCIATORI, F. P., LAURENTINO, C. L., TABOGA, S. R., et al., 2014, "Structural properties of beds packed with agro-industrial solid by-products applicable for solid-state fermentation: Experimental data and effects on process performance", *Chemical Engineering Journal*, v. 255 (nov), pp. 214–224. ISSN: 13858947. doi: 10.1016/j.cej.2014.06.040.

CASCIATORI, F. P., LAURENTINO, C. L., ZANELATO, A. I., et al., 2015, "Hygroscopic properties of solid agro-industrial by-products used in solid-state fermentation", *Industrial Crops and Products*, v. 64 (feb), pp. 114–123. ISSN: 09266690. doi: 10.1016/j.indcrop.2014.11.034.

CASCIATORI, F. P., BÜCK, A., THOMÉO, J. C., et al., 2016, "Two-phase and two-dimensional model describing heat and water transfer during solid-state fermentation within a packed-bed bioreactor", *Chemical Engineering Journal*, v. 287 (mar), pp. 103–116. ISSN: 13858947. doi: 10.1016/j.cej.2015.10.108.

CASTILHO, L. R., POLATO, C. M., BARUQUE, E. A., et al., 2000, "Economic analysis of lipase production by Penicillium restrictum in solid-state and submerged fermentations", *Biochemical Engineering Journal*, v. 4, n. 3, pp. 239–247. ISSN: 1369703X. doi: 10.1016/S1369-703X(99)00052-2.

CASTRO, A. M., CASTILHO, L. R., FREIRE, D. M., 2015, "Performance of a fixed-bed solid-state fermentation bioreactor with forced aeration for the production of hydrolases by Aspergillus awamori", *Biochemical Engineering Journal*, v. 93 (jan), pp. 303–308. ISSN: 1369703X. doi: 10.1016/j.bej.2014.10.016.

CHARNEY, J., TOMARELLI, R. M., 1947, "A colorimetric method for the determination of the proteolytic activity of duodenal juice", *J. Biol. Chem.*, v. 171, pp. 501–505.

COELHO, M. A. Z., BELO, I., PINHEIRO, R., et al., 2004, "Effect of hyperbaric stress on yeast morphology: study by automated image analysis", *Applied Microbiology and Biotechnology*, v. 66, n. 3 (dec), pp. 318–324. ISSN: 0175-7598. doi: 10.1007/s00253-004-1648-9.

COTÂRLEȚ, M., STĂNCIUC, N., BAHRIM, G. E., 2020, "Yarrowia lipolytica and Lactobacillus paracasei Solid State Fermentation as a Valuable Biotechnological Tool for the Pork Lard and Okara's Biotransformation", *Microorganisms*, v. 8, n. 8 (jul), pp. 1098. ISSN: 2076-2607. doi: 10.3390/microorganisms8081098.

DA SILVA, J. R., DE SOUZA, C. E. C., VALONI, E., et al., 2019, "Biocatalytic esterification of fatty acids using a low-cost fermented solid from solid-state fermentation with Yarrowia lipolytica", *3 Biotech*, v. 9, n. 2 (feb), pp. 38. ISSN: 2190-572X. doi: 10.1007/s13205-018-1550-2.

DA SILVEIRA, C. L., MAZUTTI, M. A., SALAU, N. P. G., 2014, "Modeling the microbial growth and temperature profile in a fixed-bed bioreactor", *Bioprocess and Biosystems Engineering*, v. 37, n. 10 (oct), pp. 1945–1954. ISSN: 1615-7591. doi: 10.1007/s00449-014-1170-0.

DAIHA, K. D. G., ANGELI, R., DE OLIVEIRA, S. D., et al., 2015, "Are Lipases Still Important Biocatalysts? A Study of Scientific Publications and Patents for Technological Forecasting", *PLOS ONE*, v. 10, n. 6 (jun), pp. e0131624. ISSN: 1932-6203. doi: 10.1371/journal.pone.0131624.

DE AZEREDO, L. A. I., GOMES, P. M., SANT'ANNA, G. L., et al., 2007, "Production and regulation of lipase activity from Penicillium restrictum in submerged and solid-state fermentations", *Current Microbiology*, v. 54, n. 5, pp. 361–365. ISSN: 03438651. doi: 10.1007/s00284-006-0425-7.

DE CASTRO, A. M., CASTILHO, L. D. R., FREIRE, D. M. G., 2016, "Characterization of babassu, canola, castor seed and sunflower residual cakes for use as raw materials for fermentation processes", *Industrial Crops and Products*, v. 83 (may), pp. 140–148. ISSN: 09266690. doi: 10.1016/j.indcrop.2015.12.050.

DE POURCQ, K., VERVECKEN, W., DEWERTE, I., et al., 2012, "Engineering the yeast Yarrowia lipolytica for the production of therapeutic proteins homogeneously glycosylated with Man8GlcNAc2 and Man5GlcNAc2", *Microbial Cell Factories*, v. 11, n. 1, pp. 53. ISSN: 1475-2859. doi: 10.1186/1475-2859-11-53.

DE PRETTO, C., GIORDANO, R. D. L. C., TARDIOLI, P. W., et al., 2018, "Possibilities for Producing Energy, Fuels, and Chemicals from Soybean: A Biorefinery Concept", *Waste and Biomass Valorization*, v. 9, n. 10 (oct), pp. 1703–1730. ISSN: 1877-2641. doi: 10.1007/s12649-017-9956-3.

DE SOUZA, C. E. C., RIBEIRO, B. D., COELHO, M. A. Z., 2019, "Characterization and Application of Yarrowia lipolytica Lipase Obtained by Solid-State Fermentation in the Synthesis of Different Esters Used in the Food Industry", *Applied Biochemistry and Biotechnology*, v. 189, n. 3 (nov), pp. 933–959. ISSN: 0273-2289. doi: 10.1007/s12010-019-03047-5.

DEEMS, R. A., 2000, "Interfacial Enzyme Kinetics at the Phospholipid/ Water Interface: Practical Considerations", *Analytical Biochemistry*, v. 287, n. 1 (dec), pp. 1–16. ISSN: 00032697. doi: 10.1006/abio.2000.4766.

DESFOUGÈRES, T., HADDOUCHE, R., FUDALEJ, F., et al., 2010, "SOA genes encode proteins controlling lipase expression in response to triacylglycerol utilization in the yeast Yarrowia lipolytica", *FEMS Yeast Research*, v. 10, n. 1 (feb), pp. 93–103. ISSN: 15671356. doi: 10.1111/j.1567-1364.2009.00590.x.

DEVECI, T., UNYAYAR, A., MAZMANCI, M. A., 2004, "Production of Remazol Brilliant Blue R decolourising oxygenase from the culture filtrate of Funalia trogii ATCC 200800", *Journal of Molecular Catalysis B: Enzymatic*, v. 30, n. 1 (jul), pp. 25–32. ISSN: 13811177. doi: 10.1016/j.molcatb.2004.03.002.

DOMÍNGUEZ, A., COSTAS, M., LONGO, M. A., et al., 2003, "A novel application of solid state culture: Production of lipases by Yarrowia lipolytica", *Biotechnology Letters*, v. 25, n. 15, pp. 1225–1229. ISSN: 01415492. doi: 10.1023/A:1025068205961.

DONGOWSKI, G., EHWALD, R., 1999, "Binding of water, oil, and bile acids to dietary fibers of the cellan type", *Biotechnology Progress*, v. 15, n. 2, pp. 250–258. ISSN: 87567938. doi: 10.1021/bp990014c.

DUAN, Y., WANG, L., CHEN, H., 2012, "Digital image analysis and fractal-based kinetic modelling for fungal biomass determination in solid-state fermentation", *Biochemical Engineering Journal*, v. 67 (aug), pp. 60–67. ISSN: 1369703X. doi: 10.1016/j.bej.2012.04.020.

DURSUN, D., DALGIÇ, A. C., 2016, "Optimization of astaxanthin pigment bioprocessing by four different yeast species using wheat wastes", *Biocatalysis and Agricultural Biotechnology*, v. 7 (jul), pp. 1–6. ISSN: 18788181. doi: 10.1016/j.bcab.2016.04.006.

FANAEI, M. A., VAZIRI, B. M., 2009, "Modeling of temperature gradients in packed-bed solid-state bioreactors", *Chemical Engineering and Processing: Process Intensification*, v. 48, n. 1 (jan), pp. 446–451. ISSN: 02552701. doi: 10.1016/j.cep.2008.06.001.

FARIAS, M. A., VALONI, E. A., CASTRO, A. M., et al., 2014, "Lipase Production by Yarrowia lipolytica in Solid State Fermentation Using Different Agro

Industrial Residues", *The Italian Association of Chemical Engineering*, v. 38, pp. 301–306. ISSN: 19749791. doi: 10.3303/CET1438051.

FATIMA, S., FARYAD, A., ATAA, A., et al., 2020, "Microbial lipase production: A deep insight into the recent advances of lipase production and purification techniques", *Biotechnology and Applied Biochemistry*, (sep), pp. bab.2019. ISSN: 0885-4513. doi: 10.1002/bab.2019.

FERNÁNDEZ-FERNÁNDEZ, M., PÉREZ-CORREA, J. R., 2007, "Realistic model of a solid substrate fermentation packed-bed pilot bioreactor", *Process Biochemistry*, v. 42, n. 2 (feb), pp. 224–234. ISSN: 13595113. doi: 10.1016/j.procbio.2006.08.003.

FERRAREZI, A. L., HIDEYUKI KOBE OHE, T., BORGES, J. P., et al., 2014, "Production and characterization of lipases and immobilization of whole cell of the thermophilic Thermomucor indicae seudaticae N31 for transesterification reaction", *Journal of Molecular Catalysis B: Enzymatic*, v. 107, pp. 106–113. ISSN: 18733158. doi: 10.1016/j.molcatb.2014.05.012.

FICKERS, P., BENETTI, P., WACHE, Y., et al., 2005, "Hydrophobic substrate utilisation by the yeast , and its potential applications", *FEMS Yeast Research*, v. 5, n. 6-7 (apr), pp. 527–543. ISSN: 15671356. doi: 10.1016/j.femsyr.2004.09.004.

FICKERS, P., FUDALEJ, F., DALL, M. L., et al., 2005a, "Identification and characterisation of LIP7 and LIP8 genes encoding two extracellular triacylglycerol lipases in the yeast Yarrowia lipolytica", *Fungal Genetics and Biology*, v. 42, n. 3 (mar), pp. 264–274. ISSN: 10871845. doi: 10.1016/j.fgb.2004.12.003.

FICKERS, P., NICAUD, J. M., DESTAIN, J., et al., 2005b, "Involvement of Hexokinase Hxk1 in Glucose Catabolite Repression of LIP2 Encoding Extracellular Lipase in the Yeast Yarrowia lipolytica", *Current Microbiology*, v. 50 (mar), pp. 133–137. ISSN: 0343-8651. doi: 10.1007/s00284-004-4401-9.

FICKERS, P., MARTY, A., NICAUD, J. M., 2011, "The lipases from Yarrowia lipolytica: Genetics, production, regulation, biochemical characterization and biotechnological applications", *Biotechnology Advances*, v. 29, n. 6 (nov), pp. 632–644. ISSN: 07349750. doi: 10.1016/j.biotechadv.2011.04.005.

FIGUEROA-MONTERO, A., ESPARZA-ISUNZA, T., SAUCEDO-CASTAÑEDA, G., et al., 2011, "Improvement of heat removal in

solid-state fermentation tray bioreactors by forced air convection", *Journal of Chemical Technology & Biotechnology*, v. 86, n. 10 (oct), pp. 1321–1331. ISSN: 02682575. doi: 10.1002/jctb.2637.

FINLAYSON, B. A., OLSON, J. W., 1987, "HEAT TRANSFER TO SPHERES AT LOW TO INTERMEDIATE REYNOLDS NUMBERS", *Chemical Engineering Communications*, v. 58, n. 1-6 (aug), pp. 431–447. ISSN: 0098-6445. doi: 10.1080/00986448708911980.

FLEURI, L. F., NOVELLI, P. K., DELGADO, C. H. O., et al., 2014, "Biochemical characterisation and application of lipases produced by Aspergillus sp. on solid-state fermentation using three substrates", *International Journal of Food Science and Technology*, v. 49, n. 12, pp. 2585–2591. ISSN: 13652621. doi: 10.1111/ijfs.12589.

FOOD AND AGRICULTURE ORGANISATION (FAO), 2020. "FAOSTAT: Statistical database." Available at: <`https://www.fao.org/faostat`>.

FRAGA, J., PENHA, A., DA S. PEREIRA, A., et al., 2018, "Use of Yarrowia lipolytica Lipase Immobilized in Cell Debris for the Production of Lipolyzed Milk Fat (LMF)", *International Journal of Molecular Sciences*, v. 19, n. 11 (oct), pp. 3413. ISSN: 1422-0067. doi: 10.3390/ijms19113413.

FRAGA, J. L., DA PENHA, A. C. B., AKIL, E., et al., 2020, "Catalytic and physical features of a naturally immobilized Yarrowia lipolytica lipase in cell debris (LipImDebri) displaying high thermostability", *3 Biotech*, v. 10, n. 10 (oct), pp. 454. ISSN: 2190-572X. doi: 10.1007/s13205-020-02444-6.

GLOVER, D. J., MCEWEN, R. K., THOMAS, C. R., et al., 1997, "pH-regulated expression of the acid and alkaline extracellular proteases of Yarrowia lipolytica", *Microbiology*, v. 143, n. 9 (sep), pp. 3045–3054. ISSN: 1350-0872. doi: 10.1099/00221287-143-9-3045.

GROENEWALD, M., BOEKHOUT, T., NEUVÉGLISE, C., et al., 2014, "Yarrowia lipolytica : Safety assessment of an oleaginous yeast with a great industrial potential", *Critical Reviews in Microbiology*, v. 40, n. 3 (aug), pp. 187–206. ISSN: 1040-841X. doi: 10.3109/1040841X.2013.770386.

GUERRAND, D., 2017, "Lipases industrial applications: focus on food and agroindustries", *OCL*, v. 24, n. 4 (jul), pp. D403. ISSN: 2272-6977. doi: 10.1051/ocl/2017031.

GUO, Q., CHEN, X., LIU, H., 2012, "Experimental research on shape and size distribution of biomass particle", *Fuel*, v. 94 (apr), pp. 551–555. ISSN: 00162361. doi: 10.1016/j.fuel.2011.11.041.

GUPTA, R. D., 2016, "Recent advances in enzyme promiscuity", *Sustainable Chemical Processes*, v. 4, n. 1, pp. 1–7. ISSN: 2043-7129. doi: 10.1186/s40508-016-0046-9.

GUTHRIE, J. P., 1972, "Aggregation of p-nitrophenyl alkanoates in aqueous solution: A caution concerning their use in enzyme model studies", *Journal of the Chemical Society, Chemical Communications*, v. 0, n. 15, pp. 897–899. ISSN: 00224936. doi: 10.1039/C39720000897.

HAGLER, A. N., MENDONÇA-HAGLER, L. C., 1981, "Yeasts from Marine and Estuarine Waters with Different Levels of Pollution in the State of Rio de Janeiro, Brazil", *Applied and environmental microbiology*, v. 41, n. 1, pp. 173–178. ISSN: 0099-2240.

HAMIDI-ESFAHANI, Z., HEJAZI, P., SHOJAOSADATI, S. A., et al., 2007, "A two-phase kinetic model for fungal growth in solid-state cultivation", *Biochemical Engineering Journal*, v. 36, n. 2 (sep), pp. 100–107. ISSN: 1369703X. doi: 10.1016/j.bej.2007.02.005.

HASAN, F., SHAH, A. A., HAMEED, A., 2009, "Methods for detection and characterization of lipases: A comprehensive review", *Biotechnology Advances*, v. 27, n. 6, pp. 782–798. ISSN: 07349750. doi: 10.1016/j.biotechadv.2009.06.001.

HERNÁNDEZ-GARCÍA, S., GARCÍA-GARCÍA, M. I., GARCÍA-CARMONA, F., 2017, "An improved method to measure lipase activity in aqueous media", *Analytical Biochemistry*, v. 530 (aug), pp. 104–106. ISSN: 00032697. doi: 10.1016/j.ab.2017.05.012.

HU, Z., HAGHJOO, K., JORDAN, F., 1996, "Further Evidence for the Structure of the Subtilisin Propeptide and for Its Interactions with Mature Subtilisin", *Journal of Biological Chemistry*, v. 271, n. 7 (feb), pp. 3375–3384. ISSN: 0021-9258. doi: 10.1074/jbc.271.7.3375.

IBGE, 2020. "Tabela 1612: Área plantada, área colhida, quantidade produzida, rendimento médio e valor da produção das lavouras temporárias". Available at: <`https://sidra.ibge.gov.br/tabela/1612`>.

IKASARI, L., MITCHELL, D. A., STUART, D. M., 1999, "Response ofRhizopus oligosporus to temporal temperature profiles in a model solid-state fermentation system", *Biotechnology and Bioengineering*, v. 64, n. 6 (sep), pp. 722–728. ISSN: 0006-3592. doi: 10.1002/(SICI)1097-0290(19990920)64:6<722::AID-BIT12>3.0.CO;2-7.

IMANDI, S. B., GARAPATI, H. R., 2007, "Lipase Production by Yarrowia lipolytica NCIM 3589 in Solid State Fermentation Using Mixed Substrate", *Research Journal of Microbiology*, v. 2, n. 5 (may), pp. 469–474. ISSN: 18164935. doi: 10.3923/jm.2007.469.474.

IMANDI, S. B., BANDARU, V. V. R., SOMALANKA, S. R., et al., 2008, "Application of statistical experimental designs for the optimization of medium constituents for the production of citric acid from pineapple waste", *Bioresource Technology*, v. 99, n. 10, pp. 4445–4450. ISSN: 09608524. doi: 10.1016/j.biortech.2007.08.071.

IMANDI, S. B., KARANAM, S. K., GARAPATI, H. R., 2010a, "Optimization of Process Parameters for the Productionof Lipase in Solid State Fermentation by Yarrowia Lipolytica from Niger Seed Oil Cake (Guizotia Abyssinica)", *Journal of Microbial & Biochemical Technology*, v. 02, n. 01, pp. 028–033. ISSN: 19485948. doi: 10.4172/1948-5948.1000019.

IMANDI, S. B., KARANAM, S. K., GARAPATI, H. R., 2010b, "Optimization of Process Parameters for the Productionof Lipase in Solid State Fermentation by Yarrowia Lipolytica from Niger Seed Oil Cake (Guizotia Abyssinica)", *Journal of Microbial & Biochemical Technology*, v. 02, n. 01, pp. 028–033. ISSN: 19485948. doi: 10.4172/1948-5948.1000019.

IMANDI, S. B., KARANAM, S. K., GARAPATI, H. R., 2010c, "Optimization of media constituents for the production of lipase in solid state fermentation by Yarrowia lipolytica from palm Kernal cake (Elaeis guineensis)", *Advances in Bioscience and Biotechnology*, v. 01, n. 02, pp. 115–121. ISSN: 2156-8456. doi: 10.4236/abb.2010.12016.

IMANDI, S. B., KARANAM, S. K., GARAPATI, H. R., 2013a, "Use of Plackett-Burman design for rapid screening of nitrogen and carbon sources for the production of lipase in solid state fermentation by Yarrowia lipolytica from mustard oil cake (Brassica napus)", *Advances in Natural Sciences: Nanoscience and Nanotechnology*, v. 44, n. 3, pp. 915–921. ISSN: 1678-4405.

IMANDI, S. B., KARANAM, S. K., GARAPATI, H. R., 2013b, "Use of Plackett-Burman design for rapid screening of nitrogen and carbon sources for the production of lipase in solid state fermentation by Yarrowia lipolytica from mustard oil cake (Brassica napus)", *Brazilian Journal of Microbiology*, v. 44, n. 3 (jan), pp. 915–923. ISSN: 2043-6262.

JIANG, Y., LI, L., ZHANG, H., et al., 2014, "Lid Closure Mechanism of Yarrowia lipolytica Lipase in Methanol Investigated by Molecular Dynamics Simulation", *Journal of Chemical Information and Modeling*, v. 54, n. 7 (jul), pp. 2033–2041. ISSN: 1549-9596. doi: 10.1021/ci500163y.

JOLIVET, P., BORDES, F., FUDALEJ, F., et al., 2007, "Analysis of Yarrowia lipolytica extracellular lipase Lip2p glycosylation", *FEMS Yeast Research*, v. 7, n. 8 (dec), pp. 1317–1327. ISSN: 15671356. doi: 10.1111/j.1567-1364.2007.00293.x.

JULIA, B. M., BELÉN, A. M., GEORGINA, B., et al., 2016, "Potential use of soybean hulls and waste paper as supports in SSF for cellulase production by Aspergillus niger", *Biocatalysis and Agricultural Biotechnology*, v. 6 (apr), pp. 1–8. ISSN: 18788181. doi: 10.1016/j.bcab.2016.02.003.

KAMOUN, J., SCHUÉ, M., MESSAOUD, W., et al., 2015, "Biochemical characterization of Yarrowia lipolytica LIP8, a secreted lipase with a cleavable C-terminal region", *Biochimica et Biophysica Acta (BBA) - Molecular and Cell Biology of Lipids*, v. 1851, n. 2 (feb), pp. 129–140. ISSN: 13881981. doi: 10.1016/j.bbalip.2014.10.012.

KAPOOR, M., GUPTA, M. N., 2012, "Lipase promiscuity and its biochemical applications", *Process Biochemistry*, v. 47, n. 4, pp. 555–569. ISSN: 13595113. doi: 10.1016/j.procbio.2012.01.011.

KARANAM, S. K., MEDICHERLA, N. R., 2010, "Application of Doehlert Experimental Design for the Optimization of Medium Constituents for the Production of L-asparaginase from Palm Kernal Cake (Elaeis guineensis)", *Journal of Microbial & Biochemical Technology*, v. 02, n. 01. ISSN: 19485948. doi: 10.4172/1948-5948.1000016.

KARASU-YALCIN, S., TIJEN BOZDEMIR, M., YESIM OZBAS, Z., 2010, "Effects of different fermentation conditions on growth and citric acid production kinetics of two yarrowia lipolytica strains", *Chemical and Biochemical Engineering Quarterly*, v. 24, n. 3, pp. 347–360. ISSN: 03529568.

KAWASSE, F. M., AMARAL, P. F., ROCHA-LEÃO, M. H. M., et al., 2003, "Morphological analysis of Yarrowia lipolytica under stress conditions through image processing", *Bioprocess Biosyst Eng*, v. 25, pp. 371–375. doi: 10.1007/s00449-003-0319-z.

KEMPKA, A. P., LIPKE, N. L., DA LUZ FONTOURA PINHEIRO, T., et al., 2008, "Response surface method to optimize the production and characterization of lipase from Penicillium verrucosum in solid-state fermentation", *Bioprocess and Biosystems Engineering*, v. 31, n. 2 (feb), pp. 119–125. ISSN: 1615-7591. doi: 10.1007/s00449-007-0154-8.

KHAN, F. I., LAN, D., DURRANI, R., et al., 2017, "The Lid Domain in Lipases: Structural and Functional Determinant of Enzymatic Properties", *Frontiers in Bioengineering and Biotechnology*, v. 5, n. MAR (mar), pp. 1–13. ISSN: 2296-4185. doi: 10.3389/fbioe.2017.00016.

KORDEL, M., HOFMANN, B., SCHOMBURG, D., et al., 1991, "Extracellular Lipase of Pseudomonas sp. Strain ATCC-21808 - Purification, Characterization, Crystallization, and Preliminary-X-Ray Diffraction Data", *Journal of Bacteriology*, v. 173, n. 15, pp. 4836–4841. ISSN: 0021-9193. doi: DS.

LAMBERT, M., BLANCHIN-ROLAND, S., LE LOUEDEC, F., et al., 1997, "Genetic analysis of regulatory mutants affecting synthesis of extracellular proteinases in the yeast Yarrowia lipolytica: identification of a RIM101/pacC homolog", *Molecular and Cellular Biology*, v. 17, n. 7, pp. 3966–3976. ISSN: 0270-7306. doi: 10.1128/MCB.17.7.3966.

LARROUDE, M., ROSSIGNOL, T., NICAUD, J.-M., et al., 2018, "Synthetic biology tools for engineering Yarrowia lipolytica", *Biotechnology Advances*, v. 36, n. 8 (dec), pp. 2150–2164. ISSN: 07349750. doi: 10.1016/j.biotechadv.2018.10.004.

LAWRENCE, J., KORBER, D., CALDWELL, D., 1989, "Computer-enhanced darkfield microscopy for the quantitative analysis of bacterial growth and behavior on surfaces", *Journal of Microbiological Methods*, v. 10, n. 2 (sep), pp. 123–138. ISSN: 01677012. doi: 10.1016/0167-7012(89)90009-2.

LEDESMA-AMARO, R., NICAUD, J.-M., 2016, "Metabolic Engineering for Expanding the Substrate Range of Yarrowia lipolytica", *Trends in Biotechnology*, v. 34, n. 10 (oct), pp. 798–809. ISSN: 01677799. doi: 10.1016/j.tibtech.2016.04.010.

LI, C.-H., FINLAYSON, B., 1977, "Heat transfer in packed beds—a reevaluation", *Chemical Engineering Science*, v. 32, n. 9, pp. 1055–1066. ISSN: 00092509. doi: 10.1016/0009-2509(77)80143-7.

LI, C., YANG, X., GAO, S., et al., 2017, "High efficiency succinic acid production from glycerol via in situ fibrous bed bioreactor with an engineered Yarrowia lipolytica", *Bioresource Technology*, v. 225, pp. 9–16. ISSN: 18732976. doi: 10.1016/j.biortech.2016.11.016.

LIU, X., YU, X., ZHANG, T., et al., 2018, "Novel two-stage solid-state fermentation for erythritol production on okara–buckwheat husk medium", *Bioresource Technology*, v. 266, n. May (oct), pp. 439–446. ISSN: 09608524. doi: 10.1016/j.biortech.2018.07.009.

LOMAN, A. A., JU, L.-K., 2016, "Soybean carbohydrate as fermentation feedstock for production of biofuels and value-added chemicals", *Process Biochemistry*, v. 51, n. 8 (aug), pp. 1046–1057. ISSN: 13595113. doi: 10.1016/j.procbio.2016.04.011.

LOPES, V. R. O., 2015, *Variação Morfológica de Yarrowia lipolytica em Fermentação no Estado Sólido*. D.sc., Universidade Federal do Rio de Janeiro.

LOPES, V. R. O., FARIAS, M. A., BELO, I. M. P., et al., 2016, "NITROGEN SOURCES ON TPOMW VALORIZATION THROUGH SOLID STATE FERMENTATION PERFORMED BY Yarrowia lipolytica", *Brazilian Journal of Chemical Engineering*, v. 33, n. 2 (jun), pp. 261–270. ISSN: 0104-6632. doi: 10.1590/0104-6632.20160332s20150146.

LÓPEZ, D. N., GALANTE, M., RUGGIERI, G., et al., 2018, "Peptidase from Aspergillus niger NRRL 3: Optimization of its production by solid-state fermentation, purification and characterization", *LWT*, v. 98, n. September (dec), pp. 485–491. ISSN: 00236438. doi: 10.1016/j.lwt.2018.09.013.

LÓPEZ-GÓMEZ, J. P., PÉREZ-RIVERO, C., WEBB, C., 2019, "Investigating a non-destructive alternative for a preliminary evaluation of fungal growth in solid state fermentations", *Journal of Microbiological Methods*, v. 160, n. March (may), pp. 60–67. ISSN: 01677012. doi: 10.1016/j.mimet.2019.03.021.

LUZ, G. R., SOUSA, L. H., JORGE, L. M., et al., 2006, "Estudo das isotermas de equilíbrio do farelo de soja", *Ciência e Tecnologia de Alimentos*, v. 26, n. 2 (jun), pp. 408–413. ISSN: 0101-2061. doi: 10.1590/S0101-20612006000200025.

MANSOLDO, F. R. P., FIRPO, R., CARDOSO, V. D. S., et al., 2020, "New method for rapid identification and quantification of fungal biomass using ergosterol autofluorescence", *Talanta*, v. 219, n. May (nov), pp. 121238. ISSN: 00399140. doi: 10.1016/j.talanta.2020.121238.

MARQUES, B. C., BARGA, M. C., BALMANT, W., et al., 2006, "A model of the effect of the microbial biomass on the isotherm of the fermenting solids in solid-state fermentation", *Food Technology and Biotechnology*, v. 44, n. 4, pp. 457–463. ISSN: 13309862.

MARTIN, H., 1978, "Low peclet number particle-to-fluid heat and mass transfer in packed beds", *Chemical Engineering Science*, v. 33, n. 7, pp. 913–919. ISSN: 00092509. doi: 10.1016/0009-2509(78)85181-1.

MASTIHUBA, V. V., KREMNICKÝ, L. L., MASTIHUBOVÁ, M., et al., 2002, "A spectrophotometric assay for feruloyl esterases", *Analytical Biochemistry*, v. 309, n. 1 (oct), pp. 96–101. ISSN: 00032697. doi: 10.1016/S0003-2697(02)00241-5.

MATIN, H. R. H., SHARIATMADARI, F., TORSHIZI, M. A. K., 2013, "Various Physico-chemical Properties of Dietary Fiber Sources of Poultry Diets", *International Journal of Agriculture and Crop Sciences.*, v. 6, n. 18, pp. 1239–1245.

MATOBA, S., MORANO, K. A., KLIONSKY, D. J., et al., 1997, "Dipeptidyl aminopeptidase processing and biosynthesis of alkaline extracellular protease from Yarrowia lipolytica", *Microbiology*, v. 143, n. 10 (oct), pp. 3263–3272. ISSN: 1350-0872. doi: 10.1099/00221287-143-10-3263.

MCEWEN, R. K., YOUNG, T. W., 1998, "Secretion and pH-dependent self-processing of the pro-form of the Yarrowia lipolytica acid extracellular protease", *Yeast*, v. 14, n. 12 (dec), pp. 1115–1125. ISSN: 0749503X. doi: 10.1002/(SICI)1097-0061(19980915)14:12<1115::AID-YEA316>3.0.CO;2-O.

MEUNCHAN, M., MICHELY, S., DEVILLERS, H., et al., 2015, "Comprehensive Analysis of a Yeast Lipase Family in the Yarrowia Clade", *PLOS ONE*, v. 10, n. 11, pp. 22. ISSN: 1932-6203. doi: 10.1371/journal.pone.0143096.

MITCHELL, D. A., VON MEIEN, O. F., KRIEGER, N., 2003, "Recent developments in modeling of solid-state fermentation: heat and mass transfer in bioreactors", *Biochemical Engineering Journal*, v. 13, n. 2-3 (mar), pp. 137–147. ISSN: 1369703X. doi: 10.1016/S1369-703X(02)00126-2.

MITCHELL, D. A., VON MEIEN, O. F., KRIEGER, N., et al., 2004, "A review of recent developments in modeling of microbial growth kinetics and intraparticle phenomena in solid-state fermentation", *Biochemical Engineering Journal*, v. 17, n. 1 (jan), pp. 15–26. ISSN: 1369703X. doi: 10.1016/S1369-703X(03)00120-7.

Mitchell, D. A., Berovič, M., Krieger, N. (Eds.), 2006, *Solid-State Fermentation Bioreactors*. Berlin, Heidelberg, Springer Berlin Heidelberg. ISBN: 978-3-540-31285-7. doi: 10.1007/3-540-31286-2.

MITCHELL, D. A., CUNHA, L. E. N., MACHADO, A. V. L., et al., 2010, "A model-based investigation of the potential advantages of multi-layer packed beds in solid-state fermentation", *Biochemical Engineering Journal*, v. 48, n. 2 (jan), pp. 195–203. ISSN: 1369703X. doi: 10.1016/j.bej.2009.10.008.

MOFTAH, O., GRBAVCIC, S., MOFTAH, W., et al., 2013, "Lipase production by Yarrowia lipolytica using olive oil processing wastes as substrates", *Journal of the Serbian Chemical Society*, v. 78, n. 6, pp. 781–794. ISSN: 0352-5139. doi: 10.2298/JSC120905005M.

MUZILLA, M., UNKLESBAY, N., HELSEL, Z., et al., 1989, "Effect of Particle Size and Heat on Absorptive Properties of Soy Hulls", *Journal of Food Quality*, v. 12, n. 4, pp. 305–318. ISSN: 17454557. doi: 10.1111/j.1745-4557.1989.tb00331.x.

MUZILLA, M., HELSEL, Z., UNKLESBAY, K., et al., 1991, "Thermal Properties of Hydrated Soybean Hulls", *Crop Science*, v. 31, n. 6 (nov), pp. 1541–1544. ISSN: 0011-183X. doi: 10.2135/cropsci1991.0011183X003100060032x.

NEUBRONNER, M., BODMER, T., HÜBNER, C., et al., 2010, "D6 Properties of Solids and Solid Materials". In: *VDI Heat Atlas*, Springer Berlin Heidelberg, pp. 551–614, Berlin, Heidelberg. doi: 10.1007/978-3-540-77877-6_26.

NICAUD, J.-M., 2012, "Yarrowia lipolytica", *Yeast*, v. 29, n. 10 (oct), pp. 409–418. ISSN: 0749503X. doi: 10.1002/yea.2921.

NUNES, P. M. B., FRAGA, J. L., RATIER, R. B., et al., 2021, "Waste soybean frying oil for the production, extraction, and characterization of cell-wall-associated lipases from Yarrowia lipolytica", *Bioprocess and Biosystems*

Engineering, v. 44, n. 4 (apr), pp. 809–818. ISSN: 1615-7591. doi: 10.1007/s00449-020-02489-0.

OGRYDZIAK, D. M., DEMAIN, A. L., TANNENBAUM, S. R., 1977, "Regulation of extracellular protease production in Candida lipolytica", *Biochimica et Biophysica Acta (BBA) - General Subjects*, v. 497, n. 2 (apr), pp. 525–538. ISSN: 03044165. doi: 10.1016/0304-4165(77)90209-4.

OLIVEIRA, T. J., CARDOSO, C. R., ATAÍDE, C. H., 2015, "Fast pyrolysis of soybean hulls: Analysis of bio-oil produced in a fluidized bed reactor and of vapor obtained in analytical pyrolysis", *Journal of Thermal Analysis and Calorimetry*, v. 120, n. 1, pp. 427–438. ISSN: 15882926. doi: 10.1007/s10973-015-4600-6.

PAIVA, A. L., BALCÃO, V. M., MALCATA, F. X., 2000, "Kinetics and mechanisms of reactions catalyzed by immobilized lipases", *Enzyme and Microbial Technology*, v. 27, n. 3-5, pp. 187–204. ISSN: 01410229. doi: 10.1016/S0141-0229(00)00206-4.

PALACIOS, D., BUSTO, M. D., ORTEGA, N., 2014, "Study of a new spectrophotometric end-point assay for lipase activity determination in aqueous media", *LWT - Food Science and Technology*, v. 55, n. 2, pp. 536–542. ISSN: 00236438. doi: 10.1016/j.lwt.2013.10.027.

PALOMO, J. M., FUENTES, M., FERNÁNDEZ-LORENTE, G., et al., 2003, "General trend of lipase to self-assemble giving bimolecular aggregates greatly modifies the enzyme functionality", *Biomacromolecules*, v. 4, n. 1, pp. 1–6. ISSN: 15257797. doi: 10.1021/bm025729+.

PEÇANHA, R., 2014, *Sistemas particulados# : operações unitárias envolvendo partículas e fluidos*. Rio de Janeiro, Elsevier Ltd. ISBN: 978-85-352-7722-7.

PEREIRA-MEIRELLES, F. V., ROCHA-LEÃO, M. H., SANT'ANNA, G. L., 2000, "Lipase location in Yarrowia lipolytica cells", *Biotechnology Letters*, v. 22, n. 1, pp. 71–75. ISSN: 01415492. doi: 10.1023/A:1005672731818.

PEREIRA-MEIRELLES, F., ROCHA-LEÃO, M., SANT'ANNA JR., G., 1997, "A Stable Lipase from Candida lipolytica", *Biotechnology for Fuels and Chemicals*, v. 63-65, pp. 73–85.

PÉREZ-CAMPO, F. M., DOMÍNGUEZ, A., 2001, "Factors Affecting the Morphogenetic Switch in Yarrowia lipolytica", *Current Microbiology*, v. 43, n. 6 (dec), pp. 429–433. ISSN: 0343-8651. doi: 10.1007/s002840010333.

PIGNÈDE, G., WANG, H., FUDALEJ, F., et al., 2000, "Characterization of an Extracellular Lipase Encoded by LIP2 in Yarrowia lipolytica", *Journal of Bacteriology*, v. 182, n. 10, pp. 2802–2810. doi: 10.1007/978-3-540-33761-4_43.

PITOL, L. O., FINKLER, A. T. J., DIAS, G. S., et al., 2017, "Optimization studies to develop a low-cost medium for production of the lipases of Rhizopus microsporus by solid-state fermentation and scale-up of the process to a pilot packed-bed bioreactor", *Process Biochemistry*, v. 62 (nov), pp. 37–47. ISSN: 13595113. doi: 10.1016/j.procbio.2017.07.019.

PIXTON, S., WARBURTON, S., 1975, "The moisture content/equilibrium relative humidity relationship of soya meal", *Journal of Stored Products Research*, v. 11, n. 3-4 (dec), pp. 249–251. ISSN: 0022474X. doi: 10.1016/0022-474X(75)90040-5.

PLASSARD, C. S., MOUSAIN, D. G., SALSAC, L. E., 1982, "Estimation of mycelial growth of basidiomycetes by means of chitin determination", *Phytochemistry*, v. 21, n. 2 (jan), pp. 345–348. ISSN: 00319422. doi: 10.1016/S0031-9422(00)95263-4.

PUNEKAR, N., 2018, *ENZYMES: Catalysis, Kinetics and Mechanisms*. Singapore, Springer Singapore. ISBN: 978-981-13-0784-3. doi: 10.1007/978-981-13-0785-0.

REIS, P., HOLMBERG, K., WATZKE, H., et al., 2009, "Lipases at interfaces: A review", *Advances in Colloid and Interface Science*, v. 147-148, n. C (mar), pp. 237–250. ISSN: 00018686. doi: 10.1016/j.cis.2008.06.001.

RIDE, J., DRYSDALE, R., 1972, "A rapid method for the chemical estimation of filamentous fungi in plant tissue", *Physiological Plant Pathology*, v. 2, n. 1 (jan), pp. 7–15. ISSN: 00484059. doi: 10.1016/0048-4059(72)90043-4.

RIGO, E., NINOW, J. L., DI LUCCIO, M., et al., 2010, "Lipase production by solid fermentation of soybean meal with different supplements", *LWT - Food Science and Technology*, v. 43, n. 7, pp. 1132–1137. ISSN: 00236438. doi: 10.1016/j.lwt.2010.03.002.

RUIZ-HERRERA, J., SENTANDREU, R., 2002, "Different effectors of dimorphism in Yarrowia lipolytica", *Arch*, v. 178, pp. 477–483. doi: 10.1007/s0020300204783.

RZECHONEK, D. A., DAY, A. M., QUINN, J., et al., 2018, "Influence of ylHog1 MAPK kinase on Yarrowia lipolytica stress response and erythritol production", *Scientific Reports*, v. 8, n. 1 (dec), pp. 14735. ISSN: 2045-2322. doi: 10.1038/s41598-018-33168-6.

SAHIR, A. H., KUMAR, S., KUMAR, S., 2007, "Modelling of a packed bed solid-state fermentation bioreactor using the N-tanks in series approach", *Biochemical Engineering Journal*, v. 35, n. 1 (jul), pp. 20–28. ISSN: 1369703X. doi: 10.1016/j.bej.2006.12.016.

SALES, J. C. S., DE CASTRO, A. M., RIBEIRO, B. D., et al., 2020, "Supplementation of watermelon peels as an enhancer of lipase and esterase production by Yarrowia lipolytica in solid-state fermentation and their potential use as biocatalysts in poly(ethylene terephthalate) (PET) depolymerization reactions", *Biocatalysis and Biotransformation*, v. 38, n. 6 (nov), pp. 457–468. ISSN: 1024-2422. doi: 10.1080/10242422.2020.1782387.

SALIHU, A., ALAM, M. Z., ABDULKARIM, M. I., et al., 2012, "Lipase production: An insight in the utilization of renewable agricultural residues", *Resources, Conservation and Recycling*, v. 58, pp. 36–44. ISSN: 09213449. doi: 10.1016/j.resconrec.2011.10.007.

SANGSURASAK, P., MITCHELL, D. A., 1998, "Validation of a model describing two-dimensional heat transfer during solid-state fermentation in packed bed bioreactors", *Biotechnology and Bioengineering*, v. 60, n. 6 (dec), pp. 739–749. ISSN: 00063592. doi: 10.1002/(SICI)1097-0290(19981220)60:6<739::AID-BIT10>3.0.CO;2-U.

SANTOS, A. G., RIBEIRO, B. D., DO NASCIMENTO, F. V., et al., 2019, "Culture Miniaturization of Lipase Production by Yarrowia lipolytica", *Current Biochemical Engineering*, v. 5, n. 1 (sep), pp. 12–20. ISSN: 22127119. doi: 10.2174/2212711905666180730101010.

SASSI, H., DELVIGNE, F., KAR, T., et al., 2016, "Deciphering how LIP2 and POX2 promoters can optimally regulate recombinant protein production in the yeast Yarrowia lipolytica", *Microbial Cell Factories*, v. 15, n. 1 (dec), pp. 159. ISSN: 1475-2859. doi: 10.1186/s12934-016-0558-8.

SHENG, J., JI, X. F., WANG, F., et al., 2014, "Engineering of Yarrowia lipolytica lipase Lip8p by circular permutation to alter substrate and temperature characteristics", *Journal of Industrial Microbiology and Biotechnology*, v. 41, n. 5 (may), pp. 757–762. ISSN: 1476-5535. doi: 10.1007/s10295-014-1428-1.

ŠIBALIĆ, D., ŠALIĆ, A., ZELIĆ, B., et al., 2020, " A New Spectrophotometric Assay for Measuring the Hydrolytic Activity of Lipase from Thermomyces lanuginosus : A Kinetic Modeling ", *ACS Sustainable Chemistry & Engineering*, v. 8, n. 12, pp. 4818–4826. ISSN: 2168-0485. doi: 10.1021/acssuschemeng.9b07543.

SIMU, S. Y., CASTRO-ACEITUNO, V., LEE, S., et al., 2018, "Fermentation of soybean hull by Monascus pilosus and elucidation of its related molecular mechanism involved in the inhibition of lipid accumulation. An in sílico and in vitro approach", *Journal of Food Biochemistry*, v. 42, n. 1 (feb), pp. e12442. ISSN: 01458884. doi: 10.1111/jfbc.12442.

SKJOLD-JØRGENSEN, J., VIND, J., SVENDSEN, A., et al., 2016, "Understanding the activation mechanism of Thermomyces lanuginosus lipase using rational design and tryptophan-induced fluorescence quenching", *European Journal of Lipid Science and Technology*, v. 118, n. 11, pp. 1644–1660. ISSN: 14389312. doi: 10.1002/ejlt.201600059.

SOARES, R. P., SECCHI, A. R., 2003, "EMSO: A New Environment for Modelling, Simulation and Optimisation", *Computer Aided Chemical Engineering*, v. 14, pp. 947–952. ISSN: 15707946. doi: 10.1016/S1570-7946(03)80239-0.

SOUZA, C. E. C., FARIAS, M. A., RIBEIRO, B. D., et al., 2017, "Adding Value to Agro-industrial Co-products from Canola and Soybean Oil Extraction Through Lipase Production Using Yarrowia lipolytica in Solid-State Fermentation", *Waste and Biomass Valorization*, v. 8, n. 4 (jun), pp. 1163–1176. ISSN: 1877-2641. doi: 10.1007/s12649-016-9690-2.

SPAGNUOLO, M., SHABBIR HUSSAIN, M., GAMBILL, L., et al., 2018, "Alternative Substrate Metabolism in Yarrowia lipolytica", *Frontiers in Microbiology*, v. 9, n. MAY (may), pp. 1–14. ISSN: 1664-302X. doi: 10.3389/fmicb.2018.01077.

STAUCH, B., FISHER, S. J., CIANCI, M., 2015, "Open and closed states of Candida antarctica lipase B: protonation and the mechanism of interfacial activation", *Journal of Lipid Research*, v. 56, n. 12 (dec), pp. 2348–2358. ISSN: 00222275. doi: 10.1194/jlr.M063388.

STEUDLER, S., BLEY, T., 2015, "Biomass estimation during macro-scale solid-state fermentation of basidiomycetes using established and novel approaches", *Bioprocess and Biosystems Engineering*, v. 38, n. 7 (jul), pp. 1313–1323. ISSN: 1615-7591. doi: 10.1007/s00449-015-1372-0.

TA, T. M. N., CAO-HOANG, L., ROMERO-GUIDO, C., et al., 2012, "A shift to 50°C provokes death in distinct ways for glucose- and oleate-grown cells of Yarrowia lipolytica", *Applied Microbiology and Biotechnology*, v. 93, n. 5 (mar), pp. 2125–2134. ISSN: 0175-7598. doi: 10.1007/s00253-011-3537-3.

THOMAS, L., LARROCHE, C., PANDEY, A., 2013, "Current developments in solid-state fermentation", *Biochemical Engineering Journal*, v. 81 (dec), pp. 146–161. ISSN: 1369703X. doi: 10.1016/j.bej.2013.10.013.

TIEMERSMA, T. P., PATIL, C. S., SINT ANNALAND, M. V., et al., 2006, "Modelling of packed bed membrane reactors for autothermal production of ultrapure hydrogen", *Chemical Engineering Science*, v. 61, n. 5, pp. 1602–1616. ISSN: 00092509. doi: 10.1016/j.ces.2005.10.004.

TIMOUMI, A., GUILLOUET, S. E., MOLINA-JOUVE, C., et al., 2018, "Impacts of environmental conditions on product formation and morphology of Yarrowia lipolytica", *Applied Microbiology and Biotechnology*, v. 102, n. 9, pp. 3831–3848. ISSN: 14320614. doi: 10.1007/s00253-018-8870-3.

TITORENKO, V. I., RACHUBINSKI, R. A., 1998, "Mutants of the Yeast Yarrowia lipolytica Defective in Protein Exit from the Endoplasmic Reticulum Are Also Defective in Peroxisome Biogenesis", *Molecular and Cellular Biology*, v. 18, n. 5, pp. 2789–2803. doi: https://dx.doi.org/10.1128/mcb.18.5.2789.

TRY, S., DE-CONINCK, J., VOILLEY, A., et al., 2018, "Solid state fermentation for the production of γ-decalactones by Yarrowia lipolytica", *Process Biochemistry*, v. 64 (jan), pp. 9–15. ISSN: 13595113. doi: 10.1016/j.procbio.2017.10.004.

TURKI, S., KRAEIM, I. B., WEECKERS, F., et al., 2009, "Isolation of bioactive peptides from tryptone that modulate lipase production in Yarrowia lipolytica", *Bioresource Technology*, v. 100, n. 10 (may), pp. 2724–2731. ISSN: 09608524. doi: 10.1016/j.biortech.2008.12.053.

TURKI, S., AYED, A., CHALGHOUMI, N., et al., 2010, "An Enhanced Process for the Production of a Highly Purified Extracellular Lipase in the Non-conventional Yeast Yarrowia lipolytica", *Applied Biochemistry and Biotechnology*, v. 160, n. 5 (mar), pp. 1371–1385. ISSN: 0273-2289. doi: 10.1007/s12010-009-8599-7.

UR REHMAN, A., RASOOL, S., MUKHTAR, H., et al., 2014, "Production of an extracellular lipase by Candida utilis NRRL-Y-900 using agro-industrial

by-products", *Turkish Journal of Biochemistry*, v. 39, n. 2, pp. 140–149. ISSN: 0250-4685. doi: 10.5505/tjb.2014.96977.

VANDERMIES, M., KAR, T., CARLY, F., et al., 2018, "Yarrowia lipolytica morphological mutant enables lasting in situ immobilization in bioreactor", *Applied Microbiology and Biotechnology*, v. 102, n. 13 (jul), pp. 5473–5482. ISSN: 0175-7598. doi: 10.1007/s00253-018-9006-5.

VARDANEGA, R., REMONATTO, D., ARBTER, F., et al., 2010, "A systematic study on extraction of lipase obtained by solid-state fermentation of soybean meal by a newly isolated strain of Penicillium sp", *Food and Bioprocess Technology*, v. 3, n. 3, pp. 461–465. ISSN: 19355130. doi: 10.1007/s11947-009-0224-9.

VARGAS, G. D. L. P., TREICHEL, H., DE OLIVEIRA, D., et al., 2008, "Optimization of lipase production byPenicillium simplicissimum in soybean meal", *Journal of Chemical Technology & Biotechnology*, v. 83, n. 1 (jan), pp. 47–54. ISSN: 02682575. doi: 10.1002/jctb.1776.

VASILEVA-TONKOVA, E., BALASHEVA, D. M., GALABOVA, D., 1996, "Influence of growth temperature on the acid phosphatase activity in the yeast Yarrowia lipolytica." *FEMS microbiology letters*, v. 145, n. 2 (dec), pp. 267–271. ISSN: 0378-1097.

VEGA, R., DOMÍNGUEZ, A., 1986, "Cell wall composition of the yeast and mycelial forms of Yarrowia lipolytica", *Archives of Microbiology*, v. 144, n. 2 (mar), pp. 124–130. ISSN: 0302-8933. doi: 10.1007/BF00414721.

VILLADSEN, J., NIELSEN, J., LIDÉN, G., 2011, *Bioreaction Engineering Principles*. Boston, MA, Springer US. ISBN: 978-1-4419-9687-9. doi: 10.1007/978-1-4419-9688-6.

VOLESKY, B., YERUSHALMI, L., LUONG, J. H. T., 2007, "Metabolic-heat relation for aerobic yeast respiration and fermentation", *Journal of Chemical Technology and Biotechnology*, v. 32, n. 6 (apr), pp. 650–659. ISSN: 01420356. doi: 10.1002/jctb.5030320607.

VONG, W. C., LIU, S.-Q., 2017, "Changes in volatile profile of soybean residue (okara) upon solid-state fermentation by yeasts", *Journal of the Science of Food and Agriculture*, v. 97, n. 1 (jan), pp. 135–143. ISSN: 00225142. doi: 10.1002/jsfa.7700.

VONG, W. C., AU YANG, K. L. C., LIU, S.-Q., 2016, "Okara (soybean residue) biotransformation by yeast Yarrowia lipolytica", *International Journal of Food Microbiology*, v. 235 (oct), pp. 1–9. ISSN: 01681605. doi: 10.1016/j.ijfoodmicro.2016.06.039.

VUONG, M.-D., THANH, N.-T., SON, C.-K., et al., 2021, "Protein Enrichment of Cassava-Based Dried Distiller's Grain by Solid State Fermentation Using Trichoderma Harzianum and Yarrowia Lipolytica for Feed Ingredients", *Waste and Biomass Valorization*, v. 12, n. 7 (jul), pp. 3875–3888. ISSN: 1877-2641. doi: 10.1007/s12649-020-01262-4.

WEI, N., YOU, J., FRIEHS, K., et al., 2007, "An in situ probe for on-line monitoring of cell density and viability on the basis of dark field microscopy in conjunction with image processing and supervised machine learning", *Biotechnology and Bioengineering*, v. 97, n. 6 (aug), pp. 1489–1500. ISSN: 00063592. doi: 10.1002/bit.21368.

WOLF, K., 1996, *Nonconventional Yeasts in Biotechnology*. Berlin, Heidelberg, Springer Berlin Heidelberg. ISBN: 978-3-642-79858-0. doi: 10.1007/978-3-642-79856-6.

WOLLMANN, T., ERFLE, H., EILS, R., et al., 2017, "Workflows for microscopy image analysis and cellular phenotyping", *Journal of Biotechnology*, v. 261, n. February (nov), pp. 70–75. ISSN: 01681656. doi: 10.1016/j.jbiotec.2017.07.019.

YANG, S., LIO, J., WANG, T., 2012, "Evaluation of Enzyme Activity and Fiber Content of Soybean Cotyledon Fiber and Distiller's Dried Grains with Solubles by Solid State Fermentation", *Applied Biochemistry and Biotechnology*, v. 167, n. 1 (may), pp. 109–121. ISSN: 0273-2289. doi: 10.1007/s12010-012-9665-0.

YANO, Y., OIKAWA, H., SATOMI, M., 2008, "Reduction of lipids in fish meal prepared from fish waste by a yeast Yarrowia lipolytica", *International Journal of Food Microbiology*, v. 121, n. 3 (feb), pp. 302–307. ISSN: 01681605. doi: 10.1016/j.ijfoodmicro.2007.11.012.

YAO, X., WANG, N., FANG, Y., et al., 2013, "Impact of surfactants on the lipase digestibility of gum arabic-stabilized O/W emulsions", *Food Hydrocolloids*, v. 33, n. 2 (dec), pp. 393–401. ISSN: 0268005X. doi: 10.1016/j.foodhyd.2013.04.013.

YAO, X., NIE, K., CHEN, Y., et al., 2018, "The influence of non-ionic surfactant on lipid digestion of gum Arabic stabilized oil-in-water emulsion", *Food Hydrocolloids*, v. 74, pp. 78–86. ISSN: 0268005X. doi: 10.1016/j.foodhyd.2017.07.043.

ZHANG, J., HU, B., 2012, "Solid-State Fermentation of Mortierella isabellina for Lipid Production from Soybean Hull", *Applied Biochemistry and Biotechnology*, v. 166, n. 4 (feb), pp. 1034–1046. ISSN: 0273-2289. doi: 10.1007/s12010-011-9491-9.

ZHANG, W., ZHAO, F., ZHAO, F., et al., 2019, "Solid-state fermentation of palm kernels by Yarrowia lipolytica modulates the aroma of palm kernel oil", *Scientific Reports*, v. 9, n. 1 (dec), pp. 2538. ISSN: 2045-2322. doi: 10.1038/s41598-019-39252-9.